T-CELL ENTOSIS IN THE LIVER: CATCHING ESCAPING T-CELLS

UNIVERSITY OF BIRMINGHAM

By Sudha Purswani

This project is submitted in partial fulfilment of the requirements for the award of the MRes

College of Medical & Dental Sciences
Department of Infection and Immunity
University of Birmingham
May 2013

Abstract

Entosis describes a form of emperipolesis, where one cell invades a host cell. Emperipolesis can result in death, division or release of the internalised cell. Preliminary data demonstrates that entosis and release of $CD4^+$T-cells occurs within primary hepatocytes and hepatoma cell lines.

This study focuses on defining the environment and stimuli necessary to induce T-cell release following entosis. A 7-Day release assay was optimised for measuring $CD4^+$T-cell release following T-cell-hepatoma co-culture and entosis. Flow cytometry was then used to quantify the release of T-cells from HepG2-CD81 and Huh-7 cell lines in response to various stimuli, doses and incubation times.

Results indicated that the majority of stimuli and dose responses were not responsible for inducing a higher or lower %T-cell release. Co-cultures also demonstrated a significantly higher %T-cell release from HepG2-CD81s at 2 hour compared to 24 hour incubations in treated and untreated co-cultures. Following optimisation of this release assay, the study concludes that further work is required to investigate the conditions which induce entosis and release of T-cells from hepatoma cell lines. Understanding the purpose and cause of T-cell entosis and release in the liver may lead to its therapeutic manipulation to prevent liver inflammation and diseases such as hepatitis.

Acknowledgements

I would like to thank my supervisor Zania Stamataki for all her guidance and support. I would also like to thank Dominik Niesen for all his help and time in the lab.

Table of Contents

List of illustrations

List of Tables

1. Introduction

1.1. The architecture & function of the liver

The liver is the largest organ in the human body, which contains the biggest reticulo-endothelial cell network(1, 2). Its functions include glycogen storage, detoxification, hormone production, digestion and metabolism(2). 80% of the liver is composed of parenchymal cells, otherwise known as hepatocytes. Other types of liver cells are demonstrated in Table 1. The architecture of the liver including the parenchymal and non-parenchymal cells is demonstrated by Figure 1.

	Type of cell	***Function/definition***
Parenchymal cells	Hepatocytes	• Detoxification of drugs • Protein synthesis and storage • Carbohydrate and fat metabolism
Non-parenchymal cells	Sinusoidal endothelial cells	• Removal of smaller particles from the circulation
	Kupffer cells	• Intravascular tissue macrophages – removal large particles from circulation
	Hepatic stellate cells	• Storage of Vitamin A
	PiT-cells	• NK cells located beneath endothelial cells and fibroblasts
	Hepatic dendritic cells	• Phagocytosis & release of cytokines in response to TLR stimulation
	NKT-cells	• Antitumor/antiviral roles
	Biliary epithelial cells	• Contribution to bile production & transportation of bile into gall bladder/intestine

Table 1*- Demonstration of parenchymal and non-parenchymal cell types and their function within the liver(2, 3).*

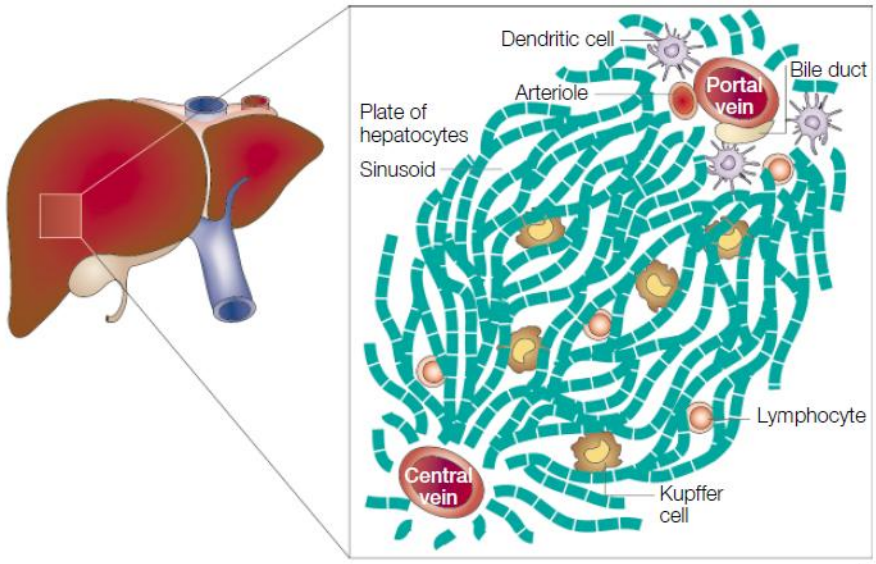

Figure 1 ***- Architecture of cells within a liver lobule. The vascular bundles known as portal tracts contain the portal vein, bile duct and arteriole. Blood travels from the portal tracts through sinusoids which exist between hepatocytes. The sinusoids contain a population of macrophages called kupffer cells.(1)***

As well as metabolic functions, the liver also performs unique immunological roles, and is involved in maintaining peripheral tolerance as well as protecting against harmful pathogens(4).

1.2. The liver immune system & hepatic T-cells

The blood from the gastrointestinal tract is rich in nutrients, harmless food antigens and pathogens that have breached the intestinal barrier(2). This blood passes through the liver via the portal vein, allowing hepatocytes to metabolise specific substances, whilst also exposing them to microbial antigens(1, 2). As well as this consistent antigen exposure, the liver is also exposed to cytokine-rich blood from the spleen and metabolite-rich blood from the systemic artery(2). This puts constant pressure on the liver to induce tolerance or immunity(1, 2, 4).

1.2.1. Liver immune cells

The sinusoidal endothelium is fenestrated and lacks a basement membrane, allowing blood, kupffer cells, DC's and lymphocytes (including T-cells) to pass from the sinusoids into the space of Disse (sub-endothelial space), where they gain direct access to hepatocytes(1).

Kupffer cells are phagocytic liver macrophages which reside in hepatic sinusoids and play a role in both tolerance, (by suppressing T-cell activation), and immunity, (by causing T-cell proliferation and cytokine synthesis)(1).

Pit Cells (PCs) recruit T-cells via cytokine/chemokine cascades. PCs release IFN-γ which induces CXCL9 secretion via hepatocytes and LSECs (Liver sinusoidal endothelial cells), promoting T-cell recruitment and immunity(1). NKT-cells are also abundant in the liver, and are involved in immunity over tolerance(1, 2, 5).

LSECs engulf and present exogenous antigen on MHCII molecules which interact with naïve $CD4^+$T-cells migrating into the liver(6). Unlike liver dendritic cells, it is unknown whether LSECs are able to prime $CD4^+$T-cells(6).

The location of immune cells found in the sinusoidal space is illustrated in Figure 2.

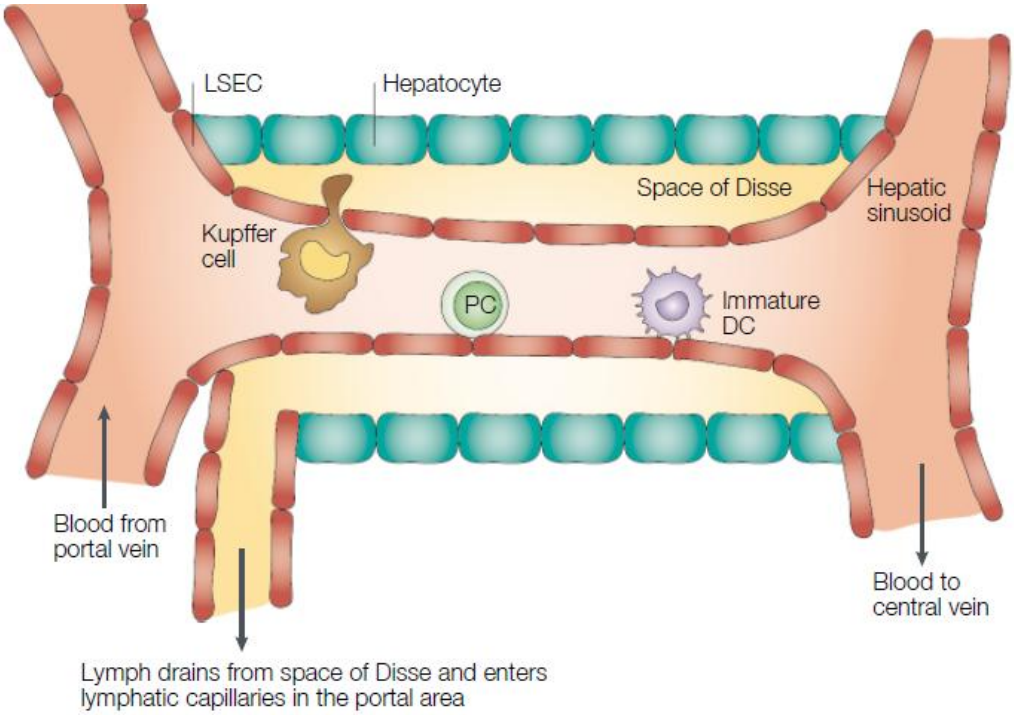

Figure 2- ***Immune cells present within the sinusoidal space can make contact with hepatocytes via the Space of Disse, which is where hepatic lymph originates from. LSECs line the fenestrated endothelium. Sinusoids contain Kupffer cells, lymphocytes, PCs and iDCs(1).***

1.2.2. Hepatic T-cells

Studies show that liver $CD4^+$ T-cells are functionally distinct compared to those in the spleen as they produce higher levels of IL-4, IL-5, IL-10 and IFN-ɤ(4). Furthermore, when naïve liver $CD4^+$Tcells make contact with IL-10 producing LSECs they differentiate into a Treg phenotype(5). In contrast, interaction of naïve $CD8^+$T-cells with LSECs results in partial T-cell activation and apoptosis, the reason for which is unknown(1, 2).

The proportion of $CD8^+$ T-cells generally outnumbers $CD4^+$T-cells in the liver although these populations fluctuate under inflammatory conditions(4, 7). For example, human liver biopsies show a higher number of activated $CD4^+$T-cells in the presence of hepatitis, relative to the number of $CD8^+$ T-cells(7). Most intrahepatic

$CD4^+$ and $CD8^+$ T-cells have an activated phenotype and circulate around the sinusoids until they encounter antigens presented by kupffer cells, immature dendritic cells, LSECs and hepatocytes(1, 2). In some cases, naïve T-cells interact directly with hepatocytes(1). Following antigen recognition these T-cells either activate, undergo apoptosis or differentiate into a regulatory/suppressive phenotype(1).

1.3. The role of cytokines in the liver and liver disease

Although the liver is enriched with cytokine-rich blood from the spleen, constitutive cytokine production in the liver itself is absent or low(2, 8, 9). Increased cytokine production within the liver can lead to hepatic inflammation, apoptosis of liver cells, choleostasis and fibrosis(8).

Unique repertoires of lymphocytes modify the immune response in the liver(2). However non-immune cells such as stellate cells, biliary epithelial cells, hepatocytes and endothelial cells are also able to produce and respond to cytokines within the liver, therefore contributing to local immunological potential(2, 8, 10). Infectious and non-infectious agents trigger the production of these cytokines, and collectively the roles of the lymphocytes and liver cells determine the outcome of immunological stimulation in the liver(2, 8).

1.3.1. Pro-inflammatory Cytokines

1.3.1.1. Tumor Necrosis Factor-α

Tumour Necrosis Factor-α (TNFα) is an inflammatory cytokine involved in chronic liver diseases and acute liver damage(10, 11). Previous data on patients with chronic liver disease show elevated levels of IL-6, IFNɤ and TNFα, irrespective of the aetiology of liver disease(8).

TNFα has been identified as a central mediator for apoptosis and necrotic damage in acute liver failure models, where infiltration of neutrophils and T-cells also occurs(8, 11). Its levels are raised in fatty liver disease, alcohol-induced liver injury, hepatitis and autoimmune liver diseases(8). These diseases lead to cirrhosis of the liver, fibrosis and angiogenesis(2, 8).

When the liver is exposed to inflammatory mediators such as LPS, kupffer cells respond by producing inflammatory cytokines such as TNFα and IFN-α, causing hepatocyte damage and liver injury(8, 11). Furthermore, when TLR4 on hepatocytes ligates to LPS, it causes the production of these pro-inflammatory cytokines such as TNFα, IL-6 and IL-12, which also causes hepatocyte damage(8, 10).

1.3.1.2. Interleukin-6

Interleukin-6 (IL-6) is produced by macrophages, T-cells and endothelial cells either constitutively or via induction of cytokines such as IL-1 or TNF(8, 12). The IL-6R has been identified on hepatocytes(13). In the liver, IL-6 induces cell growth and T-cell differentiation(8, 13). IL-6 is also secreted by kupffer cells causing hepatocytes to release acute-phase proteins, thus proving its ability to control local and systemic inflammatory reactions(12, 13). Its production increases in liver cirrhosis and has

been linked to non-alcoholic fatty liver disease, making it important in the co-ordination of the inflammatory responses in the liver(2, 8).

Some data suggests that IL-6 has an important role in liver regeneration and protection against liver disease(13, 14). One experiment demonstrated that treatment of IL-6 deficient mice with a single dose of IL-6 prevented liver damage(8). Interestingly, TNFα has also proven to be essential in hepatic regeneration. Liver regeneration is impaired when TNFα is blocked following chemical liver injury with TNFα antibodies and by knocking out TNFα(8). Collectively, this data highlights the relevance of inflammatory cytokines in liver damage, control of liver inflammatory reactions and in liver regeneration.

1.3.2. Anti-inflammatory cytokines

1.3.2.1. Transforming Growth Factor-β

The cytokine TGF-β possesses immunosuppressive and anti-inflammatory properties(8). TGF-β1 is the most common isoform found in the liver and is secreted by immune cells such as kupffer cells, stellate cells and epithelial cells(10). Whilst activated kupffer cells in the liver are a major source of inflammatory cytokines, they have also been found to secrete IL-10 and TGF-β in the non-inflamed liver(2, 15). Interestingly, previous studies show that the expression of TGF-β1 is upregulated in experimental models of CCL_4 induced hepatic fibrosis induced(10).

1.4. Characterising entosis

The formation of cell-in-cell structures can be defined by entosis, cannibalism and emperipolesis(16, 17). Phagocytosis describes cells which engulf and degrade dying or pathogenic cells(18, 19). However, cannibalism describes the process whereby passive target cells are actively consumed by non-phagocytic hosts(16). Emperipolesis is a general term for cell-in-cell structures(17, 20), which differs to phagocytosis as the target cells remain encased within a plasma membrane in the host cell in opposed entering endolysosomal compartments(16).

Entosis refers to the invasion of a target cell into its non-phagocytic host, where detachment from the extracellular matrix can promote homotypic cell-in-cell structures to form in normal and tumor cells(17, 20). Unlike cannibalism which has no preference over dead or alive cells, entosis describes a ‘live cell invasion’(21). These invading cells can die a ‘non-apoptotic cell death’ once inside the target cell(16-18). Alternatively these cells remain viable where they can divide, express movements, or exit the cell(16, 22, 23). The possible results of entosis are illustrated by Figure 3.

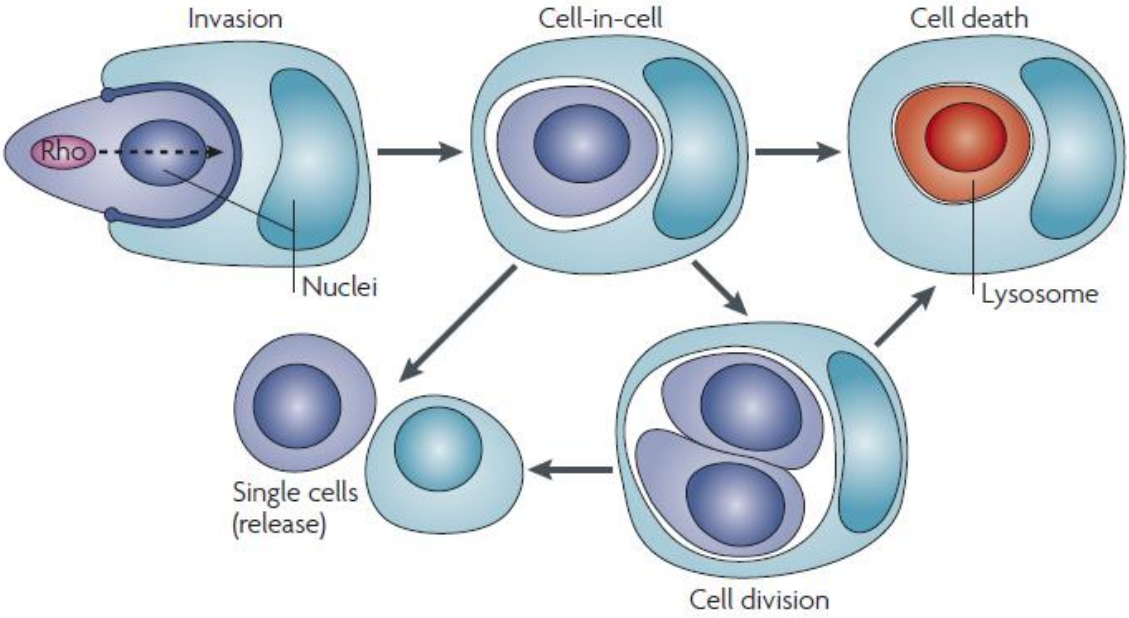

Figure 3 ***– A model of internalisation via entosis. A target cell (usually matrix detached) invades a neighbouring host cell by a Rho-dependant active mechanism. This target cell is then internalised where it can die by a non-apoptotic mechanism, survive and divide, or exit the host cell(16).***

There are numerous examples of homotypic and heterotypic interactions resulting in cell-in-cell structures. Highly metastatic tumors experience cannibalism, a homotypic interaction which results in one tumor cell engulfing another when nutrient supplies are low(21, 24).

Heterotypic interactions are more common. Previous studies show that tumor cells can engulf neutrophils and lymphocytes via cannibalism for immune evasion and survival(20, 21). One study found that live NK cells could internalise into neighbouring tumour cells via an active process similar to entosis which involved actin polymerisation(21). Furthermore, lymphocytes have also proven to be internalised by non-tumorigenic cells such as intestinal epithelial cells(16, 21).

Viable cells can internalise into host cells for protection. For example, oligodendrocytes have been observed in astrocytes within the brains of patients with MS(16). It was hypothesised that the internalised oligodendrocytes are shielded within the astrocytes to protect them from engulfment of macrophages(16). Occasionally, target and host cells both play a role in the formation of cell-in-cell structures. For example, thymocytes invade thymic nurse cells (specialised epithelial cells in the thymic cortex) via uropods, and likewise thymic nurse cells recruit actin to sites of thymocyte entry(16).

A previous study highlighted the importance of receptors in the formation of cell-in-cell structures. Human liver cells internalise Fc receptor positive NK cells via emperipolesis *in vitro*(25). Pre-incubation of liver host cells with IgG antibody (which binds to Fc receptors) increased internalisation of these NK cells, highlighting the importance of target-host cell interaction in emperipolesis(16, 25, 26).

1.5. CD4^{+} T-cells and entosis in the liver

Previous work found that autoreactive CD8^{+}T-cells invaded hepatocytes via emperipolesis where they were activated and degraded in endolysosomal compartments(27). This process of maintaining tolerance has been termed as "suicidal emperipolesis"(27). Furthermore, another study showed that NK cells had the ability to internalise in human liver cells *in vitro(25)*. These findings have led to the McKeating lab at The University of Birmingham investigating emperipolesis of CD4^{+}T-cells in the liver.

Preliminary data demonstrated that activated CD4^{+}Tcells invade primary hepatocytes where they remain viable for >16 hours (see Figure 4).

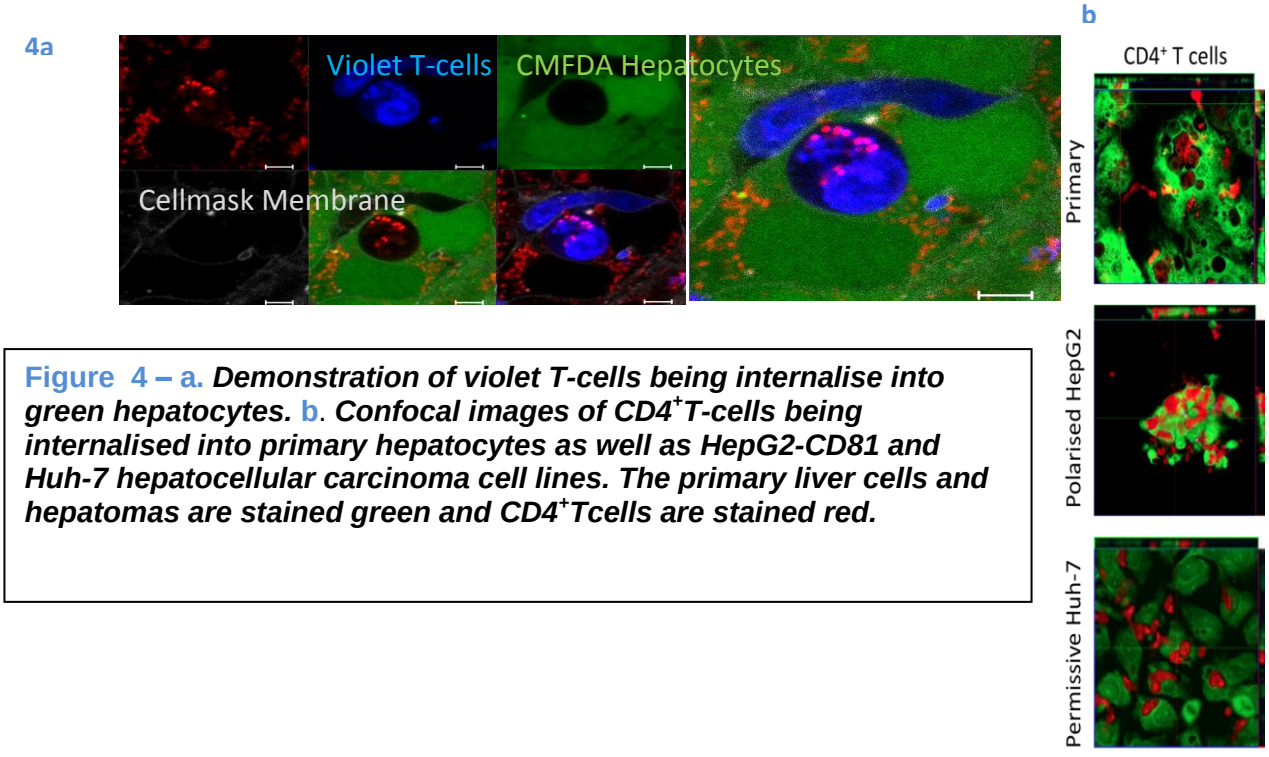

Figure 4 – a. ***Demonstration of violet T-cells being internalise into green hepatocytes.*** **b.** ***Confocal images of CD4^{+}T-cells being internalised into primary hepatocytes as well as HepG2-CD81 and Huh-7 hepatocellular carcinoma cell lines. The primary liver cells and hepatomas are stained green and CD4^{+}Tcells are stained red.***

Christine Marshallsay (BMedSci Student) constructed a protocol to demonstrate the effects of various stimuli and their doses on the numbers of $CD4^+$T-cells released from Huh-7 cells. This T-cell release assay is illustrated by Figure 5 below and the preliminary data is demonstrated in Figure 6.

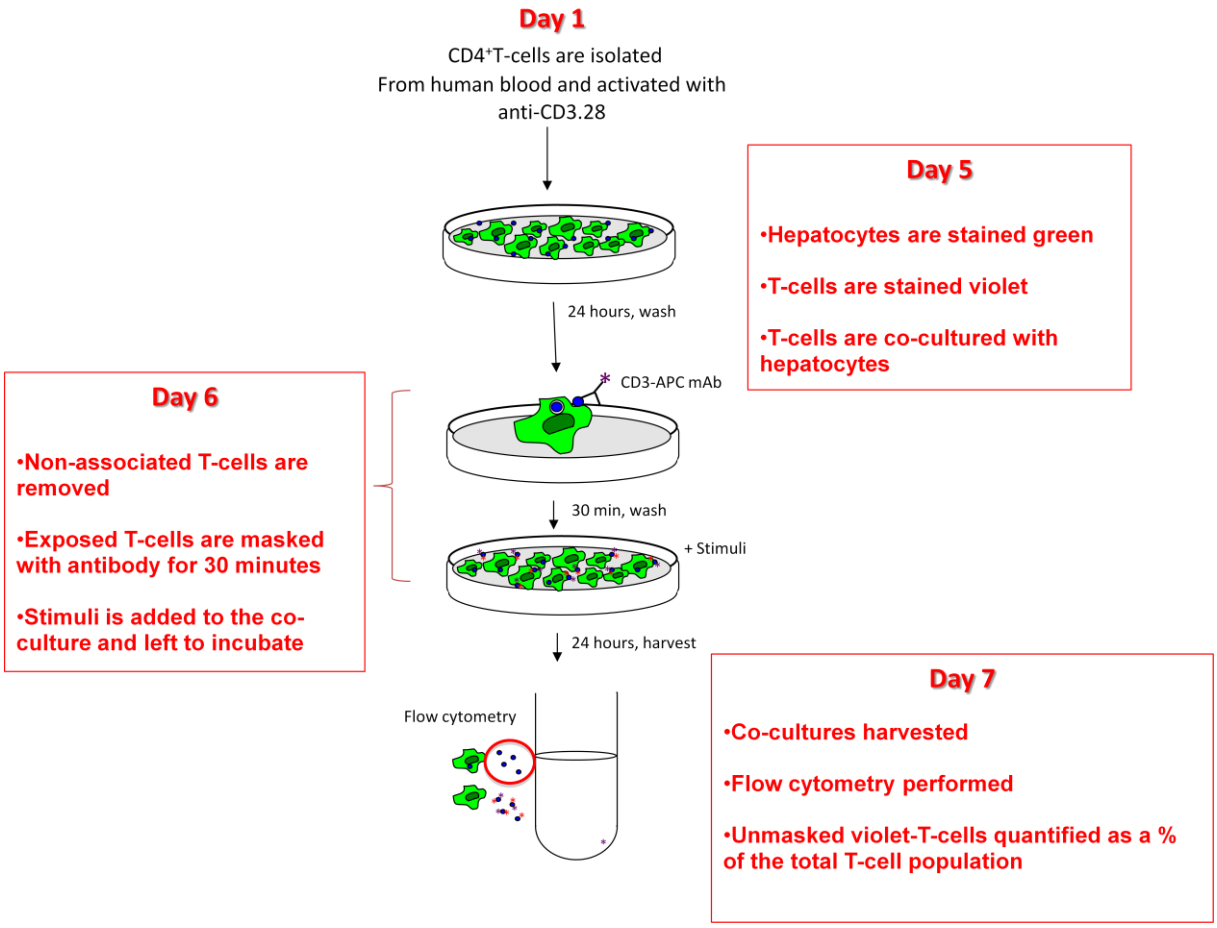

Figure 5 – ***(Adapted from Christine Marshallsay). This assay lasted 7 days. $CD4^+$T-cells were negatively selected from human peripheral blood and activated with anti-CD3.28 before being incubated in IL-2 containing medium for 4 days. On Day 5 hepatomas and T-cells were stained and co-cultured for 24 hours. Day 6 involved addition of masking antibody to mark T-cells which had not been internalised into the hepatomas. A stimulus was added to the co-cultures which were harvested the next day. Flow analysis permitted quantification of non-masked, released $CD4^+$T-cells from hepatomas.***

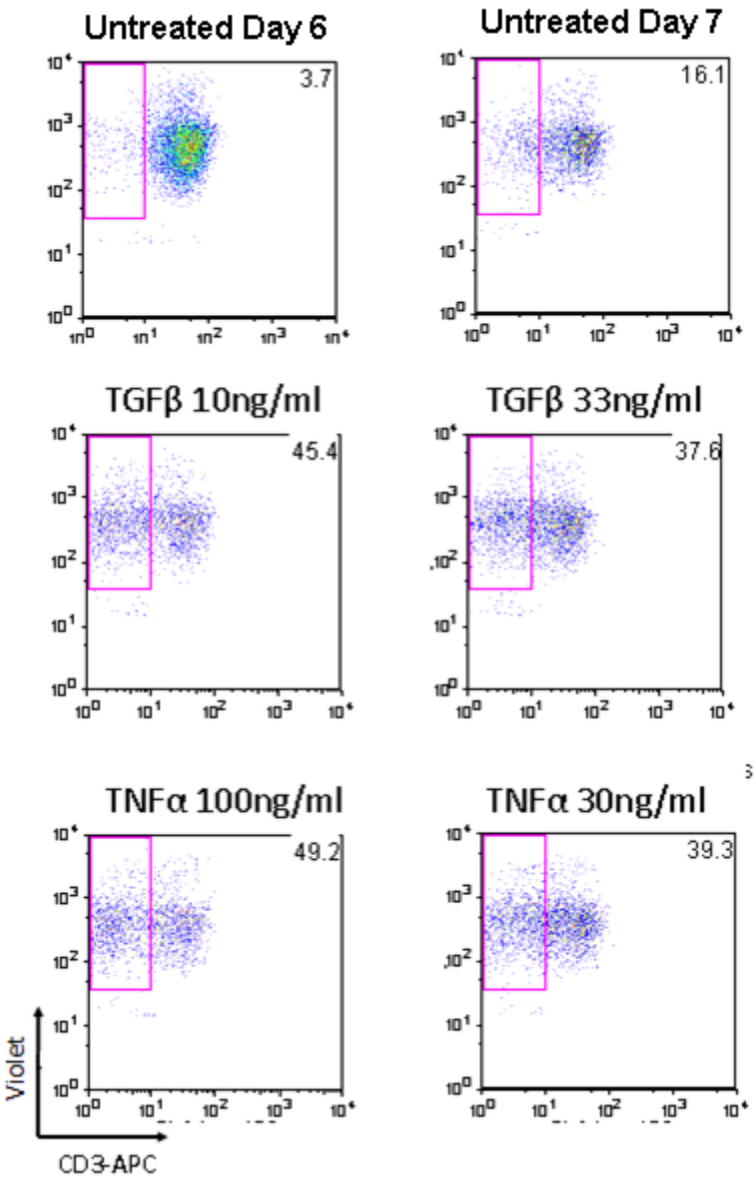

Figure 6 – ***Preliminary data demonstrating the percentage release of violet CD4^{+}T-cells from Huh-7 hepatoma lines in response to different doses of pro- and anti-inflammatory cytokines. The masking antibody used is anti-CD3 APC. The numerical value on the dot plots demonstrates the % of CD4^{+}T-cells released from hepatomas. The released T-cells are expressed as a percentage of the total T-cell population. For detailed protocol of release assay see section 2.1.***

Figure 6 suggests that pro and anti-inflammatory cytokines may have an effect on the percentage of CD4^{+}T-cells released from Huh-7 hepatomas.

1.6. Aims & Objectives

The aim is to mimic specific conditions present in the liver *in vitro* to investigate which environment causes the release of $CD4^+$T-cells from hepatocytes following entosis. First the release assay protocol originally designed by Christine Marshallsay will be optimised. This protocol will involve co-culture of T-cells with Huh-7 and HepG2-CD81 hepatoma cell lines to encourage spontaneous entosis, and quantification of T-cell release using flow cytometry. The percentage of T-cell release from the co-culture will be measured in response to stimuli, dose responses and incubation times. We hypothesise that pro-inflammatory cytokines such as TNFα, IFNɤ and IL-6 will reduce T-cell release following entosis. This would explain a tolerogenic mechanism in the liver for $CD4^+$ T-cells, to prevent further inflammation in the liver.

2. Materials & Methods

2.1. The T-cell release assay

This study was based on a 7-day release assay. On Day 1 $CD4^+$T-cells were isolated via negative selection from human peripheral blood as described in 2.5, and incubated for 4 days in IL-2 containing media. All these T-cells were $CD3^+$ ve. By incubating these T-cells with hepatomas for 24 hours on Day 5, a proportion of these cells were internalised. Anti-CD3-APC was added to the coculture on Day 6 for 30 minutes and washed off. This antibody reached all the exposed T-cells which were outside hepatomas, but did not reach internalised T-cells. This allowed use of anti-CD3 as a “masking” antibody to label all non-internalised T-cells. The co-culture was harvested after 24 hours on Day 7 and anti-CD3-APC fluorescence was analysed by flow cytometry. This permitted separation of the T-cells into $CD3^+$ and $CD3^-$ve populations. The $CD3^-$ve population represented T-cells which were released from the hepatomas after addition of the masking antibody. To confirm that the masking antibody had labelled most T-cells efficiently, some cells were harvested and fixed immediately after the masking antibody had been washed off at Day 6. Co-cultures were harvested at Day 7 to quantify the increased proportion of masking antibody -ve T-cells. These represented T-cells released spontaneously in medium only, without addition of pro-inflammatory stimuli. To assess any potential effects of inflammatory mediators, we compare the release of T-cells in medium only to T-cells released in the presence of stimuli which were added to the co-culture immediately after removal of masking antibody on Day 6.

Each condition was performed with 2 or 3 replicates (see Figure 7). T-cells and hepatomas were easy to discriminate from each other using forward and side scatter measurements. To aid this distinction further, T-cells and hepatomas were pre-labelled with CellTracker dyes in violet and green respectively. To monitor T-cell cell divisions, we used CellTrace violet, which reduces in fluorescence intensity when cells divide.

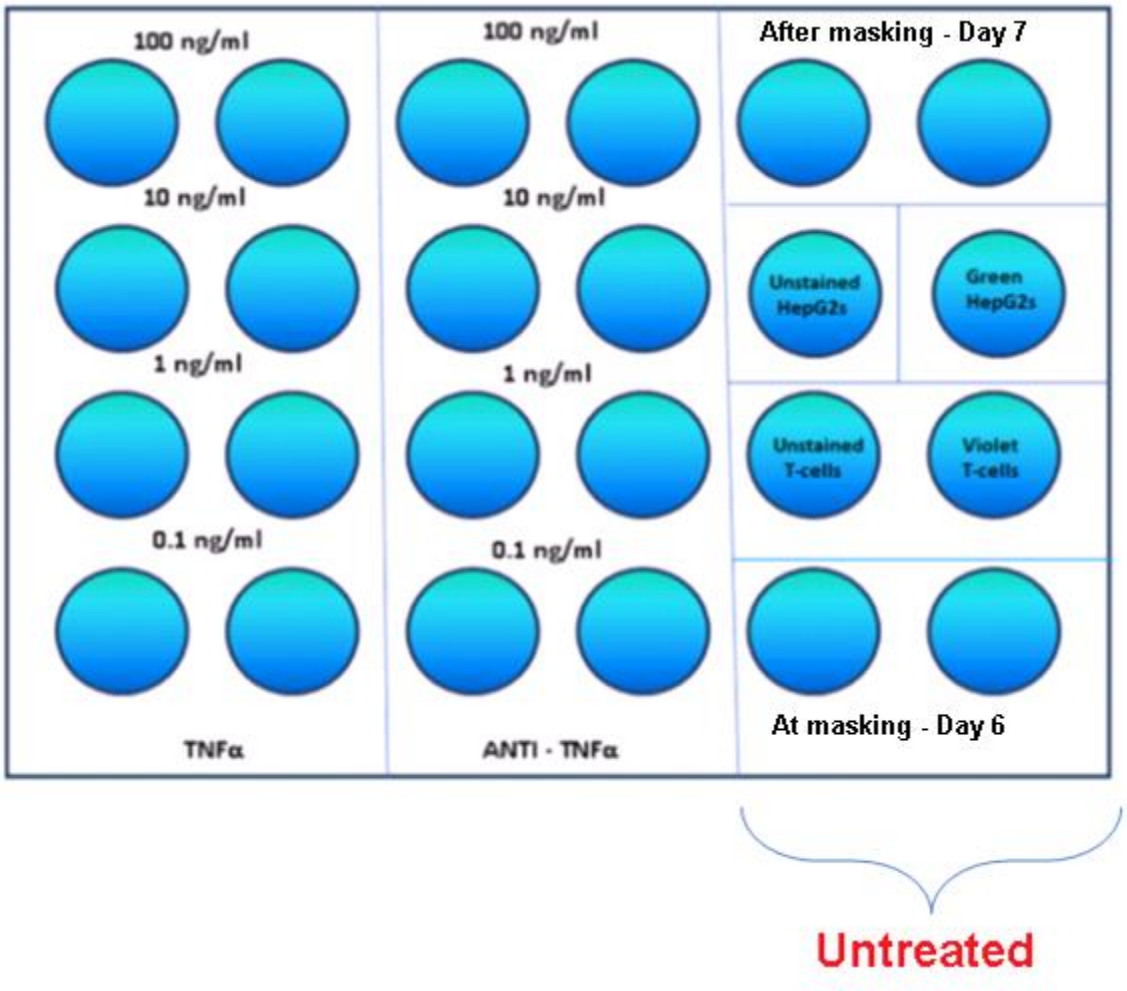

Figure 7 ***– An example of an experimental setup including treatments (TNFα +/- inhibitor) and controls on a 24-well plate. The number of wells that were treated depended on the experiment. The controls in the final column were repeated in all release assays***

2.2. The biotin assay

This assay was performed over 7 days and acted as a quality control assay to support optimisation of the release assay protocol. Biotin labels the primary amines expressed on the surface of T-cells. $CD4^{+}$T-cells were isolated from human blood (Day 1) and cultured in IL-2 containing media for 4 days. On day 5 T-cells were stained violet and biotinylated according to 2.9, before being co-cultured with the green hepatocytes for 24 hours. This allowed the biotinylated T-cells to internalise into the hepatomas. On Day 6, biotinylated T-cells which were not internalised into HepG2-CD81 cells were then masked with Streptavidin-PE antibody which binds with high affinity to biotin. Excess antibody was washed away after 30 minutes and desired treatments were incubated with the co-culture for 24 hours. On Day 7, streptavidin-APC780, which also binds with high affinity to biotin, was added for 30 minutes prior to harvesting. This masked all internalised and non-internalised biotinylated T-cells, and formed a control to confirm efficient biotinylation of all the T-cells. The co-culture was harvested and the percentages of strep-PE negative, strep-APC positive T-cells were then measured via flow cytometry. These T-cells represented the ‘released’ population of T-cells from the hepatomas. This assay is demonstrated by Figure 8.

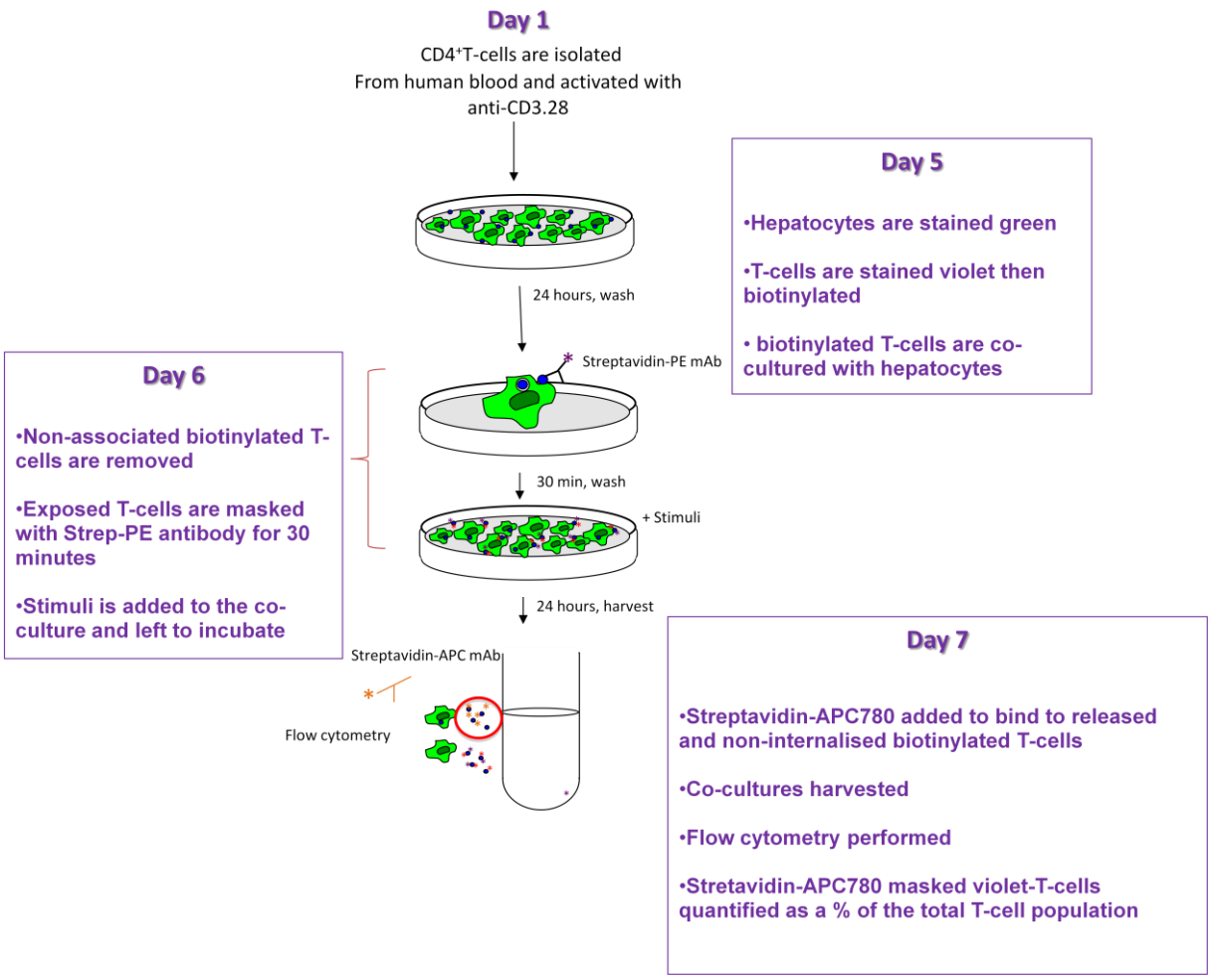

Figure 8 – ***The biotin release assay as described in 2.2, was used to optimise the original T-cell release assay described in 2.1. by Figure 5. Controls were strep-PE cultured with non-biotinylated T-cells, strep-APC780 cultured with non-biotinylated T-cells, strep-PE cultured with biotinylated T-cells, strep-APC780 cultured with biotinylated T-cells and strep-PE and APC780 cultured with biotinylated T-cells. The 'at masking' (Day 6) and 'after masking' (Day 7) controls were repeated from release assays (2.1.) using strep-PE to exposed mask biotinylated T-cells from the HepG2-CD81-T-cell co-culture.***

2.3. HepG2-CD81 hepatocyte cell line

The HepG2 line has lost CD81 expression. However, in this study HepG2 cells were transduced with CD81 under antibiotic selection in order to mimic hepatocytes *in vivo*.

Cells were cultured in DMEM (Deilbecco's modified eagle medium) supplemented with 10% Foetal Bovine Serum (FBS), 1% Streptomycin, 1% L-glutamine and 1% non-essential amino acids to form a 10%DMEM, (Gibco, Life Technologies, UK) and Zeocin used at 1mg/ml (Invitrogen, Life Technologies, UK) to select for $CD81^+$ cells. The cells were stored in an incubator at 37°C in 5% CO_2 and split every three days to prevent overgrowth and death.

2.4. Seeding HepG2-CD81 cells

The HepG2-CD81 cells were washed and incubated with 0.25% trypsin-EDTA solution (Gibco, Life Technologies, UK) for 4 minutes to dislodge the cells from the flask. The cells were lifted and the trypsin was inactivated with 10%DMEM. The cell mixture was brought to a volume of 26ml with zeocin containing media. 1ml of the cell suspension was then pipetted into each well of the 24-well plates, before being incubated for 3 days to allow T-cell populations to expand.

2.5. Isolating $CD4^+$ T-lymphocytes

Blood was provided by hematomacrosis patients at the Queen Elizabeth Hospital, Birmingham. Samples were spun for 20 minutes at 2000RPM to fractionate the blood. The leucocyte buffy coat was harvested and pooled before being diluted with sterile PBS (Gibco, Life Technologies, UK). Diluted leucocytes were layered over Lympholyte®-H (Cedarlane Labs, Canada) and spun again at 2000RPM without brake for 30 minutes. The lymphocyte layer was later removed and re-suspended in RPMI Medium-1640(L-Glu) containing 10% FBS, 1% Streptomycin and 1% non-essential amino acids (Gibco, Life Technologies, UK). The lymphocytes were centrifuged again for 5 minutes at 1500RPM before being washed with RPMI and counted.

$CD4^+$T-cells were negatively selected using an EasySep Human $CD4^+$ T-cell Enrichment Kit (Stemcell Technologies, UK) according to manufacturer's instructions. Lymphocytes were re-suspended at a concentration of $5x10^7$ cells/ml in RPMI. The EasySep Human $CD4^+$ T-cell enrichment cocktail was added to the cell suspension at 50µl/ml and incubated at room temperature for 10 minutes. Following incubation, the EasySep magnetic particles were added to the cell suspension at 100µl/ml and incubated again for 5 minutes at room temperature. The cell suspension was then brought to a specific volume using RPMI (depending on the PBMC number), before being placed into the EasySep magnet for 5 minutes. Unattached $CD4^+$T-cells were removed and activated with anti-CD3.28 human mAb at 1µg/ml (eBioscience, UK) before being incubated for 20 minutes at 37°C. Following activation, IL-2 was added to the T-cells at 500IU (PeproTech, UK) and ~2 million T-cells were seeded in a 24-well plate.

2.6. Preparing the co-culture

2.6.1. Staining HepG2-CD81 cells

CellTracker green (CMFDA) (Life Technologies, Invitrogen, UK) was diluted with Serum Free Medium (SFM) (RPMI1640 L-glutamine, 1% Streptomycin and 1% non-essential amino acids) (Gibco, Life Technologies, UK) to form a working concentration 0.02mM. 250µl of the diluted CMFDA was then added to each well of the 24-well plate and incubated at 37ºC for 40 minutes. Following incubation, wells were washed with 10% DMEM, and then incubated with 250µl of 10% DMEM until the T-cells were prepared for co-culture.

2.6.2. Staining purified T-lymphocytes

2.6.2.1. Cell Tracker Violet

Initially, T-cells were stained with CellTracker Violet (Life Technologies, Invitrogen, UK) which was diluted with SFM to form a working concentration of 0.02mM. Meanwhile, the T-cell suspension was centrifuged at 20°C for 3 minutes at 1500RPM. The violet-dye solution was used to re-suspend the T-cell pellet, before being incubated at 37°C for 30 minutes. Following incubation the violet T-cells were centrifuged again and re-suspended in 10%DMEM. 50µl containing $0.5x10^6$ violet T-cells were then co-cultured and incubated with CMFDA-labelled HepG2-CD81 cells for 24 hours.

2.6.2.2. Violet cell Trace

Following the first experiment, a CellTrace Violet Proliferation Kit (Life Technologies, Invitrogen, UK) was used to dye T-cells.

CellTrace Violet was diluted with SFM to form a working concentration of 5µM, which was mixed with the T-cells and incubated for 20 minutes at 37°C. The cells were centrifuged, re-suspended in 1ml of 10%DMEM and incubated for 10 minutes. The cell suspension was centrifuged again and the T-cell pellet was re-suspended in 10%DMEM. As previously, 50µl containing $0.5x10^6$ violet T-cells were added to each well of CMFDA-labelled HepG2-CD81 cells and incubated for 24 hours.

2.7. Co-culture Treatment

2.7.1. Masking antibody addition

Mouse anti-human CD4-APC (BD Pharmingen, BD Biosciences, UK) was used as masking antibody to stain non-internalised $CD4^+$Tcells. This masking Antibody was administered to the co-culture for 30 minutes, and excess antibody was washed away. After masking the treatment solutions were also administered to the wells.

In one experiment, a panel of anti-human antibodies were tested for their masking efficiency: CD2-APC, CD3-APC, CD5-APC (BD Pharmingen, BD Biosciences, UK), CD43-FITC and CD45-FITC (Biolegend, UK). All antibodies were used at a 1:100 dilution.

2.7.2. Treatment addition

250µl of 10%DMEM containing each treatment was added to each well and left to incubate with the co-culture for 24 hours. Figure 7 demonstrates an example of a plate used to test the T-cell release response to different concentrations of TNFα (PeproTech, UK) in the presence and absence of anti-human TNFα mAb (PeproTech, UK). In the case of the other cytokines and growth factor treatments (PeproTech, UK), varying concentrations were used (see results).

2.8. Fixing cells

On Day 7, co-cultures were harvested into FACSs tubes using 2mM EDTA (ethylenediaminetetraacetic acid) (Sigma-Aldrich, UK). All samples were fixed for 5 minutes with 4% paraformaldehyde (PFA) (Sigma-Aldrich, UK) and were filtered prior to flow analysis.

2.9. Biotinylation and streptavidin masking of $CD4^+$ T-cells

Sulfo-NHS-LC-Biotin (Thermo Scientific, UK) was re-suspended in sterile PBS to form a 2mM solution. The T-cell suspension was then washed with sterile PBS to remove amine-containing media from the cells, before being re-suspended in the biotin solution and incubated at room temperature for 30 minutes. The biotinylated T-cells were washed again with PBS and 100mM of glycine to quench excess biotin reagents, before being re-suspended in 10%DMEM. These T-cells were then added to the co-culture for 24 hours, after which streptavidin-PE (affymetrix, eBioscience, UK) was added as the masking antibody (1µg/ml). 24 hours after masking, streptavidin-APC780 (affymetrix, eBioscience, UK) was also added to the treated co-

culture for 30 minutes (at 1µg/ml). The co-culture was then harvested according to 2.8. prior to flow analysis.

2.10. Using the Huh-7 cell line

Huh-7 hepatomas were used to increase the number of T-cell internalisation events. The same experimental procedure was used as with the HepG2-CD81 and violet T-cell co-culture, however mouse anti-human CD5 PE-CY7 (BD Pharmingen, BD Biosciences, UK) was used as the masking antibody at a 1:100 dilution. Due to their rapid growth, the Huh-7 cells were seeded on a 24 well plate and co-cultured 3 hours later with violet T-cells.

2.11. Controls

The following controls were used in the T-cell release assay: unstained HepG2-CD81s containing no T-cells/treatments, CMFDA green stained HepG2-CD81s with no T-cells/treatments, $0.5x10^6$ unstained T-cells, $0.5x10^6$ violet T-cells, untreated green HepG2-CD81 and violet T-cell co-cultures at masking (fixed at Day 6), and an untreated well with green HepG2-CD81 and violet T-cell co-cultures after masking (fixed at Day 7). Figure 7 demonstrates the experimental set-up of one plate. See Figure 5 and section 2.1.for detailed assay protocol.

3. Results

The aim of this study was to optimise a method to accurately measure the percentage release of $CD4^+$T-cells from hepatoma cell lines. Once optimised, the aim was to detect the effect of various stimuli on $CD4^+$T-cell release from hepatomas. Data measuring the percentage of released unmasked $CD4^+$T-cells was then collected using a DAKO cyan flow cytometer and analysed using FlowJo.

3.1. Gating on released CD4^{+}T-cells

Flow cytometry was used to quantify CD4+T-cell and hepatoma events. A gate was placed around the T-cell population and ~20,000 T-cell events were collected (Figure 9). When analysing raw data using FlowJo, the T-cell events were backgated to ensure that no hepatoma cells fell into the T-cell gate to affect the results.

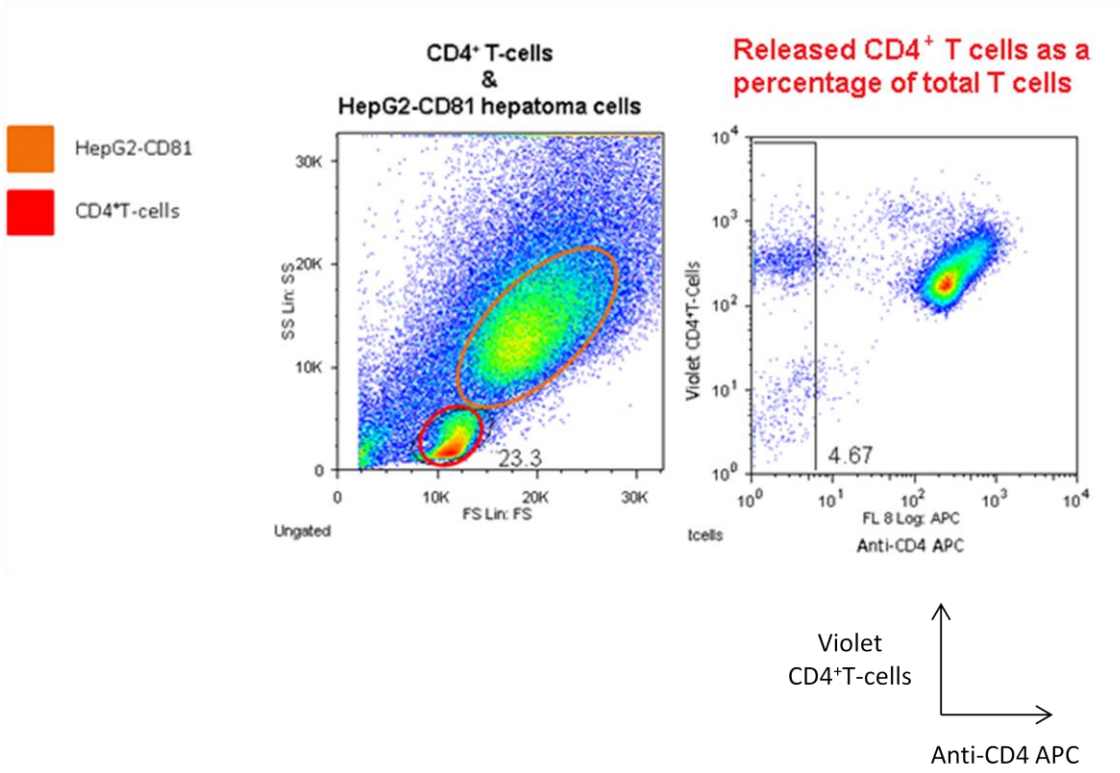

Figure 9 – ***Example of control results from Day 6 (At masking) collected by flow cytometry. The orange gate represents the HepG2-CD81 cells and the red gate represents violet CD4^{+}Tcells. These results were backgated to ensure that there was no overlap between the two cell types. The flow diagram on the right shows the % of T-cells released. Released T-cells that were not accessible to the masking antibody are anti-CD4-APC negative. The released T-cells are expressed as a percentage of the total T-cell population gated on the left (red).***

The gate around the cells negative for ‘Anti-CD4 APC’ and positive for ‘Violet $CD4^+$T-cells’ represent the percentage of T-cells released from HepG2-CD81 cells. The population positive for ‘Anti-CD4 APC’ and ‘Violet $CD4^+$T-cells’ represents non-internalised, anti-CD4 masked T-cells outside the HepG2-CD81 cells. Those negative for both anti-CD4 and Violet T-cells represent unstained T-cells, dead cells and debris.

3.2. T-cell release assays

3.2.1. *The percentage release of CD4^{+}T-cells from HepG2-CD81s does not increase in the presence of inflammatory conditions*

Experiment 1 and 2 was setup to compare %T-cell release when anti-CD4 APC masking antibody and HepG2-CD81 hepatomas were used in the release assay, in opposed to the anti-CD3 APC and Huh-7 hepatomas used in preliminary experiments. Results are displayed in Figure 10.

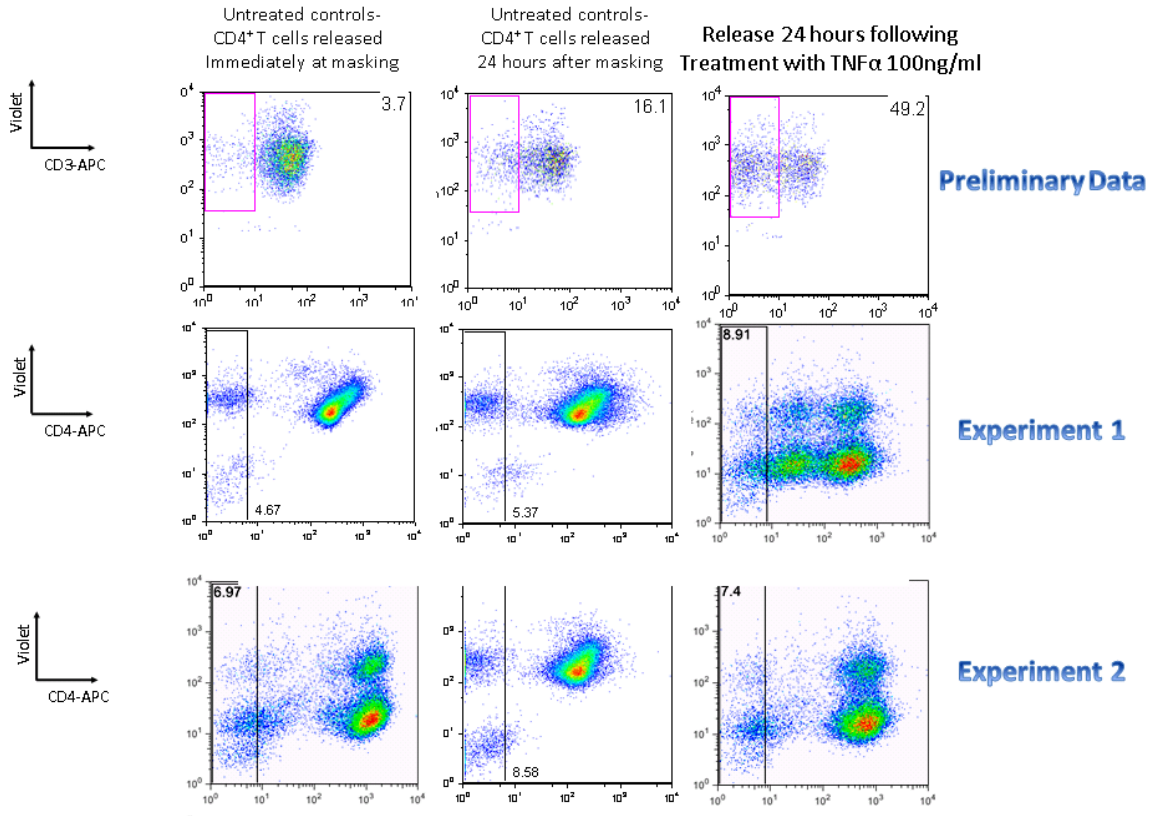

***Figure 10** – Dot plots comparing preliminary data to my Experiments 1 and 2.The preliminary experiments used anti-CD3 mAb for masking whereas Experiments 1 and 2 use anti-CD4 masking antibody to measure %T-cell release from untreated and treated (TNFα treatment 100ng/ml) co-cultures. The left column demonstrates T-cell release in the untreated controls at masking (Day 6), whereas the second column demonstrates T-cell release in the untreated controls after masking (Day 7). Co-cultures were treated for 24 hours prior to flow analysis at Day 7.*

Preliminary data in Figure 10 shows an increase in the percentage of $CD4^{+}$T-cells released 24 hours after treatment compared to untreated controls. Experiments 1 and 2 do not demonstrate a great increase in %T-cell release in the TNFα treated co-culture compared to untreated controls; however show increased T-cell proliferation compared to the preliminary data. This indicates that levels of entosis and release may differ according to the type of hepatoma cell line used.

3.2.2. Percentage release of $CD4^+$T-cells from HepG2-CD81-CD81 cells is not dependant on the dose of TNFα

This experiment measured % T-cell release in response to increasing doses to TNFα in the presence and absence of the TNFα inhibitor anti-TNF (Figure 11). The inhibitor was used to determine whether the T-cell release observed was truly induced by TNFα dose treatment.

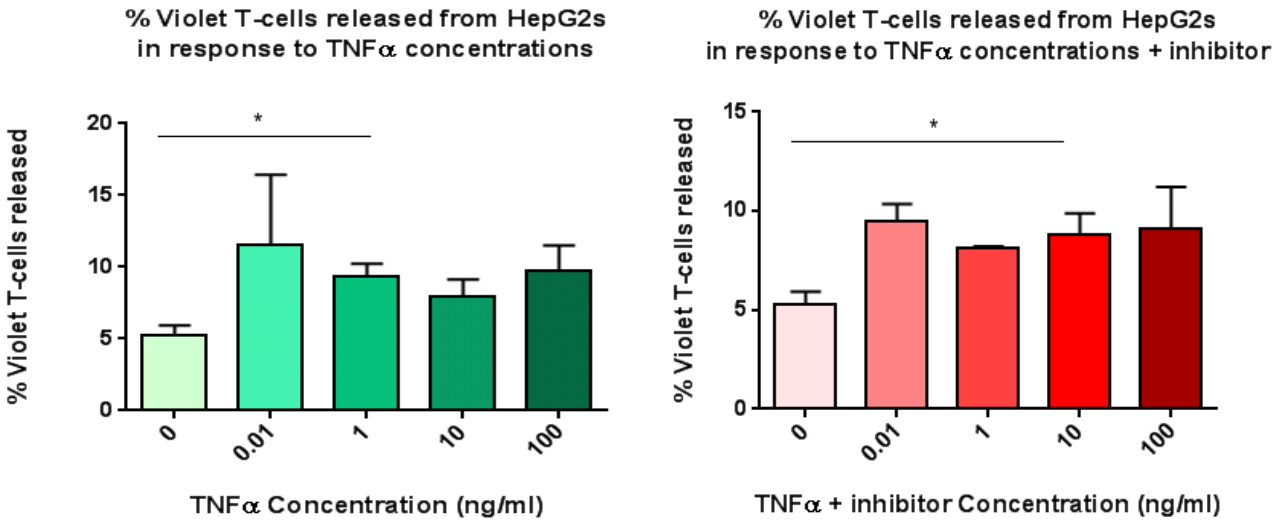

Figure 11 ***–Experiment 1: (n=2) Graphs to show the effects of different concentrations of TNFα treatment in the absence (left) and presence (right) of inhibitor (anti-TNFα), on %T-cell release from HepG2-CD81 hepatomas. The doses of TNFα used in the release assay presented a one log difference (100, 10, 1, 0.01ng/ml). TNFα +/- inhibitor was incubated with theHepG2-CD81-T-cell co-culture for 24 hours before %T-cell released was measured on Day 7. Released T-cells were expressed as percentages of the total gated T-cell population. Error bars represent the standard error of the mean (SEM). Statistically significant results are presented by a * where p<0.05.***

Figure 11 (left) shows that treatment with 1ng/ml of TNFα induces a significantly higher %T-cell release compared to the untreated control.

Figure 11 (right) shows that %T-cell release in the presence of TNFα +Inhibitor is similar compared to the TNFα treated co-cultures. The %T-cell release was significantly higher where 10ng/ml of TNFα +inhibitor was used to treat the co-culture; however the overall %T-cell release in this experiment is low.

The results imply that T-cell release from HepG2-CD81s may not be dose dependant. It is also possible that the inhibitory activity in this experiment is not effective due to the %T-cell release being similar to treated samples without inhibitor.

The next release assay involved T-cells from a different donor. This experiment measured % T-cell release in response to increasing doses to TNFα with a two log difference in the presence and absence of anti-TNF (Figure 12).

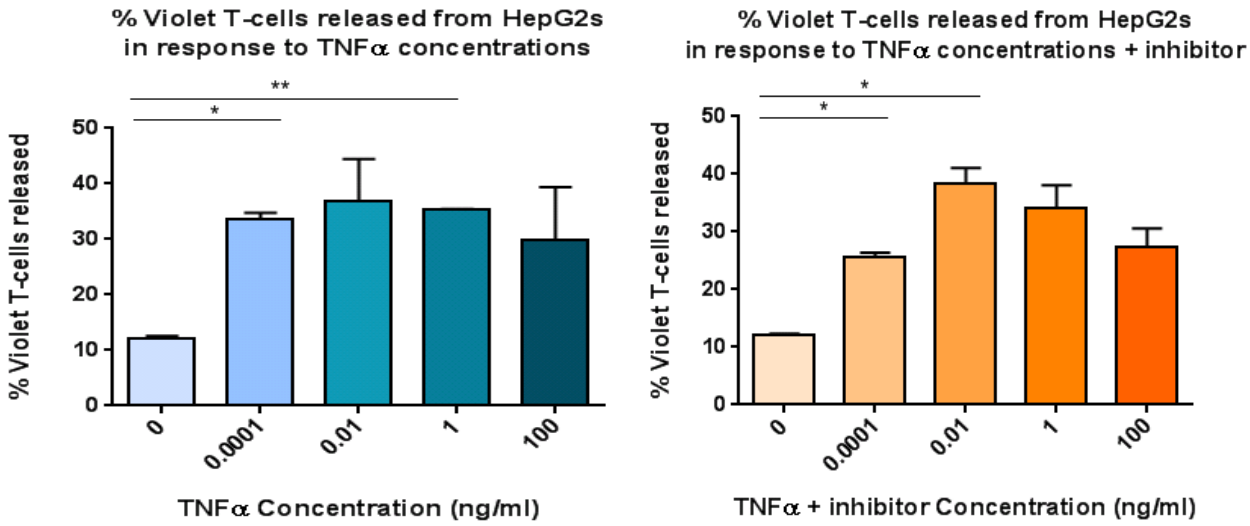

Figure 12- Experiment 2: (n=2) Graphs to show the effects of different concentrations of TNFα treatment in the absence (left) and presence (right) of inhibitor (anti-TNFα), on %T-cell release from HepG2-CD81 hepatomas. TNFα concentrations were used with a two log difference was used (100, 1, 0.01, 0.0001ng/ml). TNFα +/- inhibitor was incubated with the HepG2-CD81-T-cell co-culture for 24 hours before %T-cell released was measured on Day 7. Error bars represent the S.E.M. Statistically significant results are presented by a * where p<0.05, and ** where p<0.01.

Figure 12 (left) shows that treatment with 1ng/ml of TNFα induced a significantly higher %T-cell release compared to the untreated control where p=0.003.

In Figure 12 (Right) The Treatments of TNFα + Inhibitor show a similar %T-cell release compared to in the presence of TNFα alone (left). Treatment with 0.0001ng/ml and 0.01ng/ml of TNFα +inhibitor induced a significantly higher %T-cell release compared to untreated controls where p=0.02 and 0.04 respectively.

This data further indicates that T-release from HepG2-CD81s following entosis is probably not dose dependant.

3.2.3. TNFα +inhibitor (anti-TNFα) has a profound effect on the size and granularity of HepG2-CD81 cells

To investigate effects of TNFα on hepatoma biology, we looked at forward and side scatter profiles of these cells before and after treatment. Figure 13 shows that in the presence of TNFα +inhibitor, the size and granularity of HepG2-CD81 changes, where the population splits into two, with the larger population shifting to the left. This shows that TNFα treatment had a profound effect in hepatoma morphology. No cytotoxicity was noted by trypan blue staining.

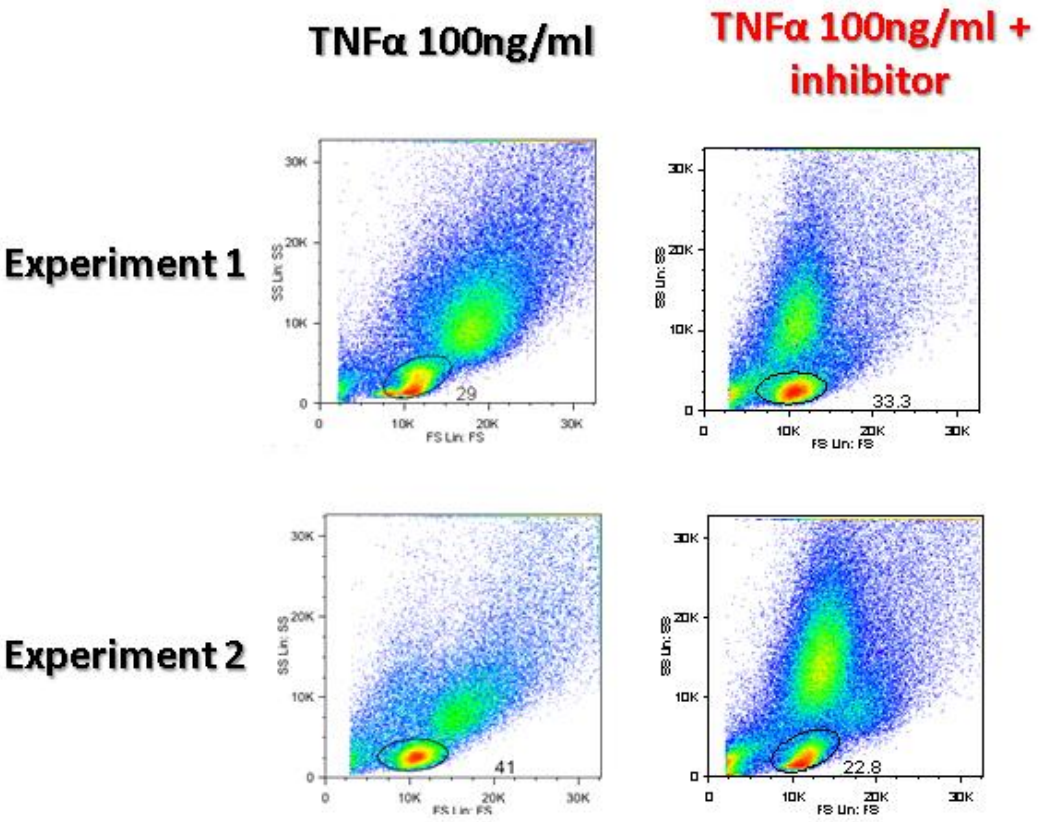

Figure 13 – ***Flow diagram from Experiment 1 and 2 demonstrating a change in HepG2-CD81 morphology in the presence of TNFα +inhibitor (anti-TNFα) compared to TNFα treated samples. TNFα +/- inhibitor was incubated with the T-cell-HepG2-CD81 co-culture on Day 6 for 24 hours. Results were collected via flow cytometry on Day 7.***

3.2.4. *Anti-CD5 antibody masks non-endocytosed Violet CD4$^+$ T-cells more efficiently compared to anti-CD4 in T-cell release assays*

As CD3 and CD4 became downregulated following stimulation of the co-cultured cells with TNFα, we set out to identify more antigens for use as masking reagents in our release assay. The optimal antigens would be present in all T-cells and would not be downregulated on the T-cell surface after treatment. Figure 14 demonstrates the masking efficiency of a panel of antibodies used in release assays.

13.

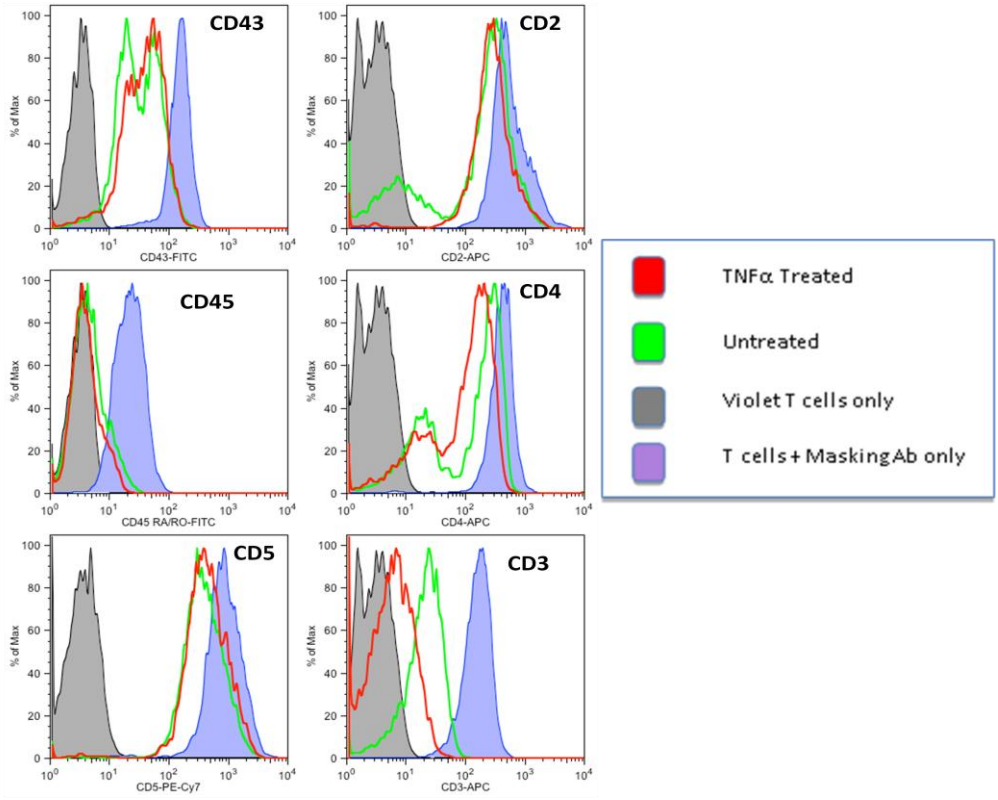

Figure 14 - ***Histograms demonstrating the efficiency of a panel of antibodies for masking CD4$^+$T-cell in TNFα (1ng/ml) treated and untreated samples. A shift of histograms to the left demonstrates loss of fluorescence and inefficient masking of T-cells. During the released assay, exposed T-cells from the T-cell-HepG2-CD81 co-cultures were masked with a panel of antibodies on Day 6 before treatment was added for 24 hours. Results were collected on Day 7 via flow cytometry.***

	Outcome	Justification
CD2	X	Bright, 100% +ve, but reduces in co-culture
CD3	X	Dim, lost following co-culture
CD4	X	Relatively bright, but some lost during co-culture
CD5	✓	Bright, almost 100% positive, with the exception of the 'untreated' anomaly
CD43	X	Intermediate brightness and loss of expression
CD45	X	Dim, lost following co-culture

Table 2 – *Description of the efficiency of each of the antibodies tested as masking antibodies in the release assay.*

Figure 14 shows that anti-CD5 PE-CY7 remains bright throughout the co-culture with HepG2-CD81 in the presence and absence of TNFα treatment. Other antibodies display reduced brightness or fluorescence is lost completely following co-culture. We therefore established that CD5 would be the optimal antigen to target for T-cell masking in the release assay.

3.2.5. Streptavidin-PE antibody efficiently masks non-internalised biotinylated $CD4^+$ T-cells

To confirm that the masking antibody assay truly reveals released T-cells, we set up a new method to identify released T-cells in the release assay using Streptavidin-PE as a masking antibody (See 2.2.). The first experiment was conducted to test whether strep-PE and strep-APC bound efficiently to biotinylated T-cells (Figure 15).

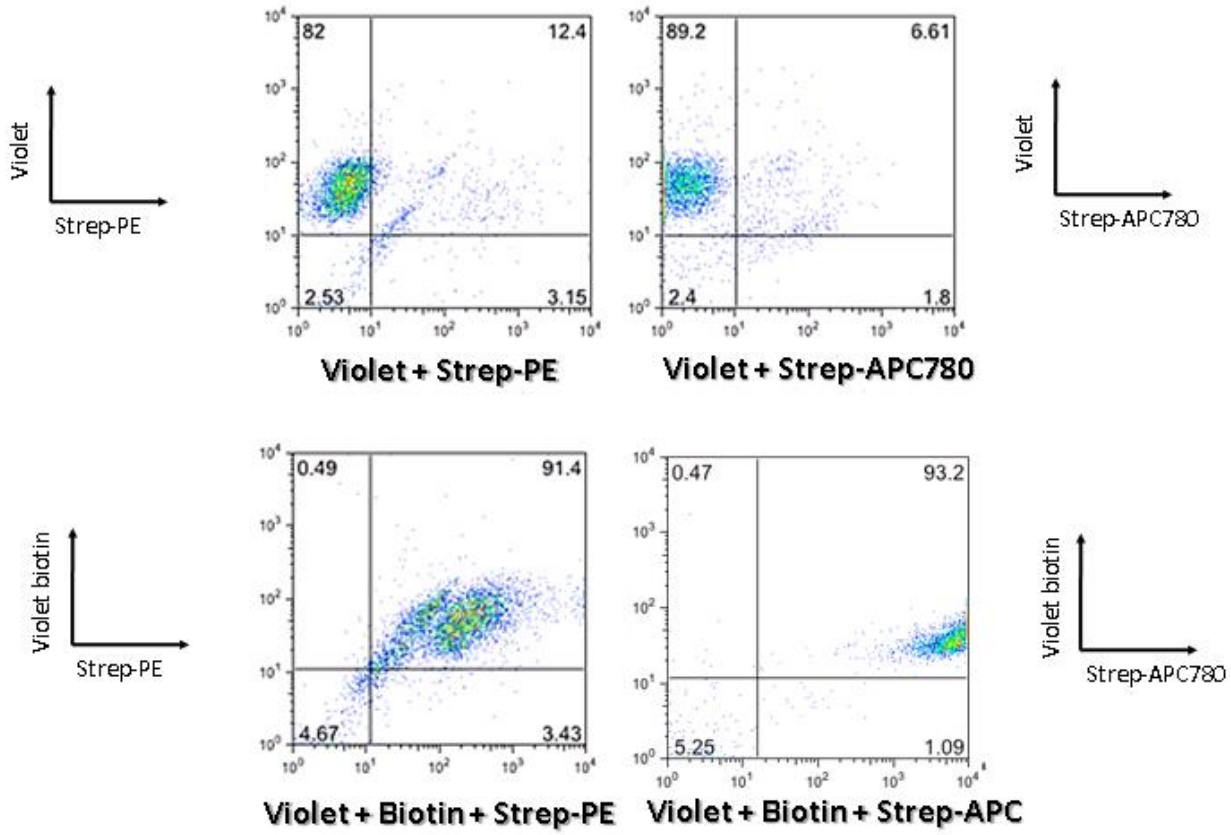

Figure 15 – ***Dot plots demonstrating the effectiveness of Streptavidin-APC and Streptavidin-PE binding to biotinylated $CD4^+$T-cells alone. T-cells were stained violet and half were biotinylated on Day 5 before being cultured in media alone for 24 hours. Streptavidin-PE was added to the biotinylated and non-biotinylated T-cells on Day 6. Streptavidin-APC780 was the control to confirm biotinylation of all T-cells and was added to the biotinylated and non-biotinylated T-cells on Day 7 for 30 minutes prior to harvesting. Results were collected on Day 7 and analysed via flow cytometry. Strep-PE/APC +ve, violet biotin +ve populations represent antibody bound T-cells.***

The top two dot plots of Figure 15 show that in the absence of biotin, Streptavidin-PE and Streptavidin-APC780 are not effective at binding to violet T-cells. The bottom two diagrams show that individually, Streptavidin-PE and APC bind effectively to biotinylated violet T-cells (where in both cases >90% of bionylated T-cells are bound by Streptavidin APC/PE). Results from this experiment show that streptavidin-PE may be an effective masking antibody of biotinylated T-cells.

The aim of the next experiment was to test if strep-PE and strep-APC780 could simultaneously bind to the majority of the biotinylated T-cell population (Figure 16).

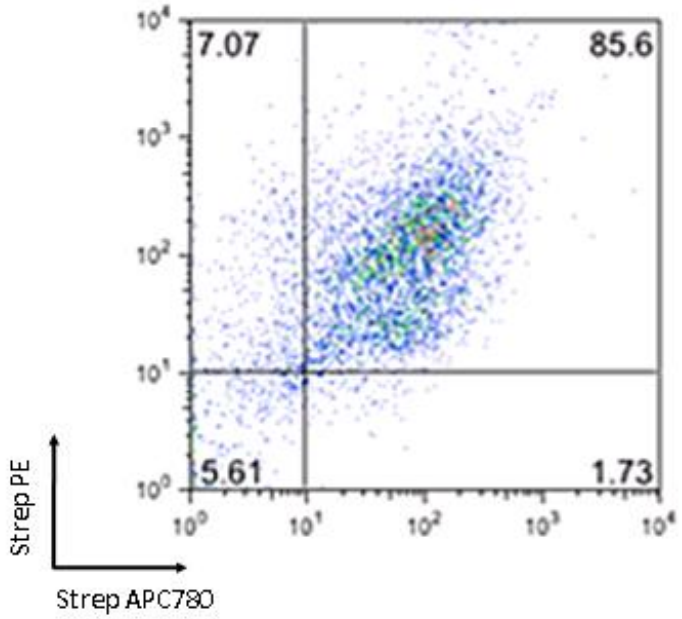

Figure 16 – ***Diagram demonstrating the effectiveness of both Strep-PE and Strep-APC at binding to biotinylated violet CD4^{+}Tcells. A population of the T-cells were biotinylated on Day 5 and cultured alone for 24 hours. On Day 6 streptavidin-PE was added to biotinylated T-cells for 30 minutes. On Day 7 strep-APC780 was also added to the biotinylated T-cells for 30 minutes after which the double-masked T-cells were harvested and analysed via flow cytometry. Strep-PE +ve, strep-APC +ve T-cells represent the double masked T-cells population.***

Figure 16 shows that in the presence of both Streptavidin-APC and Streptavidin-PE, (the double positive population) >85% of biotinylated violet T-cell population is masked. These results show that streptavidin-PE would be effective as a masking antibody of biotinylated T-cells and streptavidin-APC780 would effective as a control marker to confirm T-cell biotinylation in release assays.

3.2.6. Anti-CD5 antibody efficiently masks non-internalised $CD4^+$Tcells

The next experiment used streptavidin-PE in parallel to anti-CD5 PE-CY7 to confirm the efficiency of anti-CD5 PE-CY7 as a masking antibody in release assays (Figure 17).

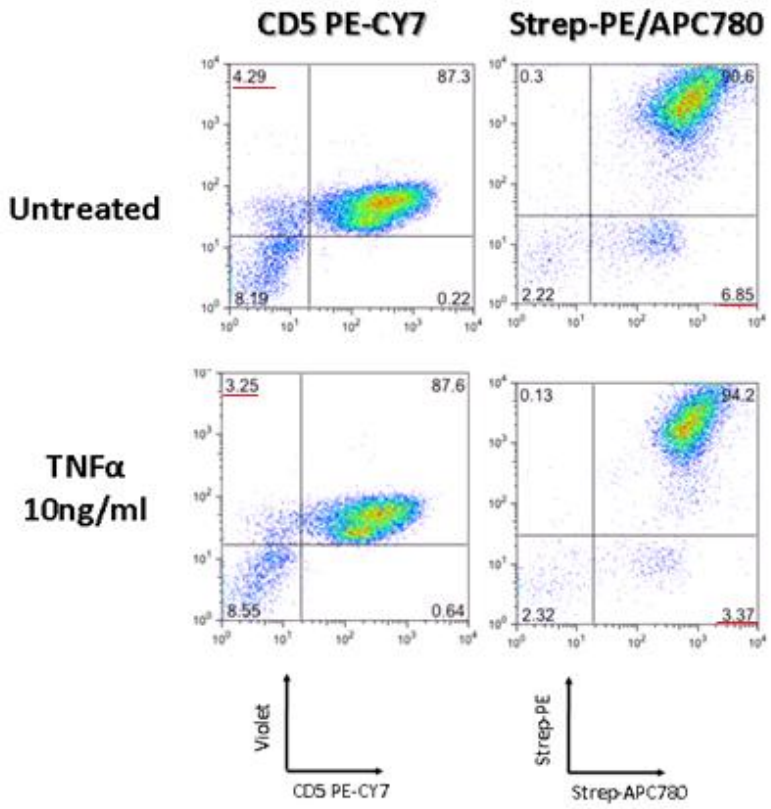

Figure 17 – ***Dot plots comparing %T-cell release from HepG2-CD81s in treated and untreated co-cultures, using anti-CD5 PE-CY7 and streptavidin-PE as masking antibodies. Values underlined in red demonstrate the percentage of violet $CD4^+$T-cells released from HepG2-CD81s. T-cells were stained violet and half were biotinylated prior to co-culture on Day 5. The streptavidin-PE was then added as the masking antibody in co-cultures containing biotinylated T-cells on Day 6. Streptavidin-APC780 acted as the control to prove complete T-cell biotinylation, and was added to the co-culture on Day 7 for 30 minutes prior to harvesting. Anti-CD5 was used to mask un-biotinylated violet T-cells from the release assay as Figure 6 states. Results were collected on Day 7 via flow cytometry. Violet +ve, CD5 –ve populations represent released T-cells in anti-CD5 masked assays. Strep-APC +ve, strep-PE –ve populations represent released T-cells in strep-PE masked assays.***

Figure 17 shows that where anti-CD5 is used as a masking antibody, the %T-cell release is similar in treated and untreated co-cultures. This result is repeated where streptavidin-PE is used as a masking antibody, as the %T-cell release is similar between treated and untreated co-cultures.

The similar T-cell release measured by both strep-PE and anti-CD5 PE-CY7, provides confirmation that anti-CD5 is a suitable to use as a masking antibody during subsequent release assays.

3.2.7. Percentage release of violet $CD4^+$T-cells from Huh-7s is not stimuli dependant

After optimising the release protocol, the effects of stimuli on T-cell release was investigated in another hepatoma cell line. Huh-7 cells from a confluent monolayer and are different from HepG2-CD81 cells because they do not polarise in culture. The effects of pro-inflammatory, anti-inflammatory and hypoxia treatment on the percentage T-cell release from Huh-7s were tested (Figure 18 and 19).

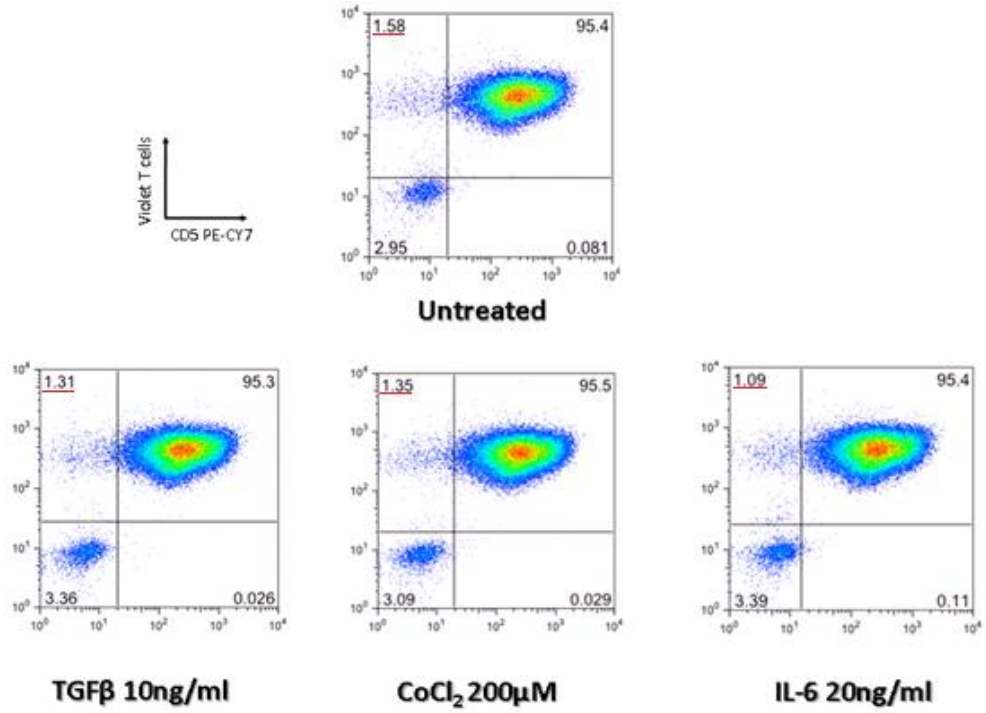

Figure 18 – ***Dot plots to demonstrate the % release of violet T-cells from Huh-7s 3 hours following incubation with treatments (in opposed to 24 hours). Here the T-cells were masked with anti-CD5 PE-CY7, treated and harvested on Day 6. Here anti-inflammatory (TGF), pro-inflammatory (IL-6) and hypoxic conditions (CoCl2) were tested. The anti-CD5 negative, violet positive population represents %released T-cells underlined in red.***

Figure 18 shows that the percentages of released T-cells are similar both between the treatments and in comparison to the control. This implies that the release of $CD4^{+}$T-cells from Huh-7s is not stimuli dependant.

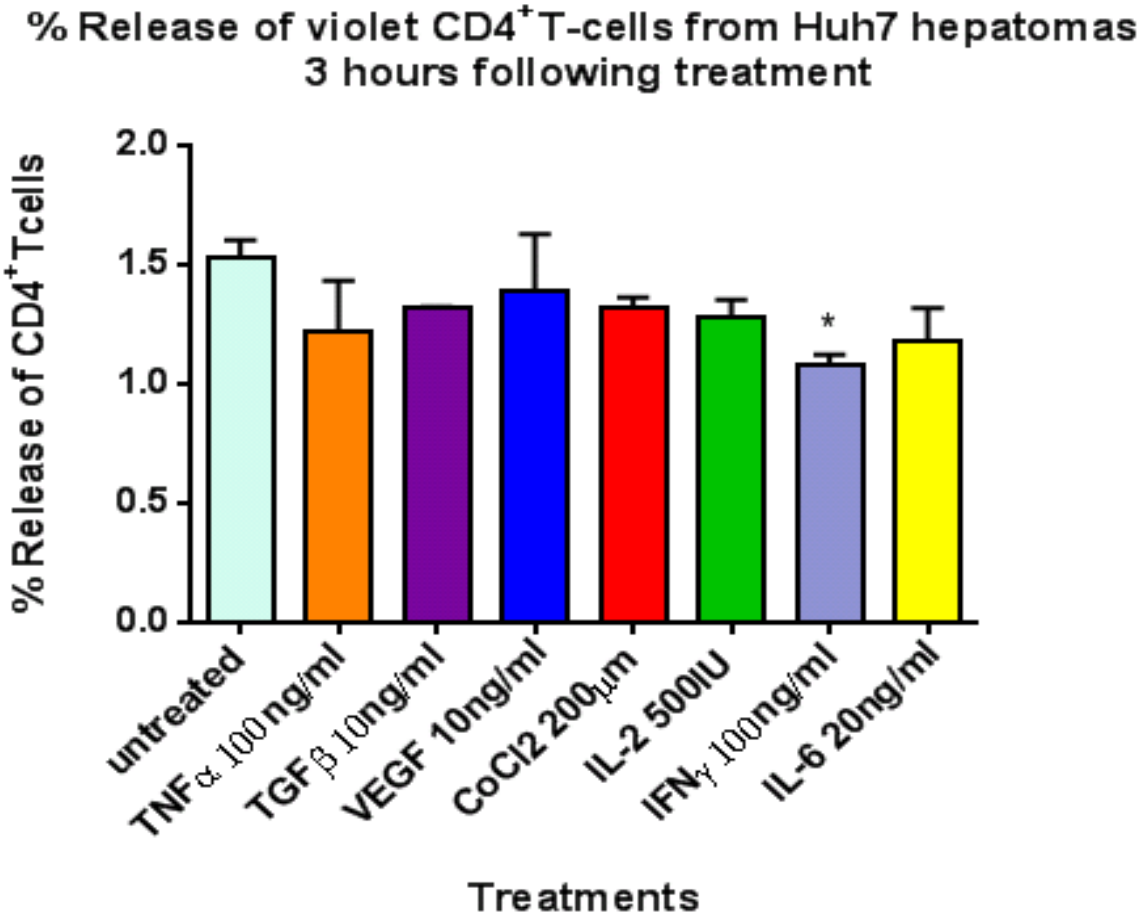

Figure 19 - ***Bar graph (n=2) Demonstrating the effects of 3 hour treatments on percentage T-cell release from Huh-7s.Co-cultures were masked with anti-CD5 and treatments were incubated with co-cultures for 3 hours before harvesting and flow analysis (All on Day 6). Here anti-inflammatory (TGFβ), pro-inflammatory (IL-6, TNFα, IFNɣ, IL-2), growth factors (VEGF) and hypoxic conditions (CoCl2) were added as treatments in release assays. Bars represent S.E.M. Results which are significantly lower compared to the untreated co-culture are presented by a * where p<0.05. To calculate statistical significant data a paired T-test was performed.***

Figure 19 shows that pro and anti-inflammatory cytokines, growth factors and hypoxic conditions mostly induce a similar %T-cell release from 3 hour Huh-7 co-cultures. However, the % T-cell release is significantly lower with IFNɣ treatment compared to that of untreated controls. Collectively this data implies that IFNɣ may have an effect on %T-cell release from Huh-7s.

3.2.8. 2 hour incubations with treatments results in significantly increased %T-cell release from HepG2-CD81s compared to 24 hour incubations

To determine whether treatment incubation times influenced %T-cell release in release assays, an experiment was conducted using 2 and 24 hour incubations in the presence of IFNɣ (Figure 20).

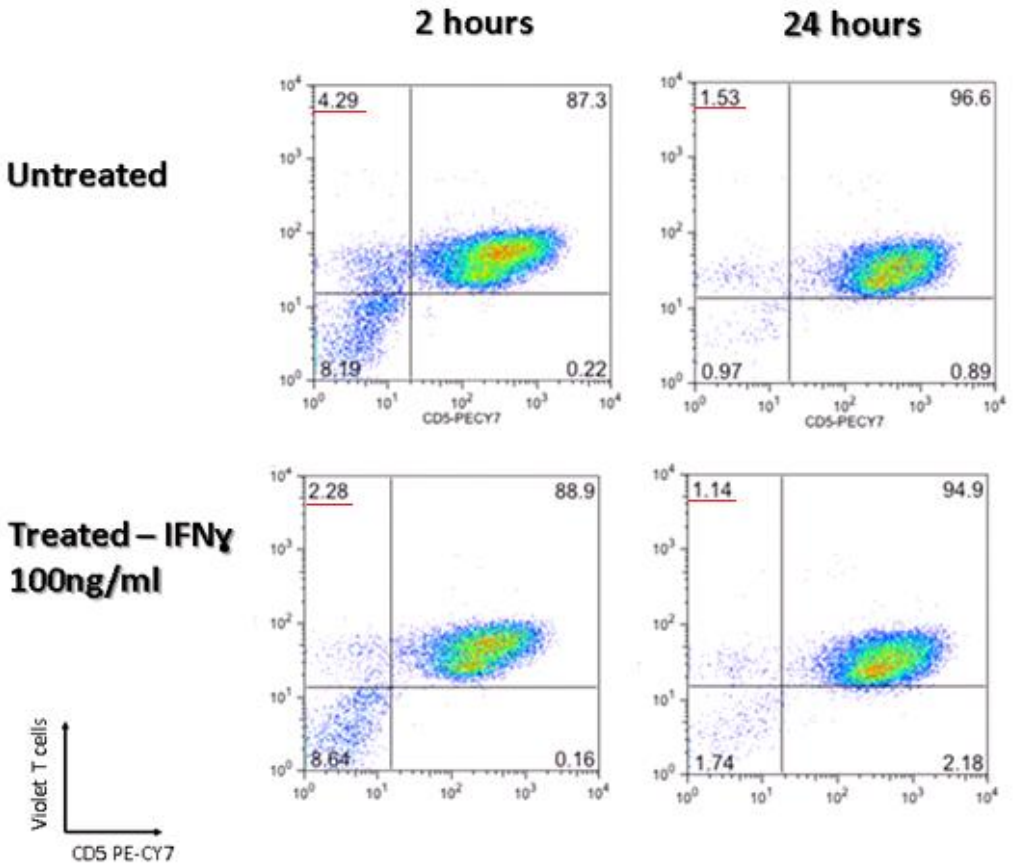

Figure 20 – ***Dot plots demonstrating the effects of incubation time and cytokine treatment (IFNɣ 100ng/ml) on T-cell release from HepG2-CD81 hepatomas. The anti-CD5 PE-CY7 negative, violet positive populations represent the % of released T-cells, where the values are underlined in red. Here the non-internalised T-cells were masked with anti-CD5 before being treated with IFNɣ on Day 6. Co-cultures were harvested for flow analysis at 2 hours and 24 hours (Day 6 and 7 respectively).***

Figure 20 shows that the %T-cell release is greater in treated and untreated co-cultures at 2 hours compared to 24 hours. The results show that IFNɣ treatment induced lower %T-cell release from HepG2-CD81s at 2 hours compared to untreated controls. This reinforces the possibility that IFNɣ may be involved in preventing T-cell release following entosis.

An experiment was performed to determine whether incubation times (2h and 24h) in the presence of other stimuli influenced %T-cell release in release assays (Figure 21).

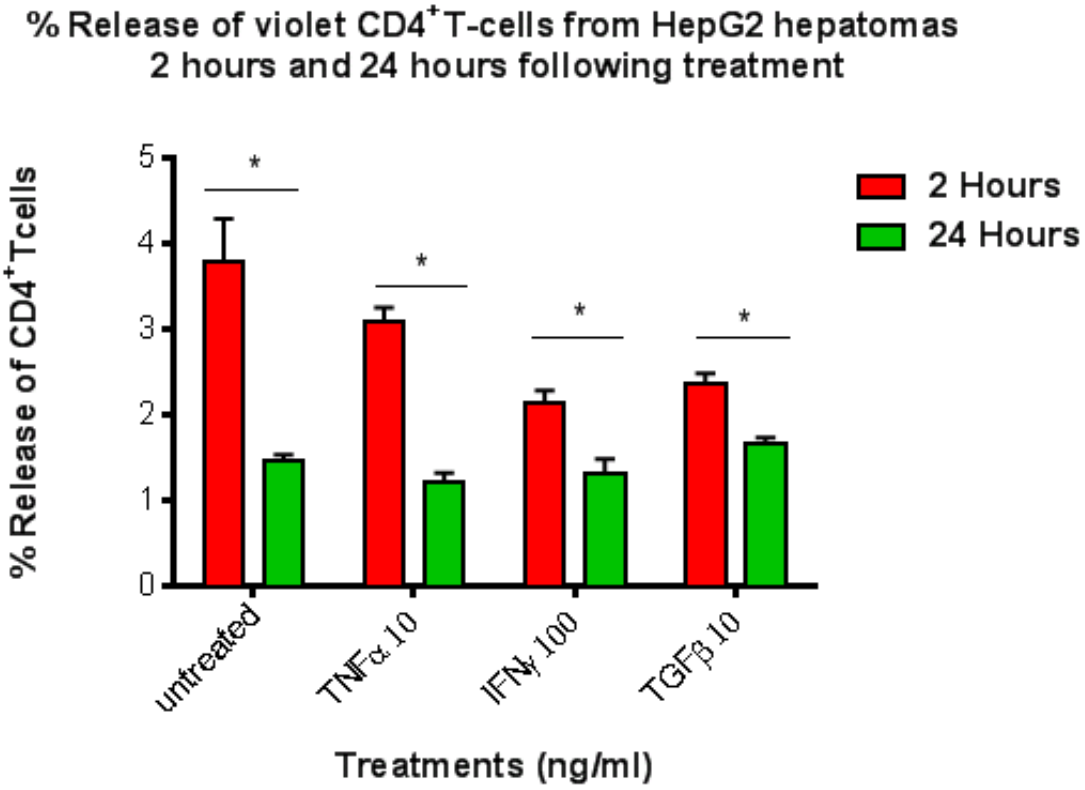

Figure 21– ***Bar graph (n=2) demonstrating the effects of 2 hour and 24 hour treatment incubation times on percentage T-cell release from HepG2-CD81 cells. Non-internalised T-cells were masked with anti-CD5 before being treated with various stimuli and harvested for flow analysis at 2 hours and 24 hours (Day 6 and 7) respectively. Here pro-inflammatory (TNFα, IFNɣ) and anti-inflammatory cytokines (TGFβ) were used as treatments. Error bars represent the S.E.M. Statistically significant results are presented by a * where p<0.05. To calculate statistical significances within the data a paired T-test was performed.***

Figure 21 demonstrates that the percentage release of T-cells is significantly greater at 2 hours compared to 24 hours in the untreated and treated co-cultures.

These results indicate that T-cell release is time dependant rather than stimuli dependant.

3.2.9. There is no significant change in %T-cell release from Huh-7 cells with 2 hour treatment incubations compared to 24 hour treatment incubations

The same experiment was repeated to assess whether 2 hour and 24 hour incubations had an effect on release assays involving Huh-7s. It is also possible that T-cell release from hepatomas is induced by a combination of treatments in opposed to a single stimulus. Therefore some treatments in this experiment were used in combination to test their effects on %T-cell release (Figure 22).

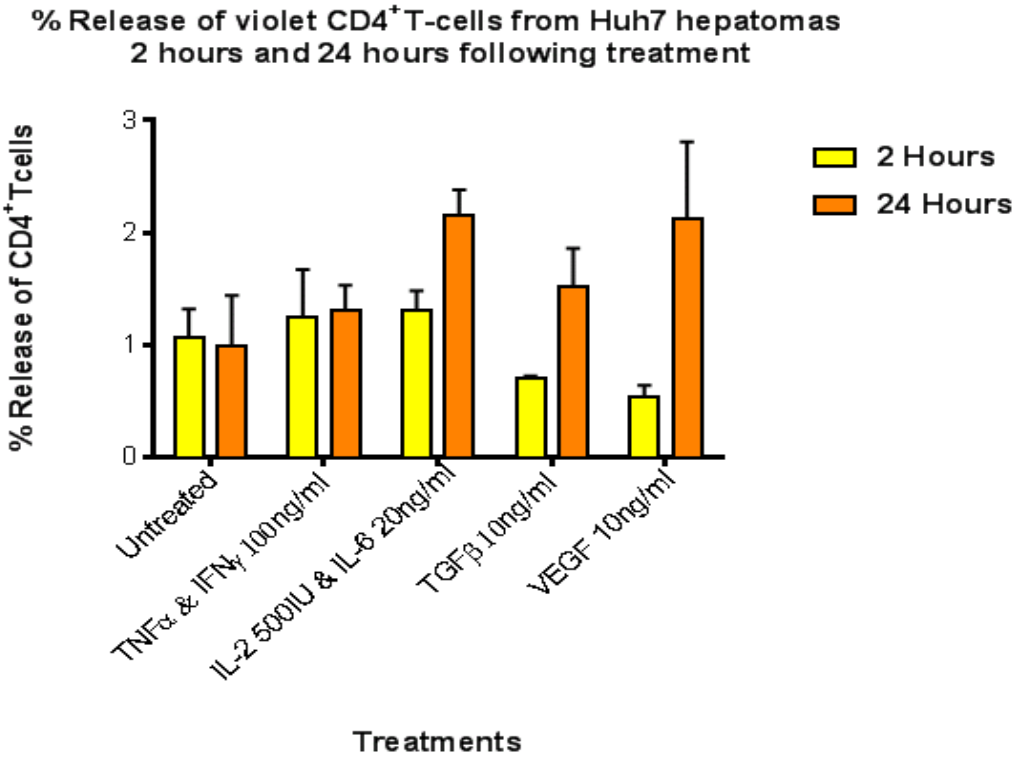

Figure 22 - ***Bar graph (n=2) demonstrating the effects of 2 hour and 24 hour treatment incubation times on percentage T-cell release from Huh-7 cells. Non-internalised T-cells were masked with anti-CD5 on Day 6 before being treated with various stimuli and harvested for flow analysis at 2 hours and 24 hours (Day 6 and 7) respectively. Here pro-inflammatory cytokines were used in combination (TNFα, IFNɣ and IL-2,IL-6). Anti-inflammatory cytokines (TGFβ) and growth factors (VEGF) were also used as treatments. Error bars represent the S.E.M.***

Figure 22 shows that none of the treated co-cultures show a significantly different %T-cell release compared to untreated co-cultures. There is also no significant difference in %T-cell release between 2-hour and 24-hour treated co-cultures.

This shows that the higher T-cell released observed at 2 hours in the previous experiment may be HepG2-CD81 specific.

3.3. Lymphocyte-hepatocyte interactions

3.3.1. Co-culture of hepatocytes with T-cells causes downregulation of CD2 on CD4^{+}T-cells

When screening for optimal masking antigens for our release assay, we discovered that CD2 becomes downregulated upon co-culture with hepatomas. To investigate this further we did a time course experiment in the presence or absence of IL-2 and IL-6. These cytokines were used to mimic a liver inflammatory response *in vitro(8)*.

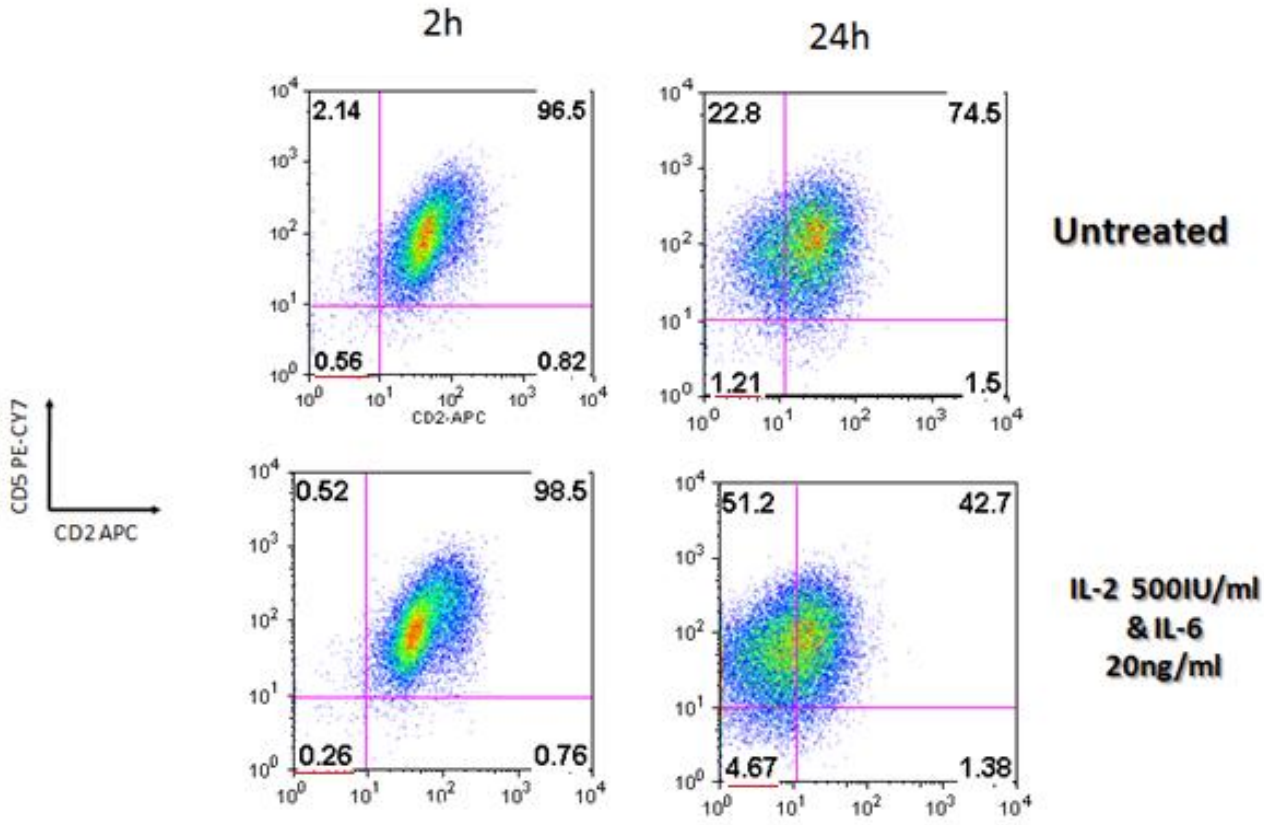

Figure 22- ***Dot plots demonstrating violet T-cell release from Huh-7 cells, 2 and 24 hours following incubation with IL-2 and IL-6. Both anti-CD2 APC and anti-CD5 PE-CY7 are used as masking antibodies at Day 6 and released T-cells are demonstrated as negative for both anti-CD2 and anti-CD5 (values underlined in red). Co-cultures were then harvested for flow analysis on Day 6 and 7 after 2 and 24 hour treatments respectively.***

Figure 22 shows that in the presence of co-culture with Huh-7 hepatomas, CD2 on T-cells is down-regulated, which is demonstrated by the shift in T-cell population to the left in the untreated samples at 24 hours. This downregulation of CD2 on T-cells increases in the presence of the pro-inflammatory cytokines IL-6 and IL-2, 24 hours following stimulation.

This shows that the pro-inflammatory cytokines IL-2 and IL-6 may influence CD2 surface expression on $CD4^{+}$T-cells.

4. Discussion

From these experiments, a well-defined release assay has been established to accurately measure T-cell release from HepG2-CD81s and Huh-7 cell lines. However, there is no strong evidence to suggest that pro-inflammatory cytokines (TNFα, IL-6, IL-2, IFNɤ), anti-inflammatory cytokines (TGF-β), growth factors (VEGF) or hypoxic conditions (CoCl2) significantly increase or reduce the release of T-cells from hepatomas following entosis.

The HepG2-CD81 hepatocellular carcinoma cell line used in parts of this study presents epithelial cell morphology. They were used in this *in vitro* study due to their ability to polarise and form apical and basolateral surface domains, which resemble the bile canalicular and sinusoidal domains observed *in vivo* within polarized human hepatocytes.

4.1. The effects of TNFα on T-cell release from HepG2-CD81 hepatomas

TNF-α was used to treat the T-cell-HepG2-CD81 co-culture, in order to mimic pro-inflammatory conditions in the liver.

Preliminary data (Figure 10) showed that TNFα treatment may be promoting T-cell release following entosis using an assay based on identifying released cells by lack of anti-CD3 antibody access (see section 2.1.). A potential interpretation for the increase in the CD3 –ve population in the cytokine treated co-culture is the downregulation of CD3 by the T-cells. To investigate this, I used anti-CD4 in this assay and found that CD4 indeed becomes downregulated, but not completely undetectable from the T-cell surface by flow cytometry like CD3. This 'loss' of anti-CD3 mAb makes it difficult to distinguish between released and non-released T-cell populations, therefore affecting accurate positioning of the 'released T-cell gate'. This partly eliminated the previous problem, however showed that there was now no significant increase in T-cell release from HepG2-CD81s following treatment with TNFα (100ng/ml), but increased T-cell proliferation. To rule out the effect of TNFα on T-cell proliferation, cells were labelled with CellTrace violet. This reagent confers violet fluorescence that reduces by half after each cell division. This way we could monitor if a treatment truly increases T-cell release or causes existing T-cell proliferation.

4.2. The effects of TNFα doses +/- inhibitor on T-cell release from HepG2-CD81 hepatomas

Results from Figures 11 and 12 implied that %T-cell release is not dependant on the dosage of TNFα as there is no correlation between TNFα dosages and T-cell release.

Previous work demonstrated that under certain circumstances, hepatocytes are able to produce TNFα(9).The absence of correlation between TNFα doses and T-cell release could be because the hepatomas themselves are producing TNFα, therefore inducing large amounts of T-cell release and eliminating the effects of TNFα dose responses on T-cell release. This may explain why the overall %T-cell release in the treated and control groups are low (Figures 11 and 12).

The overall %T-cell release was similar in the TNFα treated groups compared to those with TNFα +inhibitor, suggesting that the inhibitor was ineffective at blocking TNF-induced release. If the hepatomas themselves are producing TNFα, it may be that that the concentration of inhibitor was not high enough to saturate the amount of TNFα present.

Further results show that TNFα +inhibitor affected the granularity and morphology of the HepG2-CD81s (Figure 13). This may be because in the presence of TNFα alone the HepG2-CD81s become depolarised and therefore have a different shape and size compared to in the presence of the inhibitor, where the majority of TNFα is blocked.

4.3. Establishing a masking antibody for non-internalised violet T-cells

The downregulation of CD3 and CD4 described in 4.1, led to an investigation to find a suitable masking antibody that would target an antigen on T-cells which was not downregulated. Anti-CD5 PE-CY7 was identified as the most suitable masking antibody from an antibody panel which were tested in release assays (Figure 14). This is because this anti-CD5 did not lose fluorescence during co-culture and CD5 was not downregulated on T-cells throughout the assay.

As the efficiency of streptavidin-PE was already confirmed as a masking antibody for biotinylated T-cells (Figure 15 and 16), this protocol was used in parallel to anti-CD5, to confirm its masking efficiency. Figure 17 demonstrates that anti-CD5 PE-Cy7 is efficient at masking $CD4^{+}$T-cells as the percentage release of T-cells from HepG2-CD81s in these experiments match those where Strep-PE is used for masking. As a result the following experiments used anti-CD5 PE-CY7 as a masking antibody for non-internalised T-cells.

4.4. The effects of time on T-cell release from HepG2-CD81 and Huh-7 hepatomas

Results show that T-cell release was significantly greater at 2 hours compared to 24 hours in untreated and treated co-cultures involving HepG2-CD81 hepatomas (Figure 21). When the assay was repeated in Huh-7s, no significant differences were found. It is possible that entosis and T-cell release occurs in a continuous cycle. This cycle may occur at a slower rate in HepG2-CD81 co-cultures due to the HepG2 polarised cluster morphology, which restricts T-cell access to these hepatomas. As T-cells have easier access to the confluent Huh-7 monolayers, they may be undergoing constant entosis and release, which explains why a significant difference in %T-cell release is not present between 2 hour and 24 hours incubations (Figure 22).

4.5. The effects of stimuli on T-cell release from Huh-7 hepatomas

One experiment involved a three hour treatment of Huh-7-T-cell co-cultures with pro-inflammatory and anti-inflammatory cytokines, growth factors and hypoxic conditions (Figure 19). These results showed that most treatments had no significant effect on T-cell release compared to the untreated control.

However, IFNɣ treatment significantly reduced %T-cell release from Huh-7s in comparison to untreated controls. Previous work demonstrates that IFNɣ has a role in stimulating hepatic inflammation and aggravating liver damage(28). Furthermore, hepatocyte entry and degradation of self-reactive $CD8^+$T-cells recently demonstrated a novel tolerogenic mechanism within the liver(27). This decrease in T-cell release

may represent another form of tolerance whereby T-cells 'hide' in hepatocytes in order to avoid exacerbating the inflammatory response induced by IFNɣ.

4.6. CD2 downregulation on $CD4^+$T-cells in hepatoma co-cultures

Results from Figure 22 show that CD2 surface expression on T-cells is lost significantly during co-culture. This effect increases in the presence of pro-inflammatory cytokine IL-6. Both these antibodies were used at saturating concentrations pre-determined by titration, which suggests that CD2 expression is being down-regulated or lost in the presence of co-cultures with hepatoma cell lines.

The reduced expression of CD2 on $CD4^+$T-cells in the presence of hepatomas could be a response to cytokines secreted by the hepatomas (HepG2-CD81s/Huh-7s). Hepatocytes are known to produce IL-6 and TNFα(8, 13). These inflammatory cytokines may be responsible for inducing CD2 downregulation on T-cells.

CD2 has been implicated in the induction of T-cell anergy(29, 30), where previous experiments show that down-modulation of CD2 on T-cells can result in reduced proliferation and IL-2 production(29). Re-expression of CD2 can then restore these functions(29, 30). The inflammatory conditions may be inducing anergy in the $CD4^+$T-cells, therefore increasing CD2 downregulation on T-cells and reducing their IL-2 production. This describes a possible tolerogenic mechanism for T-cells in the liver, where further inflammation is prevented.

CD2 is also required for T-cell adhesion to APCs via the cell adhesion molecules CD58 (LFA-3) and CD59(29, 31). If T-cells are unable to bind to other cells it makes them more difficult to activate which again explains CD2-downregulation as a tolerogenic function of T-cells in the presence of inflammation.

4.7. Future work

This work has optimised a flow cytometry based assay for the detection of T cells released by hepatomas *in vitro*. Expansion of this study would lead to greater confidence in the results obtained from this experiment and would provide a clearer understanding towards the reasons for T-cell entosis and release from hepatocytes.

The data in the experiment was collected using flow cytometry. It would be beneficial however, to confirm these results using a different method. To do this one could to set up an overnight experiment to visualise the release of violet $CD4^+$Tcells from green hepatomas using a Zen confocal microscope. The effect of treatment can then be recorded visually and a Z-stack can confirm internalisation of the T-cells within the hepatomas.

Hepatoma cells are cancer derived and so may differ from the *in vivo* situation in important aspects. Recent studies show that many proteins are down-regulated in hepatoma cell lines compared to primary hepatocytes(14). In order to be able to translate this T-cell entosis model to an *in vivo* situation, the release assay should be repeated using primary hepatocytes.

The results from this study show that cytokines, growth factors and hypoxic conditions do not significantly affect the percentage release of $CD4^+$T-cells from hepatoma cell lines. It may be that another factor induces increased release of T-cells such as a viral infection. Further release assays could be repeated on co-cultures infected with a viral infection, which could mimic hepatitis based model. It is also possible T-cell release responses to stimuli were not observed because they require a specific environment requiring a combination of stimuli rather than a single stimulus alone. It is possible that percentage T-cell release from hepatomas may

differ to controls when stimuli are used in combinations with each other, which could also be used to closely mimic various *in vivo* situations.

Lastly, future experiments would measure the % of entosis prior to measuring the %T-cell release so that all experiments can be made relative and comparable to each other. From this study the % of T-c0ells internalised via entosis is unknown. If the numbers of entosis events are low at the beginning of the assay, it may explain why %T-cell release has also been low throughout the study.

4.8. Conclusion

In conclusion, this study has optimised a protocol to quantify the percentage of $CD4^+$T-cell release from hepatomas following entosis, however further work is required to fully investigate the causes of entosis and $CD4^+$T-cell release from hepatocytes. Although most treatments did not significantly affect the percentage release of T-cells from hepatomas, shorter incubation times with stimuli showed a larger % of T-cell release from HepG2-CD81s compared to 24 hour treatments, demonstrating how the organisation of hepatomas may influence the speed and frequency at which entosis and release occurs. Understanding the reasons for entosis and release of $CD4^+$T-cells is important; so that the T-cells may be manipulated therapeutically to function against the development of infections and diseases in the liver such as HCV.

5. References

1. Crispe IN. Hepatic T cells and liver tolerance. Nat Rev Immunol. 3. England2003. p. 51-62.

2. Ishibashi H, Nakamura M, Komori A, Migita K, Shimoda S. Liver architecture, cell function, and disease. Semin Immunopathol. 2009;31(3):399-409.

3. Hsu W, Shu S, Gershwin E, Lian Z. The current immune function of hepatic dendritic cells. Cellular & Molecular Immunology. 2007;4(5):321-8.

4. Katz SC, Pillarisetty VG, Bleier JI, Kingham TP, Chaudhry UI, Shah AB, et al. Conventional liver CD4 T cells are functionally distinct and suppressed by environmental factors. Hepatology. 2005;42(2):293-300.

5. Lau A, de Creus A, Lu L, Thomson A. Liver tolerance mediated by antigen presenting cells: fact or fiction? Gut. 2003;52(8):1075-8.

6. Kruse N, Neumann K, Schrage A, Derkow K, Schott E, Erben U, et al. Priming of CD4+ T cells by liver sinusoidal endothelial cells induces CD25low forkhead box protein 3- regulatory T cells suppressing autoimmune hepatitis. Hepatology. 2009;50(6):1904-13.

7. PHAM B, MOSNIER J, WALKER F, NJAPOUM C, BOUGY F, DEGOTT C, et al. FLOW-CYTOMETRY CD4+/CD8+ RATIO OF LIVER-DERIVED LYMPHOCYTES CORRELATES WITH VIRAL REPLICATION IN CHRONIC HEPATITIS-B. Clinical and Experimental Immunology. 1994;97(3):403-10.

8. Tilg H. Cytokines and liver diseases. Canadian Journal of Gastroenterology. 2001;15(10):661-8.

9. Takano M, Sugano N, Mochizuki S, Koshi R, Narukawa T, Sawamoto Y, et al. Hepatocytes produce tumor necrosis factor-alpha and interleukin-6 in response to Porphyromonas gingivalis. Journal of Periodontal Research. 2012;47(1):89-94.

10. Braunersreuther V, Viviani G, Mach F, Montecucco F. Role of cytokines and chemokines in non-alcoholic fatty liver disease. World Journal of Gastroenterology. 2012;18(8):727-35.

11. Schwabe R, Brenner D. Mechanisms of liver injury. I. TNF-alpha-induced liver injury: role of IKK, JNK, and ROS pathways. American Journal of Physiology-Gastrointestinal and Liver Physiology. 2006;290(4):G583-G9.

12. Snyers L, De Wit L, Content J. Glucocorticoid up-regulation of high-affinity interleukin 6 receptors on human epithelial cells. Proc Natl Acad Sci U S A. 1990;87(7):2838-42.

13. Fischer CP, Bode BP, Takahashi K, Tanabe KK, Souba WW. Glucocorticoid-dependent induction of interleukin-6 receptor expression in human hepatocytes facilitates interleukin-6 stimulation of amino acid transport. Ann Surg. 1996;223(5):610-8; discussion 8-9.

14. Pan C, Kumar C, Bohl S, Klingmueller U, Mann M. Comparative Proteomic Phenotyping of Cell Lines and Primary Cells to Assess Preservation of Cell Type-specific Functions. Molecular & Cellular Proteomics. 2009;8(3):443-50.

15. Shi F, Ljunggren H, La Cava A, Van Kaer L. Organ-specific features of natural killer cells. Nature Reviews Immunology. 2011;11(10):658-71.

16. Overholtzer M, Brugge J. The cell biology of cell-in-cell structures. Nature Reviews Molecular Cell Biology. 2008;9(10):796-809.

17. Overholtzer M, Mailleux AA, Mouneimne G, Normand G, Schnitt SJ, King RW, et al. A nonapoptotic cell death process, entosis, that occurs by cell-in-cell invasion. Cell. 2007;131(5):966-79.

18. White E. Entosis: it's a cell-eat-cell world. Cell. 2007;131(5):840-2.

19. Caruso RA, Fedele F, Finocchiaro G, Arena G, Venuti A. Neutrophil-tumor cell phagocytosis (cannibalism) in human tumors: an update and literature review. Exp Oncol. 2012;34(3):306-11.

20. Yang Y, Li J. Progress of Research in Cell-in-Cell Phenomena. Anatomical Record-Advances in Integrative Anatomy and Evolutionary Biology. 2012;295(3):372-7.

21. Qian Y, Shi Y. Natural killer cells go inside: Entosis versus cannibalism. Cell Research. 2009;19(12):1320-1.

22. SHAMOTO M. EMPERIPOLESIS OF HEMATOPOIETIC-CELLS IN MYELOCYTIC-LEUKEMIA - ELECTRON-MICROSCOPIC AND PHASE-CONTRAST MICROSCOPIC STUDIES. Virchows Archiv B-Cell Pathology Including Molecular Pathology. 1981;35(3):283-90.

23. Boll I, Domeyer C, Buhrer C. Human megakaryoblastic proliferation and differentiation events observed by phase-contrast cinematography. Acta Haematologica. 1997;97(3):144-52.

24. Fais S. Cannibalism: A way to feed on metastatic tumors. Cancer Letters. 2007;258(2):155-64.

25. SANDILANDS G, REID F, GRAY K, ANDERSON J. LYMPHOCYTE EMPERIPOLESIS REVISITED .1. DEVELOPMENT OF INVITRO ASSAY AND PRELIMINARY CHARACTERIZATION OF LYMPHOCYTE SUB-POPULATION INVOLVED. Immunology. 1978;35(2):381-9.

26. REID F, SANDILANDS G, GRAY K, ANDERSON J. LYMPHOCYTE EMPERIPOLESIS REVISITED .2. FURTHER CHARACTERIZATION OF THE LYMPHOCYTE SUB-POPULATION INVOLVED. Immunology. 1979;36(2):367-72.

27. Benseler V, Warren A, Vo M, Holz LE, Tay SS, Le Couteur DG, et al. Hepatocyte entry leads to degradation of autoreactive CD8 T cells. Proc Natl Acad Sci U S A. 108. United States2011. p. 16735-40.

28. Knight B, Lim R, Yeoh G, Olynyk J. Interferon-gamma exacerbates liver damage, the hepatic progenitor cell response and fibrosis in a mouse model of chronic liver injury. Journal of Hepatology. 2007;47(6):826-33.

29. Bachmann M, Barner M, Kopf M. CD2 sets quantitative thresholds in T cell activation. Journal of Experimental Medicine. 1999;190(10):1383-91.

30. Fortner K, Russell J, Budd R. Down-modulation of CD2 delays deletion of superantigen-responsive T cells. European Journal of Immunology. 1998;28(1):70-9.

31. KORETZ K, BRUDERLEIN S, HENNE C, MOLLER P. EXPRESSION OF CD59, A COMPLEMENT REGULATOR PROTEIN AND A 2ND LIGAND OF THE CD2 MOLECULE, AND CD46 IN NORMAL AND NEOPLASTIC COLORECTAL EPITHELIUM. British Journal of Cancer. 1993;68(5):926-31.

THE EXPRESSION OF E3 UBIQUITIN LIGASES IN T-CELLS

UNIVERSITY OF BIRMINGHAM

By Sudha Purswani

This project is submitted in partial fulfilment of the requirements for the award of the MRes

College of Medical & Dental Sciences
Department of Infection and Immunity
University of Birmingham
May 2013

Abstract

E3 ubiquitin ligases have been identified as key regulators of the immune system. They function in T-cell tolerance by targeting molecules for degradation, thereby affecting T-cell signalling and activation. By understanding the role of E3 ubiquitin ligases in different T-cell subsets, we may be able to manipulate them therapeutically to stop or promote T-cell activation, thereby preventing development of autoimmune diseases and cancer respectively.

This study induces anergy in human $CD4^+$T-cells through plate-bound anti-CD3 antibody stimulation. Anergy in anti-CD3 stimulated cells was determined by quantifying the number of proliferating T-cells by flow cytometry following a secondary anti-CD3.28 stimulus. Quantitative RT-PCR was also used to establish differences in E3 ubiquitin ligase expression between T-cell subsets. Results showed some induction of anergy in anti-CD3 stimulated T-cells.

When comparing E3 ubiquitin ligase expression between different T-cell subsets, many of the genes were not detectable. This may be due to large amounts of cell death during assays resulting in low cDNA recovery and insufficient material to detect gene expression. This study concludes that further work is required to confirm the anergic state of the T-cells. Furthermore, in order to accurately compare E3 ligase expression between T-cell subsets, RT-PCR needs to be repeated using more material.

Acknowledgements

I would like to thank John Curnow for all his support and guidance. I would also like to thanks Siobhan Restorick and Lindsay Durant for all their time and help in the lab.

3 Contents

List of illustrations

List of Tables

1. Introduction

1.1. The role of T-cells in tolerance and autoimmunity

Immunological self tolerance occurs when the body's immune system prevents mounting an immune response to self antigens. $CD4^+$T-cells are able to mount strong immune responses to foreign antigens and are mostly unresponsive to self antigens(1). Many autoimmune diseases occur due to a breakdown of tolerance within the $CD4^+$T-cell population(2). Two types of T-cell tolerance exist: central tolerance (induced in the thymus) and peripheral tolerance (induced in the secondary lymphoid and peripheral tissues)(2, 3).

1.1.1. Central Tolerance and nTregs

Central tolerance occurs largely throughout fetal life, and involves the deletion of T-cells which bind self-antigen with high affinity(1). Deletion occurs prior to T-cell maturation, preventing self-reactive T-cells from leaving the thymus and causing autoimmunity(1, 4).

Self-antigens are processed and presented by thymic antigen presenting cells (APCs) in association with self-MHC (Major Histocompatibility Complexes)(1, 4, 5). First, T-cells in the thymus undergo positive selection where the T-cell receptors (TCR) bind to self-MHC molecules with sufficient affinity. They are then selected to develop into a single positive $CD4^+CD8^-$ or $CD4^-CD8^+$ thymocytes(1, 5). T-cells which do not show sufficient affinity to self-antigens are deleted via 'death by neglect'(1, 4, 5). Negative selection occurs next whereby T-cells with a high affinity for self-MHC molecules undergo apoptotic cell death(1, 4, 5), preventing dangerous self-reacting

T-cells from escaping into the periphery and causing damage. The thymic selection process is illustrated by Figure 1.

Figure 1 – ***Central tolerance in the thymus. (A) Death by neglect - double positive T-cell does not recognise APC and MHC-self-peptide complex. This causes apoptosis. (B) Positive selection - low-affinity interactions between the thymocyte and peptide-MHC complex leads to development of a single positive T-cell which escapes to the periphery. (C) Negative selection - Strong binding between the thymocyte and MHC-peptide complex leads to apoptosis. This prevents self reactive T-cells from becoming single positives and escaping into the periphery to cause host damage. (5)***

Impaired development and function of naturally arising $CD4^+CD25^+$ Treg cells (nTregs), has been associated with several autoimmune diseases(6). nTregs arise from T-cell progenitors in the bone marrow and develop in the thymus. Here they are positively selected on an intermediate TCR-affinity strength which lies between that required for the positive and negative selection for conventional T-cells(7, 8). nTregs then migrate into the periphery where they contribute to 5-10% of the mature peripheral $CD4^+$T-cell population(8). They are characterised by their expression of the transcription factor forkhead box p3 (Foxp3). The survival of nTregs in the periphery is dependent on exogenously produced IL-2(9), whereas their function depends on the production of cytokines such as IL-10, IL-35 and TGFβ, which exert suppressive effects on conventional T-cells(4).

1.1.2. Mechanisms of Peripheral tolerance

Not all self-antigens are expressed in the thymus during lymphocyte development, allowing some self-reactive lymphocytes to escape into the periphery(4). This highlights the importance of peripheral tolerance; when lymphocytes first encounter self-antigens outside the thymus (e.g. food antigens)(4). Peripheral tolerance processes involve deletion or hyporesponsiveness of self-reactive T-cells, which meet self-antigens outside the thymus(4, 10). It includes the action of regulatory T-cells, deletion of self-reactive T-cells, anergy and immune ignorance(1, 4).

1.1.2.1. Immune Ignorance

Immune ignorance describes the process when self-reactive T-cells fail to react to their autoantigen(4).This occurs when antigens are present at low concentrations, therefore are incapable of overcoming the lymphocyte-receptor threshold to trigger a response(11). Furthermore, some self-antigens are present in immune-privileged sites. These Immune-privileged sites describe locations which are tolerant to the presence of antigens without responding with a potentially damaging inflammatory response(4, 11). Immune-privileged sites include the brain, the testes and the eye(4).

1.1.2.2. $CD4^+CD25^+$T-cells (iTreg Cells)

ITreg $CD4^+CD25^+$ cells (inducible regulatory T-cells) are distinct from nTregs and form in the presence of chronic inflammation and disease(12). They mature from naïve $CD4^+$T-cells in the periphery in response to TGFβ, where they acquire the expression of CTLA4 and CD25 markers, and upregulate the transcription factor FOXP3(12). Like nTregs, iTregs are involved in tolerance to self-antigen and suppression of the immune system(7). More specifically, they suppress T-cell proliferation and autoimmune reactions through IL-10 and TGFβ production, causing apoptosis of effector T-cells and blocking co-stimulation and maturation of dendritic cells(13). The development and action of Tregs are presented in Figure 2.

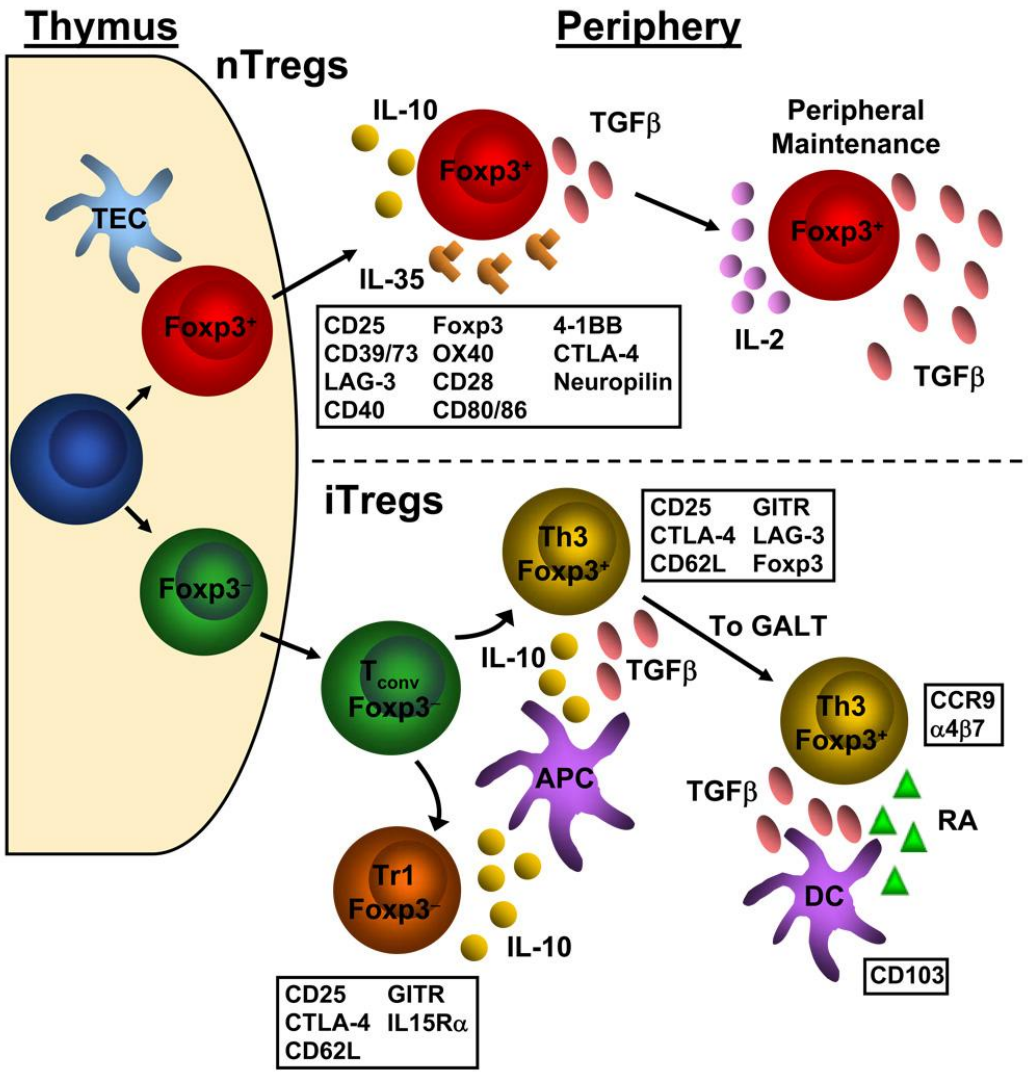

Figure 2 - ***(8) nTregs (top) differ from naïve conventional T-cells in the thymus. The cell surface markers expressed by nTregs are indicated in the top box however none of these markers are solely expressed by Tregs and can also be located on activated conventional T-cells. iTregs (bottom) can develop from T-cell precursors in the periphery in the presence of IL-10 and TGFβ secreted from APCs (DCs and macrophages). iT-regs share similar surface markers to nTregs, and can be induced to form Foxp3$^-$ Tr1 cells or Foxp3$^+$ Th3 cells.***

$CD4^+Foxp3^+$ Treg cells differ from $CD4^+Foxp3^-$ conventional $CD4^+$T-cells. The conventional T-cell population is diverse and consists of subpopulations characterised according to cytokine production(14). They include the populations Th1, Th2 and Th17, wherein central memory and effector memory subpopulations exist(15).

1.1.2.3. Anergic T-cells

1.1.2.3.1. $CD4^+$T-cell activation

Two signals are required for $CD4^+$T-cell activation and the mounting of an effective immune response. An example of $CD4^+$ T-cell activation is presented in Figure 3 below.

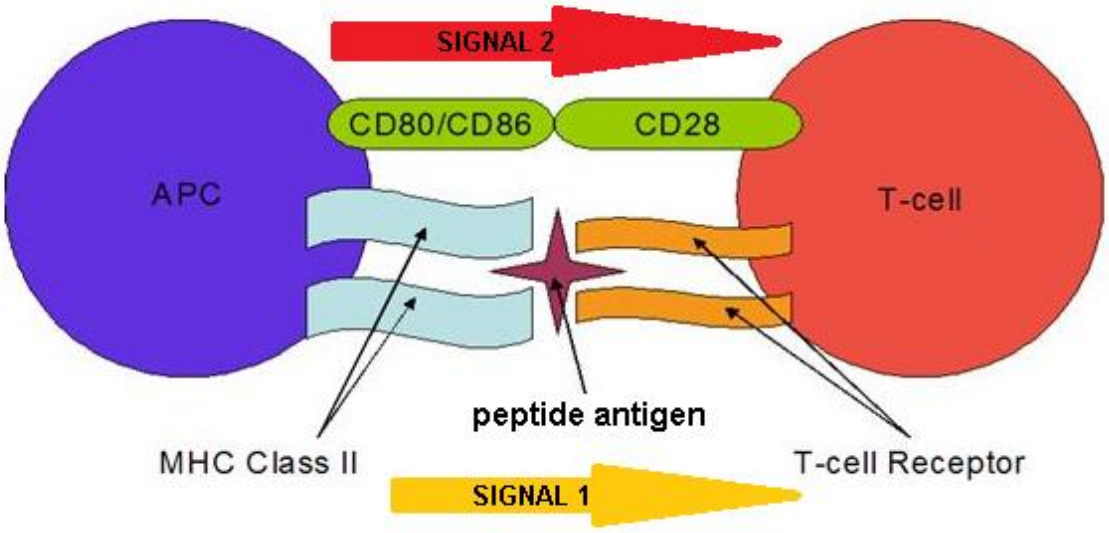

Figure 3 - ***(16, 17) Signal 1 occurs when the TCR binds to the MHCII-peptide complex presented by APCs(17). The MHCII molecule is restricted to professional APCs (dendritic cells, B cells and macophages)(10, 17). Signal 2 occurs through co-stimulation. The co-stimulatory receptor CD28 is constitutively expressed by naïve $CD4^+$T-cells and binds to co-stimulatory ligands CD80/CD86 on APCs(17). Both the TCR and co-stimulatory molecule on the $CD4^+$T-cells must simultaneously engage with the MHCII-peptide complex and the co-stimulatory molecules on the APC, in order for effective T-cell activation to occur.***

1.1.2.3.2. CD4+T-cell anergy

Anergy is a negative regulatory process of T-cell activation(10, 18). By understanding the mechanism of anergy, unwanted T-cell activation may be targeted, therefore preventing the development of autoimmune disease(10). By definition, anergy is a T-cell intrinsic state of unresponsiveness which occurs when T-cells are activated through the TCR in the absence of co-stimulation(10, 17). Upon re-stimulation with antigen, anergic T-cells remain viable, but demonstrate long lived hyporesponsiveness, including defects in cell-cycle progression and effector function(17) (See Figure 4).

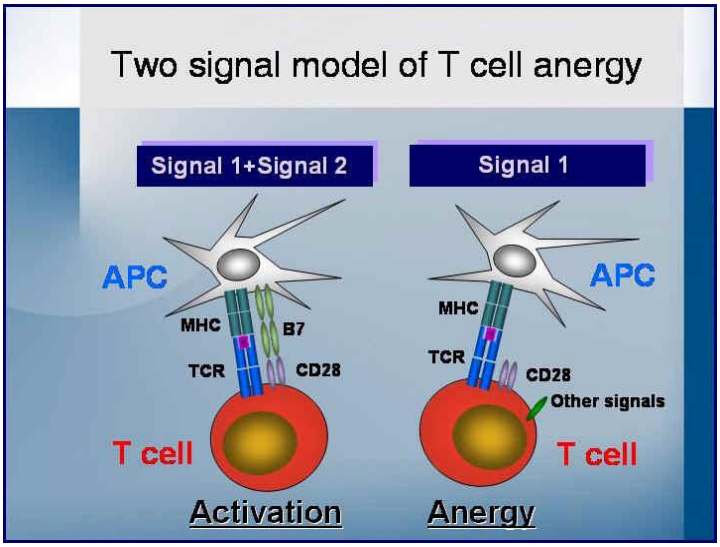

Figure 4 – ***(Left) Normal T-cell activation requiring Signal 1 (MHC-peptide with TCR) and Signal 2 (CD60/86 with CD28). (Right) Anergy occurs in the presence of Signal 1 but absence of Signal 2 (no CD80/86-CD28 co-stimulation). This means that the T-cell is not efficiently activated therefore enters an 'anergic' state(19).***

Anergy has been identified *in vivo* and *in vitro*(17). *In vitro*, T-cells undergo clonal anergy, where they are unresponsive to recall stimulation in the absence of co-stimulation(10, 17). Clonal anergy is characterised by reduced IL-2, IL-3 and IFN-ɤ secretion and reduced proliferation(10, 17, 20). It was first characterised in $CD4^{+}$T-helper cells stimulated through the TCR in the absence of CD28 co-stimulation(10, 17), and is reversible with strong stimuli or exogenous IL-2/IL-15 upon re-stimulation(10, 17, 20). Previous data suggests that induction of clonal T-cell anergy in naïve T-cells is difficult, however may be possible when induced via plate bound anti-CD3 mAb in the absence of soluble anti-CD28 mAb(10, 21). Various other methods are also used to induce T-cell anergy *in vitro*, including the mitogen concanavalin A and altered peptide ligands with lower avidity TCR ligation(17).

In vivo anergy models are termed adaptive tolerance(10). Adaptive tolerance results from peripheral T-cells being challenged by superantigen or specific peptides which results in T-cell activation in the absence of antigen-APC stimulation(17). One *in vivo* study showed that antigen challenge of TCR-transgenic mice caused large amounts of T-cell death(10). The T-cells which survived were anergic and displayed reduced proliferation and IL-2 production, just as demonstrated by *in vitro* models(10).

Anergy in naïve T-cells can be induced *in vivo*, however may not always be induced in naïve T-cell *in vitro*(10). Furthermore, the anergic state of T-cells *in vivo* cannot be rescued by IL-2, and instead recovers over time due to loss of the antigen from the periphery(10).

1.2. The ubiquitination pathway

Ubiquitin is a 76-amino-acid globular molecule present in all tissues, which determines the fate of the protein it is attached to(10, 20). Normally, ubiquitin targets proteins for degradation and recycling via the 26S proteasome(10, 20, 22). However other purposes of protein ubiquitylation include re-directing proteins within the cell, conformational changes of proteins and protein stabilisation(10, 20).

Ubiquitin is part of the ubiquitination pathway. The transfer of ubiquitin to target proteins involves coordination between the ubiquitin enzymes: E1, E2 and E3(10, 20, 22, 23). De-ubiquitylating enzymes and ubiquitin-binding proteins are also involved in this pathway(20, 23). Figure 5 illustrates the steps involved in the ubiquitin-proteasome pathway.

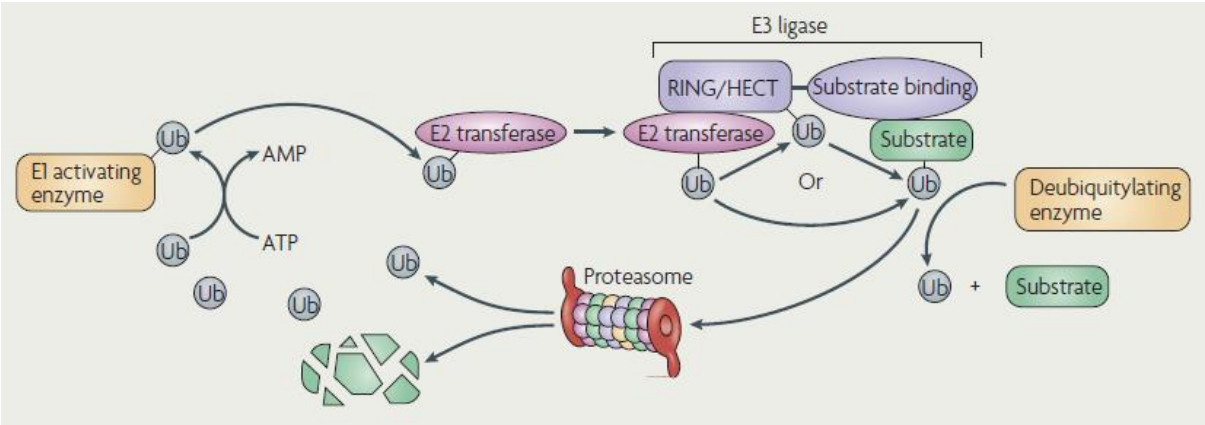

Figure 5(10) – ***The ubiquitin-proteasome pathway. Ubiquitin is activated in an ATP-dependant manner by E1 ubiquitin-activating enzyme. This activated ubiquitin is transferred to an E2 ubiquitin-conjugating enzyme (E2 ubiquitin transferase). The E2 enzyme binds to the recruitment domain of E3 ubiquitin ligase (such as the RING/HECT domain), which brings together the substrate and activated ubiquitin. The ubiquitinated protein can now be targeted for proteasome degradation. De-ubiquitylating enzymes can remove ubiquitin from the protein substrate(10)***.

1.3. E3 Ubiquitin protein ligases and their role in T-cell anergy

E3 ubiquitin ligases consist of a large complex superfamily of >500 enzymes(17) which catalyse the covalent bonding of the ubiquitin molecule to the target protein via the ubiquitination pathway(10, 17). In recent years, E3 ubiquitin ligases have been identified as critical in the regulation of T-cell responses by influencing T-cell signalling pathways(10).

Upregulation of E3 ubiquitin ligase genes Cbl-b(24), GRAIL(18) and ITCH(24) have been associated with T-cell activation and anergy(10, 20). However, recent research has identified TRAC1 (RNF125)(25), NEDD4(26), Peli1(27) and TRAF6 to also be involved in T-cell activation(26-28), suggesting that these genes may also be involved in maintaining the anergic state of T-cells.

1.3.1. Cbl-b

Cbl-b is a 982-amino acid containing protein with high sequence homology to CBL(10, 24). This RING-type E3 ligase was the first to be identified to have a role in i*n vivo* tolerance and T-cell activation(10). Previous research shows that peripheral T-cells from Cbl-b$^{-/-}$ mice express increased IL-2 secretion and hypoproliferation following stimulation compared to wild-type cells(20). Cbl-b$^{-/-}$ mice also develop spontaneous autoimmunity by 6 months of age(10, 23, 24). Furthermore, studies show that murine Cbl-b$^{-/-}$ T-cells are resistant to anergy induction *in vitro* and i*n vivo(22)*. Collectively, this data indicates that Cbl-b is involved in negative regulation of T-cell activation in the periphery and anergy.

1.3.2. GRAIL

GRAIL (RNF128), is a 428-amino acid type1 transmembrane protein which contains an extracellular protease-associated domain, a cytosolic coiled domain and RING-finger domains(10, 18). GRAIL is upregulated in ionomycin-induced anergic murine T-cells(10, 18) and constitutive expression of GRAIL has been associated with anergy in T-cells(23). Further studies show that overexpression of GRAIL in naïve $CD4^{+}$T-cells abolishes IL-2 production and proliferation upon peptide-APC stimulation(17). This data demonstrates the suppressive role of GRAIL in T-cell activation and its role in anergy.

As with Cbl-b and ITCH, GRAIL also contributes to Treg function and is highly expressed in nTregs(20, 23). Results show that GRAIL expression levels correlate with the immunosuppressive activity of murine Treg cells induced *in vivo* through superantigen exposure(23). These results indicate that GRAIL also has a vital function in T-cell tolerance(10).

1.3.3 ITCH

ITCH is a 864-amino acid cytosolic E3 ubiquitin ligase(10) which plays a role in TCR signalling and T-cell activation through ubiquitination(10). This is demonstrated by *in vitro* studies, where ITCH-deficient cells show enhanced proliferation and activation on TCR-engagement(23). Furthermore, *in vivo* studies show ITCH mutations in 18^{H} mice cause persistent itching of the skin and lymphoproliferative disease, indicating its role in peripheral tolerance(10, 24). $ITCH^{-/-}$ mice are also resistant to ionomycin-induced anergy and their $CD4^{+}$T-cells are resistant to Treg-dependant immunosupression(10, 20, 23, 24) reinforcing the importance of ITCH in tolerance and as a negative regulator of T-cell activation.

1.3.4. NEDD4, TRAC1 and PELI1

TRAC-1 (RNF125) contains an N-terminal RING-finger domain(25). Investigation into high expression of TRAC-1 in lymphoid tissues has shown that antisense oligonucleotides reduce TRAC-1 mRNA levels in primary T-cells, and inhibit T-cell activation in response to TCR cross-linking(25). This indicates that TRAC-1 is a positive regulator of T-cell activation(25), and therefore its expression may be downregulated in anergic T-cells.

Recent studies have revealed that Nedd4 also positively regulates T-cell activation(10, 20). Although Nedd4$^{-/-}$ T-cells develop normally, they show reduced proliferation and IL-2 production(26). Nedd4$^{-/-}$T-cells also contain more of the E3 ubiquitin ligase Cbl-b. Studies show that Nedd4 promotes the ubiquitin-mediated degradation of Cbl-b in activated T-cells and promotes the conversion of naïve T-cells into activated T-cells(20, 26). In other words, Nedd4 can be described as a positive regulator of T-cell activation(23), which functions by targeting an E3 ubiquitin ligase which negatively regulates T-cell activation.

Peli1 belongs to the Pellino family of E3 ubiquitin ligases and is one of three members (PELI1, 2 and 3)(27). The function of PELI depends on the C-terminal RING domain. Investigations show that Peli1 is crucial as a negative regulator of T-cell activation and in preventing autoimmunity(27). Peli1 deficiencies cause hyperactivation of T-cells which are resistant to Treg and TGFβ supression(27). Furthermore Peli1$^{-/-}$ mice develop autoimmunity and accumulation of the transcription factor c-Rel, which has important roles in T-cell activation(20, 27). These results highlight the importance of Peli1 in maintaining peripheral tolerance(17, 27).

1.4. Aims & objectives

The aim of this study is to construct a protocol to induce anergy in human $CD4^+$T-cells using existing literature. Furthermore, the expression of E3 ubiquitin ligases will be compared between Tregs, conventional $CD4^+$T-cells, anergic $CD4^+$T-cells and non-anergic $CD4^+$T-cells through the use of $CD4^+$T-cell isolation assays and quantitative RT-PCR. This will clarify whether E3 Ubiquitin ligases are associated with T-cell anergy and are differentially expressed between different T-cell phenotypes.

We hypothesise that all the E3 ubiquitin ligases which are negative regulators of T-cell activation will be upregulated, and positive regulators of T-cell activation such as RNF125 and Nedd4 will be downregulated in anergic and Treg populations. This is because the hyporesponsive and tolerogenic functions of anergic T-cells indicate that the threshold for T-cell activation in these subsets may be higher compared to non-anergic T-cells and $CD4^+CD25^-$T-cells.

2. Methods

6. The T-cell anergy assay

The T-cell anergy assay was performed over a period of 8 days. On Day 0, PBMCs were isolated from human peripheral blood using Ficoll. $CD4^+CD25^+$ (Conventional T-cells) and $CD4^+CD25^-$ cells (Tregs) were isolated using a $CD4^+CD25^+$ Treg Isolation Kit (MACS, Miltenyi Biotec, UK) as described in 2.2. Pellets of Tregs and a proportion of conventional T-cell pellets were stored in a -80°C freezer for future experiments via PCR. The remaining conventional T-cells were incubated in complete media alone, or were treated with plate-bound anti-CD3 mAb or plate-bound anti-CD3 mAb with soluble anti-CD28 antibody. The treatment groups were incubated for 24 hours. On Day 1 the T-cells were washed and rested in complete media until Day 4. On Day 4 T-cells from all the treatment groups were stained with proliferation dye then either re-stimulated (using anti-CD3.28 Dynabeads) or not re-stimulated. 3 hours following re-stimulation samples of each treatment group were taken and frozen down for future PCR experiments (Figure 7). The remaining T-cells were incubated until Day 8 where they were analysed for T-cell proliferation via flow cytometry. The process of this assay is displayed by Figure 6.

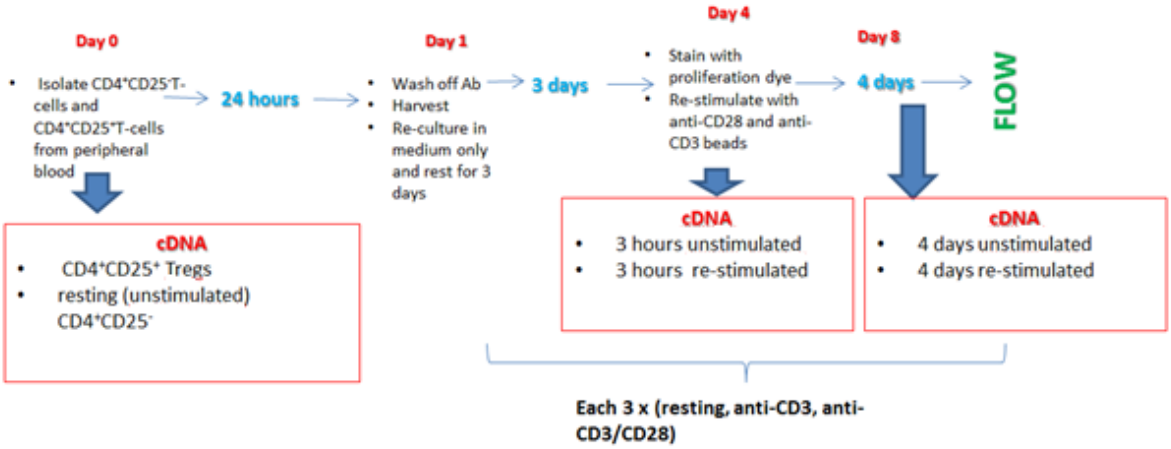

Figure 6 – ***Overview of anergy assay (Day 0-8). Boxes headed cDNA indicates where cell pellets will be frozen and cDNA isolated for PCR.***

2.2. Isolating $CD4^+CD25^-$ and $CD4^+CD25^+$ T-cells from human peripheral blood

Two 50ml universal tubes were prepared with 125µl of heparin and 25ml of blood from the same donor. The blood was diluted with an equal volume of RPMI-1640 (1%GPS, 1% hepes, Sigma-Aldrich Life Science, UK) and prepared with Ficoll (GE Healthcare Life-Sciences, UK) to isolate PBMCs according to the manufacturer's instructions.

The PBMC buffy coat layer was harvested and washed twice with RPMI before being counted and 50µl was isolated for a purity check. The $CD4^+$ T-cells were negatively selected from $CD4^-$ cells using a $CD4^+CD25^+$ Treg Isolation Kit (MACS, Miltenyi Biotec, UK). This involved using MACS buffer (PBS, 0.1% BSA, 2mM EDTA (Sigma-Aldrich, UK, E7889)), Biotin antibody cocktail, anti-biotin microbeads (Miltenyi Biotec 130-045-101, UK) and an LD column (Miltenyi Biotec 130-042-201, UK) according to the manufacturer's instructions.

Next the $CD4^+CD25^-$ cells were separated from the $CD4^+CD25^+$ T-cells using MACS buffer and an MS column (Miltenyi Biotec, UK) according to the manufacturer's instructions. 50µl of the $CD4^+CD25^-$ and $CD4^+CD25^+$ cells were stored for flow cytometry purity checks.

The cells were counted and cell suspensions of between 100,000 and 200,000 $CD4^+CD25^+$ and $CD4^+CD25^-$ T-cells were centrifuged. The supernatant was discarded and the pellet was frozen in a -80°C freezer for future PCR experiments.

2.3. Stimulating $CD4^+CD25^-$ with plate bound anti-CD3 antibody

Three conditions were tested in these experiments: unstimulated (resting) T-cells, anti-CD3 antibody treated T-cells and anti-CD3.28 antibody treated T-cells. The anti-CD3 human antibody (eBiosciences, clone:0KT3, UK) was diluted to a concentration of 2µg/ml with sterile PBS(29, 30). 1ml of this anti-CD3 solution was added 2 wells on a 24-well plate and left to incubate at 37°C for 1 hour (29, 30). Following incubation the antibody solution was washed from the wells three times using sterile PBS.

From the T-cell isolation, 2-3million conventional $CD4^+CD25^-$ T-cells suspended in 1ml RPMI, were plated into each of the three wells (including the plate-bound anti-CD3 coated wells). Soluble anti-CD28 human antibody (eBiosciences, clone:CD28.2, UK) was added to one of the wells to form a final concentration of 2µg/ml (31). The plate was incubated for 24 hours at 37°C. following incubation, the T-cells were transferred to Falcon tubes and washed in complete RPMI-1640 media (1%GPS, 1% hepes, 10%HIFCS) (Sigma-Aldrich Life Science, UK) before being transferred to a fresh 24-well plate where they were rested for 3 days in the incubator at 37°C(31).

2.4. Staining the $CD4^+CD25^-$ T-cells with proliferation dye

The T-cells were transferred to falcon tubes and washed once with PBS to remove any serum. They were then re-suspended in room temperature PBS at twice the final required concentration. The cell proliferation dye (eFluor 450, eBioscience, 65-0842, UK) was diluted in PBS to form a 20µM solution, before being added to the cell suspension in a 1:1 dilution, and left to incubate in the dark at 37°C for 10 minutes. Cold complete media was used to stop labelling and the cell suspension was incubated on ice for a further 5 minutes before being washed twice in complete

media. After the washes, the cells were counted, re-suspended in complete media and plated on a round-bottom 96-well plate. Each condition was plated three times so that T-cells could be harvested at 3 hours following re-stimulation, 4 days following re-stimulation and for flow cytometry (Figure 7).

.

2.5. Re-stimulating $CD4^{+}CD25^{-}$ T-cells with anti-CD3 & anti-CD28 Dynabeads

Anti-CD3.28 human T-activator Dynabeads (Gibco, Life Technologies, UK) were used to re-stimulate the three different T-cell conditions. The bead stock solution was diluted with complete medium according to the manufacturer's instructions and 100µl of bead solution was added to all the 're-stimulated' wells. Figure 7 demonstrates the layout of conditions on the 96-well plate. Figure 8 shows the solutions added to the 'stimulated' and 'un-stimulated' wells. The pellets of T-cells harvested at 3 hours following re-stimulation and 4 days following re-stimulation were frozen in a -80°C freezer for future PCR experiments. Figure 6 illustrates the process of the entire assay in the form of a flow diagram.

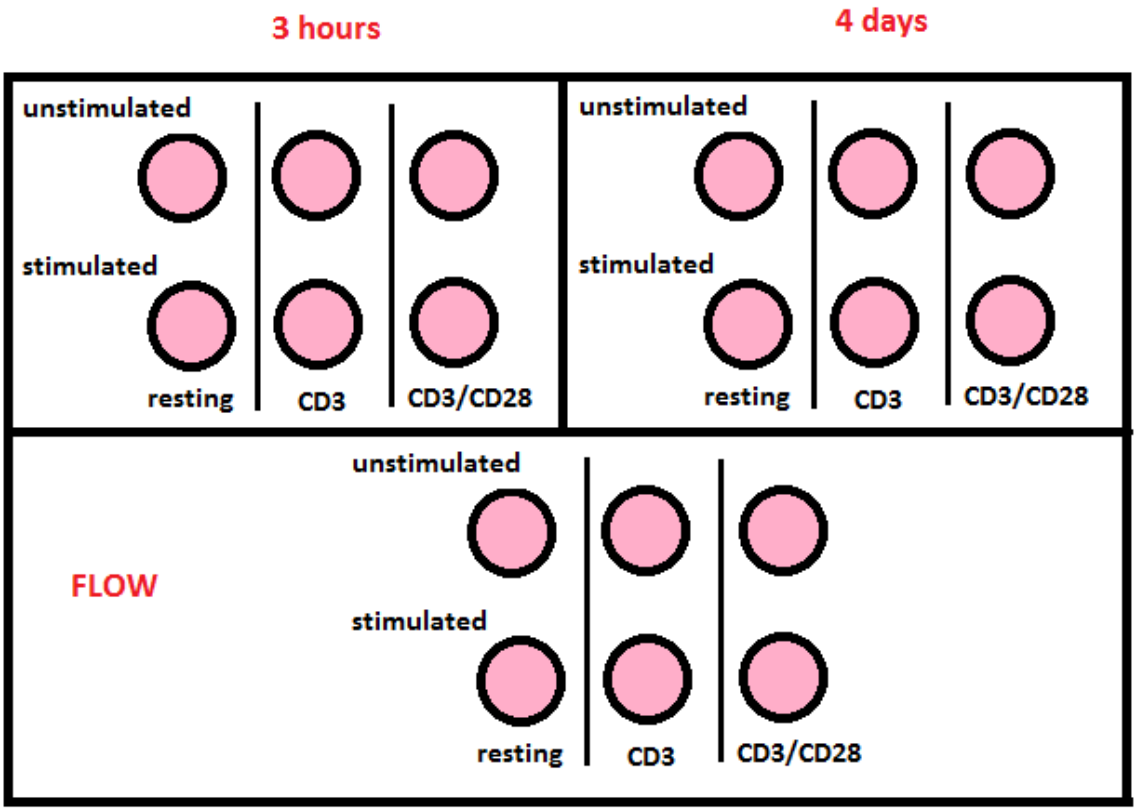

Figure 7 – ***Diagram demonstrating the treatment groups of T-cells of on a 96-well plate. The three treatment groups are resting T-cells (initially unstimulated), anti-CD3 stimulated T-cells and anti-CD3.28 stimulated T-cells. 3 days following stimulation these groups were then either re-stimulated with anti-CD3.28 beads or not re-stimulated. At 3 hours and 4 days following re-stimulation, T-cells were harvested and the pellets frozen for future PCR experiments***

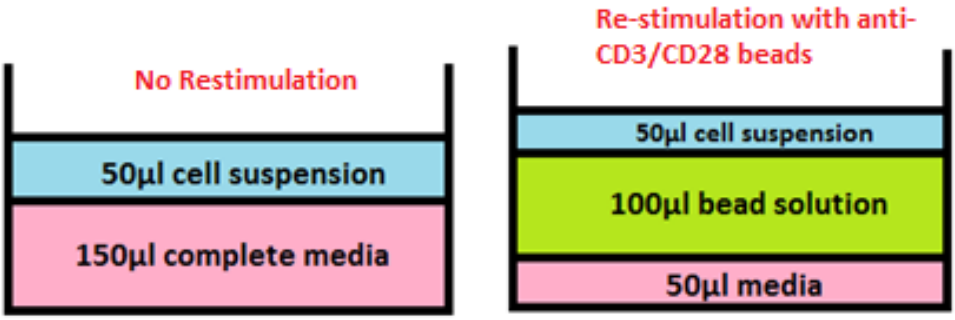

Figure 8 – ***Diagram demonstrating the contents of re-stimulated and non re-stimulated wells on the round-bottom 96-well plate. The total volume of a well on a 96-well plate did not exceed 200µl. unstimulated wells (left) contain the T-cell suspension in media. Re-stimulated wells (right) contain media, cell suspension and anti-CD3/28 antibody bead solution.***

2.6. Re-stimulating $CD4^{+}CD25^{-}$ T-cells with anti-CD3 & anti-CD28 Antibody

In some experiments, T-cells were re-stimulated via plate bound anti-CD3 and soluble anti-CD28 antibody. As previously, the anti-CD3 antibody was diluted from a to forma 2µg/ml with sterile PBS. 200µl of anti-CD3 solution was then added to all re-stimulated wells of the 96-well plate and left to incubate at 37°C for 1 hour. Following incubation the antibody solution was washed from the wells three times using sterile PBS. 100,000 cells were suspended in complete media containing anti-CD28 antibody (diluted to form a final concentration of 2µg/ml), and were added to the anti-CD3 coated wells on the 96-well plate and left to incubate until day 8.

2.7. Re-stimulating $CD4^{+}CD25^{-}$ T-cells with anti-CD3 & anti-CD28 Treg suppressor beads

Other experiments used Treg human suppression inspector beads (MACS, Miltenyi Biotec, 130-092-909, UK) to re-stimulate the T-cells. The bead stock solution was diluted with complete medium according to the manufacturer's instructions and 100µl of bead solution was added to all the 're-stimulated' wells in the same way as the CD3.28 Dynabeads.

2.8. Isolating cDNA

A µMACS^{TM}One-step cDNA Kit (MACS, Miltenyi Biotech, UK) was used according to manufacturer's instructions, to isolate cDNA from sample pellets from anergy assays.

Cells were lysed with lysis buffer and the cellular DNA was sheared through a 21G needle attached to a 1-5ml syringe. The sheared lysate was then spun for 1 minute at

x13000g before being applied to the LysateClear column where it was spun for a further 3 minutes at x13000g.

The µMACS column was placed in the magnetic field and prepared with 100µl of binding/lysis buffer. Following centrifugation, 50µl of Oligo(dT) Microbeads was added to the 1ml of lysate and mixed thoroughly before being added to the column matrix. The column was rinsed withLysis/Binding buffer to remove protein and DNA, and then rinsed with Wash Buffer to remove rRNA and DNA. Equilibration/Wash Buffer was then added to the column matrix.

The Enzyme Mix was dissolved in 20µl Re-suspension Buffer and also added to the top of the column. Sealing solution was added directly on top of the column and the thermoMACS Separator was set to 42° and left to incubate for 1 hour. Following incubation, the column was rinsed twice again with Equilibration/Wash buffer. 20µl cDNA Release Solution was then applied the column matrix and left to incubate for 10mins at 42°C before the synthesized cDNA was eluted with 50µl cDNA Elution Buffer.

2.9. PCR

The concentration of cDNA was measured using the Nanodrop2000/2003 Thermoscientific and the cDNA samples were aliquoted into a 384-well PCR plate with master-mix (Fast start universal probe master, Rox, Roche Applied Science, UK) GAPDH reference probe (Hs02758991_g1) (TaqMan Gene Expression Assays, Applied Biosystems, UK), RNase free water and the target primer probe. Target probes included RNF125 (Hs00215201_m1), RNF128 (Hs00226053_m1), ITCH (Hs00395201_m1), PELI1 (Hs00900505_m1), Nedd4 (Hs00406454_m1), CBLB (Hs00180288_m1)) (TaqMan Gene Expression Assays, Applied Biosystems, UK).

The reaction volume was 5µl. Each condition was plated as a triplicate and the control consisted of 2.5µl master mix with 2.5µl RNase free water. The PCR was run on the Light Cycler480 II (Roche Applied Biosystems) for 45 cycles before being analysed via basic relative quantification. The cycle conditions are shown in Table 1.

Stage	Cycles	Temp °C	Hold Time (h:min:sec)	Ramp Rate (°C/s)
Pre-incubation	1	95	00:10:00	4.4
Amplification	**50**	**95**	**00.00.15**	**4.4**
		60	**00.01.00**	**2.2**
		72	**00.00.01**	**4.4**
Melt curve	1	95	00.00.10	4.4
		40	00.00.30	2.5
		80	continuous	0.06
Cooling	1	40	00.00.10	2

Table 1 – *PCR cycle conditions performed by the Light Cyler480 II to detect E3 ubiquitin ligase gene expression in T-cell subsets*

2.10. Statistics

AccuCheck counting beads (Life Technologies, Invitrogen, UK) were added to samples from anergy assays according to manufacturer's instructions prior to flow cytometry. This allowed the number of proliferated cells counted via flow to be calculated in order to make all results from the same experiment relative. These results were then plotted on a bar graph using the mean. Error bars presented in graphs displayed the SEM. Results which displayed significant differences were marked with a * where $p<0.05$, ** where $p<0.01$ and *** where $p<0.001$.

The ΔCt values and $2^{-\Delta Ct}$ values were calculated from the PCR results. The replicate $2^{-\Delta Ct}$ values were then plotted on a bar graph to display the mean and standard error of the mean (SEM) which was calculated via Prism.

3. Results

3.1. Methods used to initially stimulate conventional CD4$^+$T-cells affects T-cell proliferation

Different methods were used to stimulate conventional CD4$^+$T-cells to define which method could be used in anergy assays to induce T-cell proliferation, but allow T-cells to return close to rest by day 4 (Figure 9).

9a.

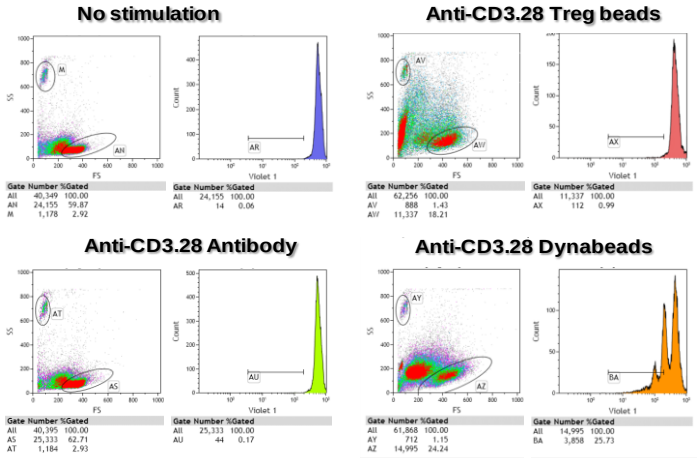

9b.

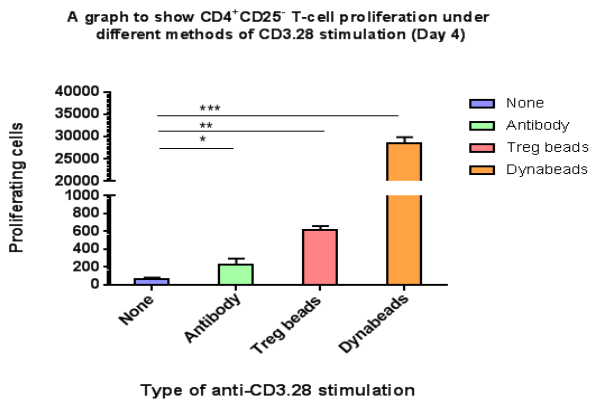

Figure 9- a. ***Flow diagrams and histograms demonstrating effects of anti-CD3.28 stimulation methods on CD4$^+$T-cell proliferation. T-cells were stimulated for 4 days. The T-cell population was gated and the proportion of proliferating T-cells calculated using counting beads. b. Graph comparing effects of anti-CD3.28 stimulation methods on numbers of proliferating CD4$^+$T-Cells (Day 4). Each condition was performed in triplicates therefore the graph shows means and the error bars represent the SEM where n=3. Significant differences to the untreated control are represented by * where p<0.05, ** where p<0.01 and *** where p<0.001. The stimulation methods used in this experiment were Dynabeads, Treg suppressor beads and CD3.28 antibody.***

Gate AR in Figure 9a shows that the non-stimulated $CD4^+$T-cell population experiences the lowest % T-cell proliferation. Figure 9b shows that the antibody stimulated population demonstrates a significantly higher amount of proliferation compared to unstimulated controls where p=0.049. T-cells stimulated with Treg suppressor beads induced significantly higher T-cell proliferation numbers compared to unstimulated controls, where p=0.004. Dynabead stimulation induced the highest significant T-cell proliferation number compared to unstimulated populations where p=0.0009.

The results show that antibodies are the most effective at both stimulating the T-cells and allowing them to return to rest by Day 4.

3.2. Anergy induction is not dependant on the method of CD4^{+}T-cell re-stimulation

This experiment was performed to determine whether re-stimulating T-cells via different methods following initial antibody stimulations, would affect T-cell proliferation numbers and trends in the data (Figure 10).

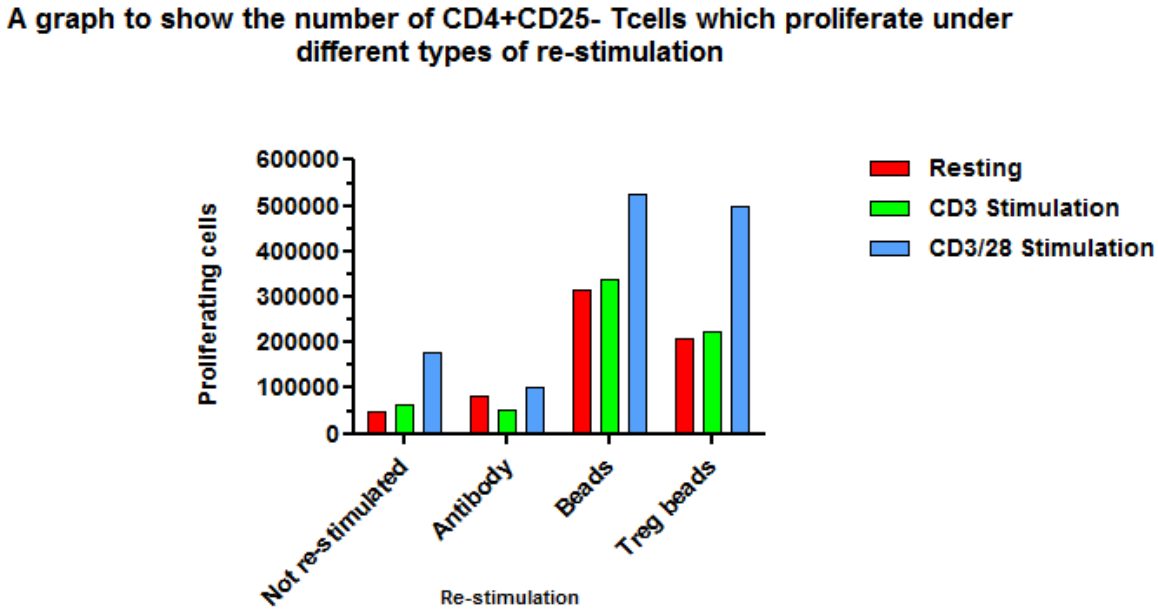

***Figure 10*– Results from Experiment 4 anergy assay at Day 8, where different methods of re-stimulation are used (n=1). T-cells are stimulated using anti-CD3 or anti-CD3.28 antibody at Day 1, then re-stimulated (CD3.28) using antibody, Dynabeads or Treg suppressor beads at Day 4. Results demonstrate the number of conventional CD4^{+}T-Cells which have proliferated 4 days after re-stimulation.**

Figure 10 shows where there is no re-stimulation, the anti-CD3.28 stimulated $CD4^+$T-cells from day 4, are still proliferating at Day 8. The proliferation numbers of this population are higher compared to the resting and anti-CD3 stimulated populations which have also not been re-stimulated.

In the antibody re-stimulated populations, anti-CD3 stimulated groups contain the lowest number of proliferating cells, with the resting and CD3.28 stimulated population showing increased proliferation respectively.

The numbers of proliferating cells induced by Dynabead re-stimulated populations were the highest compared to other re-stimulation methods and the non-re-stimulated control populations. Dynabead re-stimulation of resting and anti-CD3 stimulated T-cells induce a similar level of T-cell proliferation with the number or proliferating cells increasing from resting and anti-CD3 stimulated populations respectively. Anti-CD3.28 Dynabead stimulated populations induced the highest T-cell proliferation number. Collectively, the trends in the data from the Dynabead re-stimulated populations were repeated in Treg bead re-stimulated and non-re-stimulated populations.

Overall this data shows that Dynabeads induce the highest number of T-cell proliferation in all three treatment groups without affecting the trend in the data, implying that if anergy exists, it is not broken by Dynabead re-stimulation. Therefore, Dynabead re-stimulation was used for the remainder of the anergy assays.

3.3. Re-stimulated conventional CD4^{+}T-cells initially stimulated via anti-CD3 antibody proliferate less compared to those initially stimulated with anti-CD3.28 antibody.

In order to visualise the effects of initial stimulation and re-stimulation on CD4^{+}T-cells, and anergy assay was conducted and presented in dot plots in Figure 11.

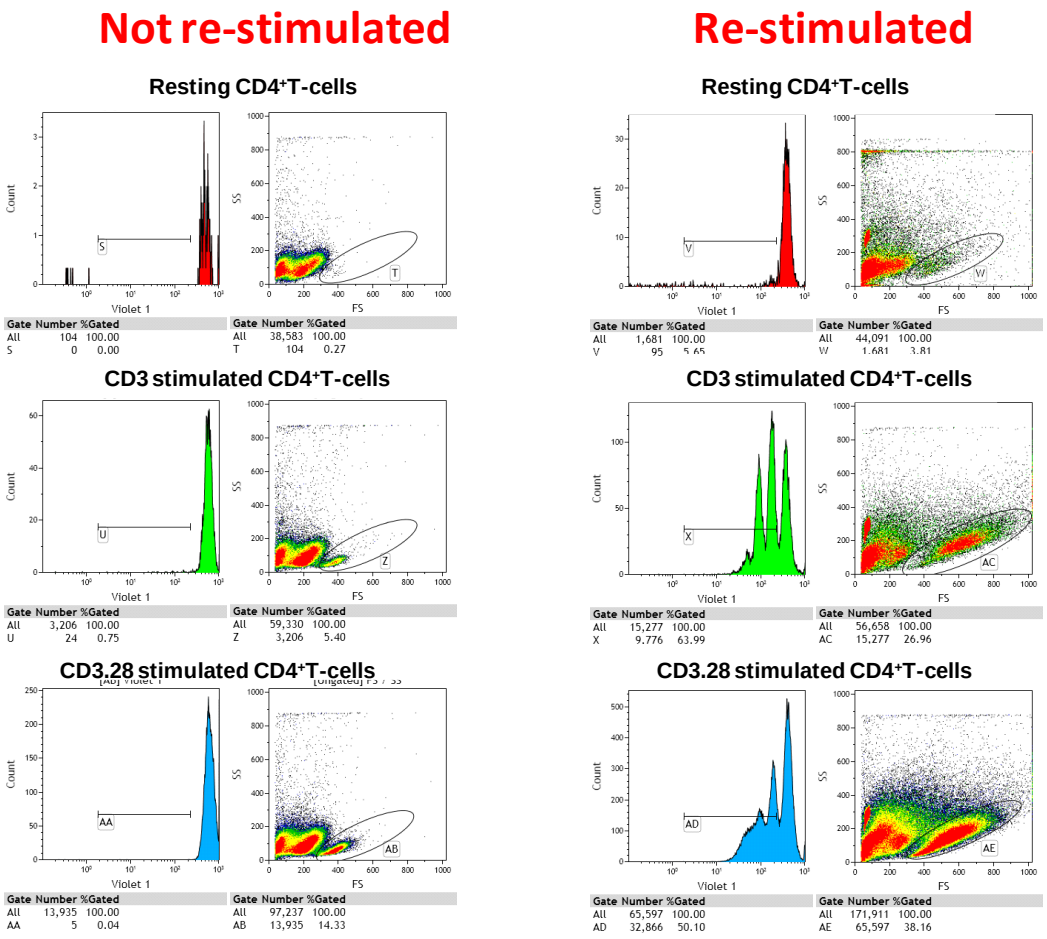

***Figure 11** – Dot plot results from Experiment 1 (Day 8) demonstrating the degree of T-cell proliferation when cells undergo no initial stimulation, anti-CD3 stimulation only, or anti-CD3.28 stimulation only. These populations are either re-stimulated by anti-CD328 Dynabeads or not re-stimulated at Day 4. Results were collected via flow cytometry on Day 8.*

Results from Figure 11 show that the majority of unstimulated resting cells with and without re-stimulation die. An increased population of $CD4^+$T-cell survive with anti-CD3 stimulation alone, with an even higher population of T-cells surviving with initial stimulation of anti-CD3.28.

Anti-CD3.28 re-stimulation of the anti-CD3 and anti-CD3.28 stimulated groups, induce increased T-cell proliferation in these populations respectively. The T-cell death which exists upon re-stimulation correlates with this increase in T-cell proliferation, reflecting activation-induced cell death.

Results show that T-cell survival increases with increased stimulation, implying that CD3.28 stimulation induces full activation and CD3 stimulation induces partial activation of $CD4^+$T-cells.

3.4. Anergy is variably induced in anti-CD3 stimulated cells

Multiple anergy assays were performed to compare T-cell proliferation numbers between treatment groups, to identify whether anergy may have been induced (Figure 12).

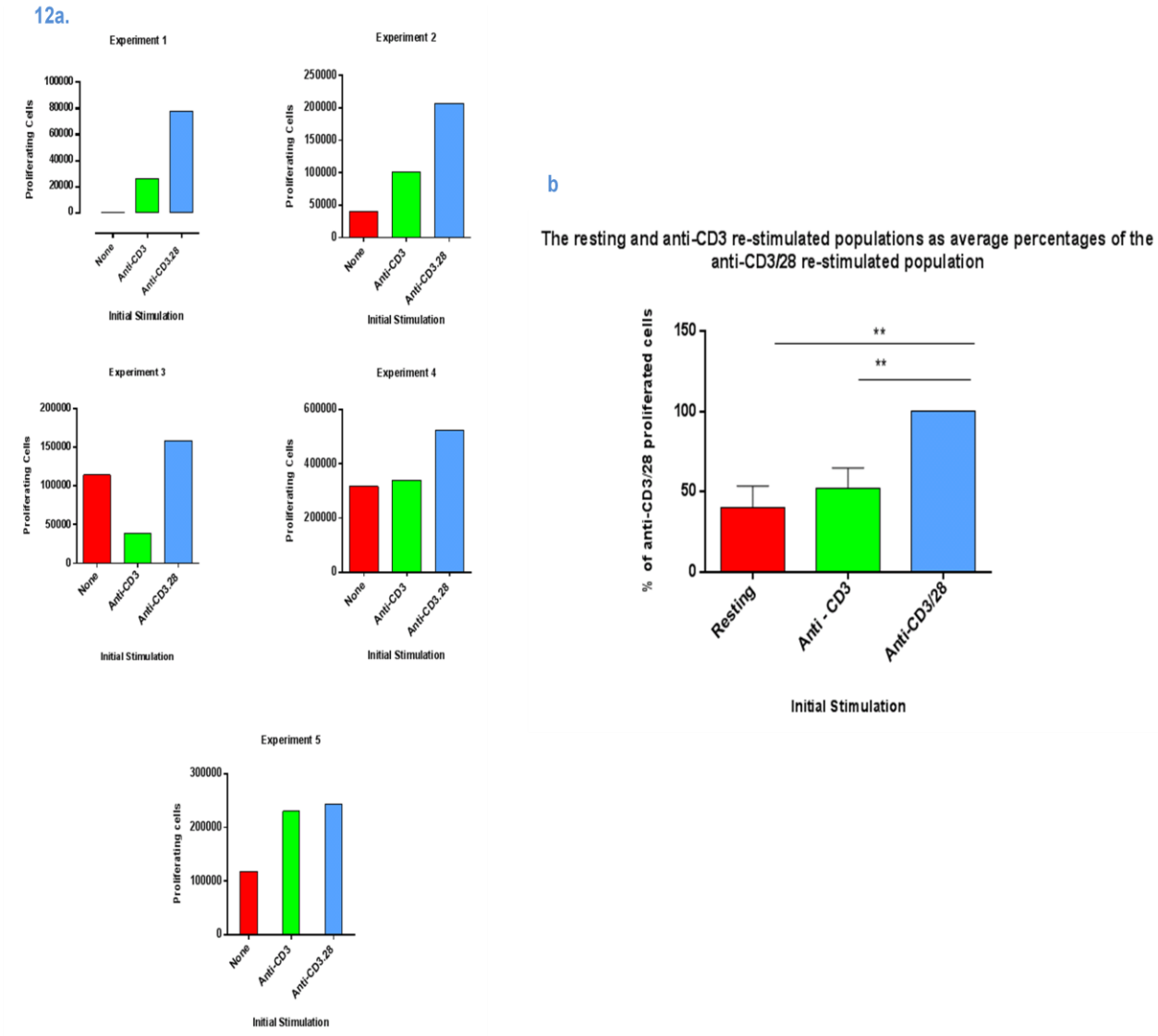

Figure 12- a. ***Results from anergy assays at Day 8, where n=1. Shows the number of proliferating cells in unstimulated, CD3 and CD3.28 stimulated T-cell populations, 4 days after Dynabead anti-CD3.28 re-stimulation.*** ***b.*** ***Graph showing the % of anti-CD3.28 re-stimulated, proliferated T-cells from anergy experiments 1-5 (Figure 11a). Each value is presented as a percentage of the anti-CD3.28 initially stimulated, re-stimulated population (100%) and averaged. Error bars represent the SEM. n=5.***
***** demonstrates a significant difference where p<0.01.***

In all experiments shown in Figure 12a the anti-CD3.28 stimulated, re-stimulated population demonstrates the highest number of proliferating conventional $CD4^+$T-cells. Experiments 1, 2 and 4 show that T-cell proliferation is higher in the anti-CD3 stimulated population in comparison to the resting population.

Where results were averaged and expressed as percentages in Figure 12b, both the resting and anti-CD3 stimulated populations showed a significantly lower % of proliferating T-cells upon re-stimulation, compared to anti-CD3.28 stimulated populations, with p-values of 0.005 and 0.009 respectively. However there was no significant difference in percentages between resting and anti-CD3 stimulated populations following re-stimulation (Figure 12b).

Overall results indicate that anergy may be induced in some experiments; however this anergy induction may be donor dependant.

In order to determine the health of the resting population of T-cells, an experiment was conducted to count the number of non-proliferated cells from the stimulated, non-re-stimulated treatment groups (Figure 13).

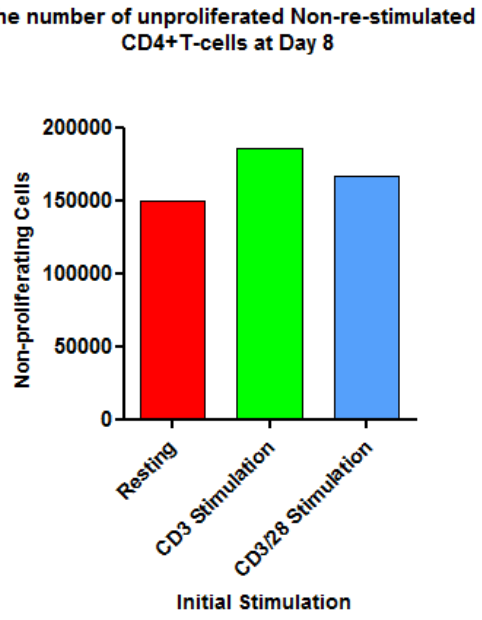

***Figure 13** – Results from Experiment 4 demonstrating the number of non-proliferated cells. T-cells were treated at Day 1 with anti-CD3 or anti-CD3.28 antibody (untreated control). These populations were not re-stimulated. The number of non-proliferating cells were quantified using counting beads and flow cytometry at Day 8.*

Figure 13 shows that the lowest numbers of non-proliferated cells were found in the resting non-re-stimulated population, with an increasing number of non-proliferated cells in the anti-CD3.28 and anti-CD3 stimulated populations respectively.

The low number of viable non-proliferated resting cells implies that this population may be dying or non-functional therefore making it more probable that anergy may be induced in previous experiments.

3.5. The $CD4^+CD25^+$ and $CD4^+CD25^-$ T-cells isolated from peripheral blood has high purity

Percentage purities of Tregs and conventional isolated T-cells were checked to ensure that the PCR samples were not contaminated with other cell subsets (Figure 14).

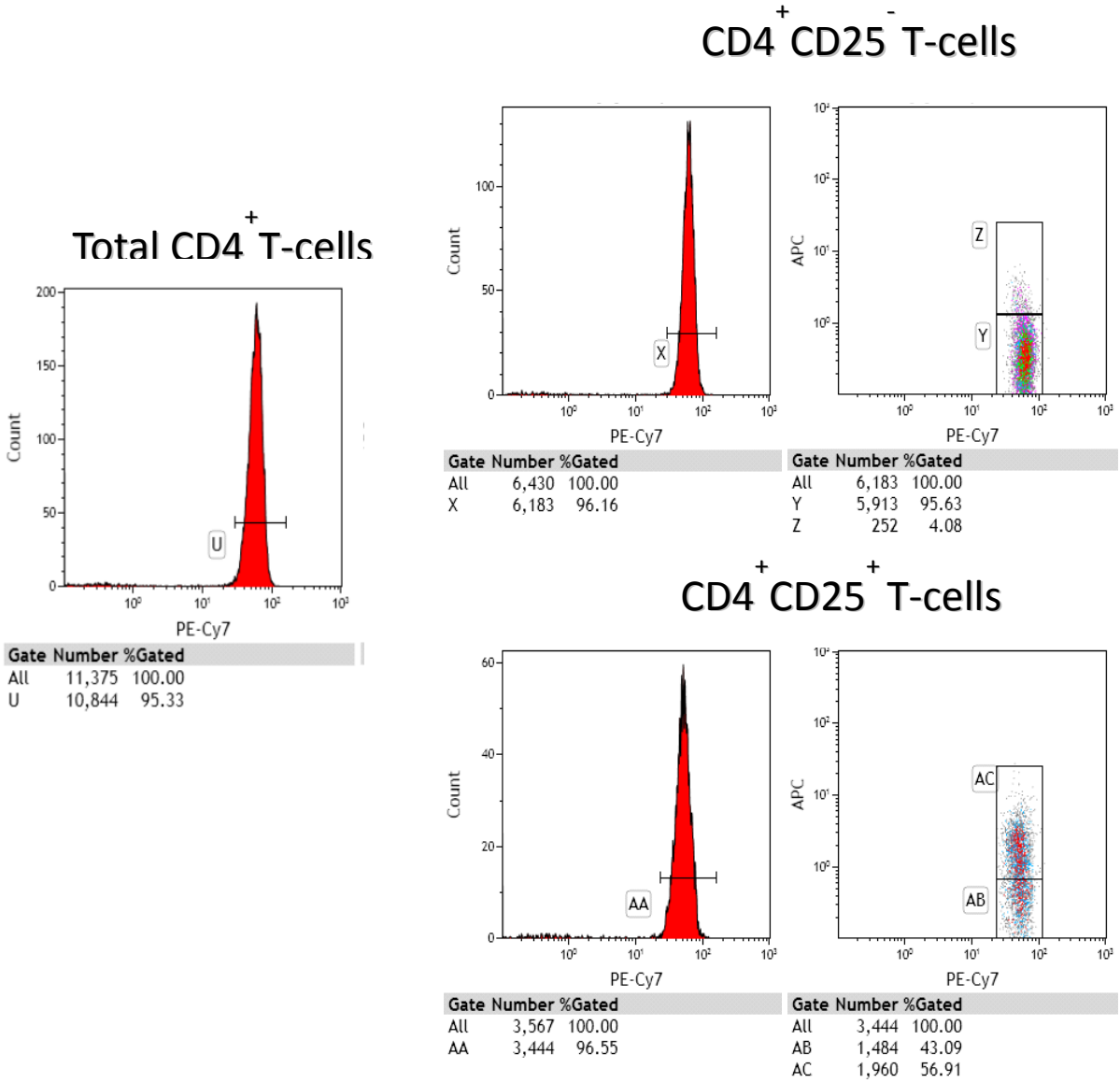

***Figure 14** – Histograms and dot plots representing a purity check from $CD4^+CD25^-$ and $CD4^+CD25^+$ T-cell isolations taken from human peripheral blood. (Left) Represents the purity of the entire $CD4^+$T-cell population. (Top right) indicates the purity of the conventional $CD4^+$T-cell population. (Bottom right) demonstrates the purity of the Treg population.*

Figure 14 demonstrates that the total $CD4^+$T-cell population was 95.33% pure. The purity of $CD4^+CD25^-$ T-cells was 95.63% and the percentage purity of $CD4^+CD25^+$T-cells (Tregs) was 56.91%, which shows that the $CD4^+CD25^+$population were enriched with Treg cells.

These results however, indicate that the Treg population is not as pure as the conventional T-cell population, and is contaminated with some $CD4^+CD25^+$ T-cells.

3.6. Peli1 is expressed to a similar degree in both Treg cells and conventional CD4^{+}T-cells

Quantitative RT-PCR was performed to detect the expression of E3 ubiquitin ligase genes in Tregs and conventional T-cells, to assess whether E3 ligase expression was specific to the function of these T-cell subsets (Figure 15).

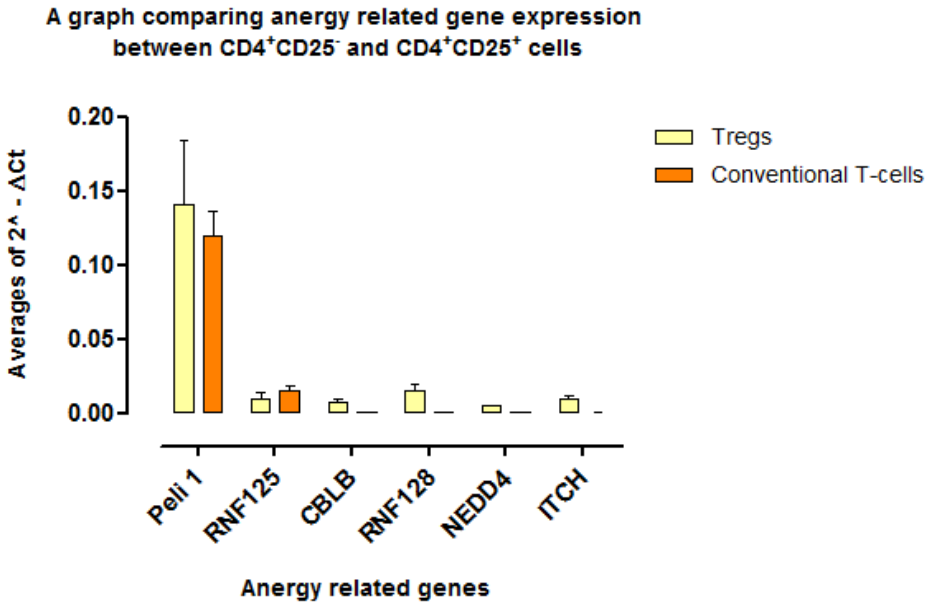

***Figure 15** – A graph comparing the expression of 6 anergy related E3 ubiquitin ligase genes between conventional CD4^{+}T-cells (CD4^{+}CD25^{-}) and Tregs (CD4^{+}CD25^{+}). Both these T-cell subsets were isolated from human blood at Day 0 and frozen. Each condition was repeated in triplicate and displayed as a mean. The error bars represent the SEM. The single lines on the graph indicate where genes were not detectable (N/D), where the reference gene GAPDH was detected however the target anergy gene was not. n=2/3 except where no error bars are present in which case n=1.*

Cbl-b, RNF128 (GRAIL), NEDD4 and ITCH expression were not detectable in the conventional $CD4^+$T-cells isolated at Day 0, but were detectable at a very low level in Tregs. E3 ligase genes which were detectable were expressed at very low levels in both these T-cell populations. The highest gene expression existed for Peli1 which was expressed at similar levels between Tregs and conventional T-cells.

Where E3 ligase genes were detectable in Tregs but not detectable in conventional T-cells, implies that these E3 ubiquitin ligases may have a role in Treg function.

3.7. The overall expression of anergy related E3 ligases in anti-CD3 stimulated/re-stimulated and anti-CD3.28 stimulated/re-stimulated conventional CD4^{+}T-cells is low

The raw data curves from the PCR reactions were analysed to explain why some E3 ubiquitin ligase genes were not detectable from Figures 15 and 17.

16a.

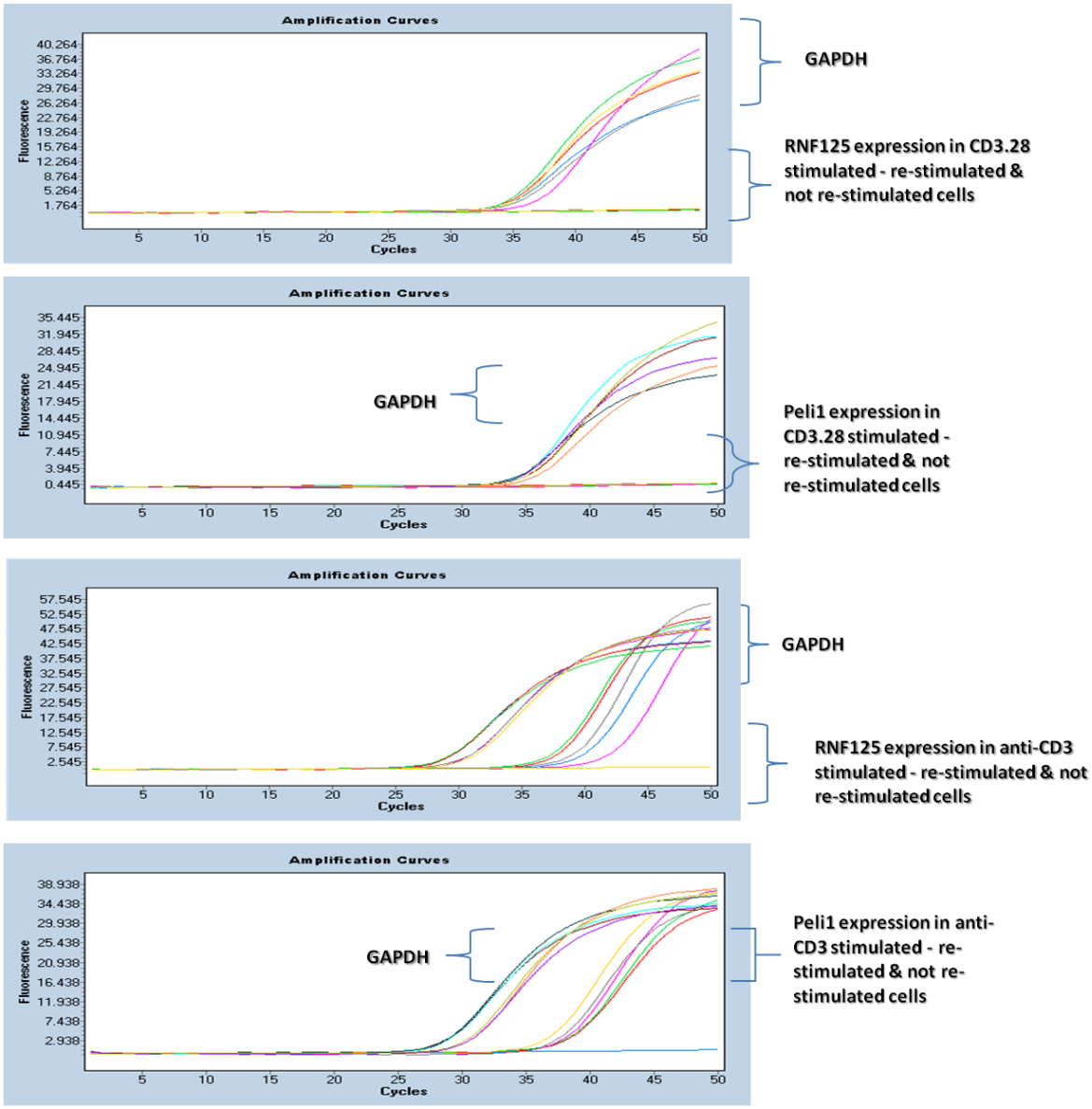

***Figure 16a, b** – PCR curves demonstrating raw data. Represents the expression of RNF125 and Peli1 respectively against reference gene GAPDH between anti-CD3 stimulated and anti-CD3.28 stimulated CD4^{+}T-Cells +/- anti-CD3.28 Dynabead re-stimulation. **c,d** -Represents expression of RNF125 and Peli 1 respectively against GAPDH between anti-CD3 stimulated and anti-CD3.28 stimulated CD4^{+}T-Cells +/- anti-CD3.28 Dynabead re-stimulation.*

Figure 16 c and d demonstrates that where GAPDH is detected early at ~25 cycles, the target genes (Peli1 and RNF125) are detectable at ~10 cycles later in the anti-CD3 stimulated, re-stimulated and non-re-stimulated populations.

Figures 16a and b show that when GAPDH is detected at later cycles (~33-35 cycles), the target genes Peli1 and RNF125 are not detected in the anti-CD3.28 re-stimulated and non-re-stimulated populations.

These results imply that the gene expression may have been detectable either after 45 cycles into the PCR reaction, or if the T-cell subsets were purer.

Quantitative RT-PCR (Figure 17) was performed to detect the expression of E3 ubiquitin ligase genes in anergic and non-anergic $CD4^+$T-cell populations, to assess whether E3 ligase gene expression was specific to the function of either of these T-cell subsets (Figure 15).

17a.

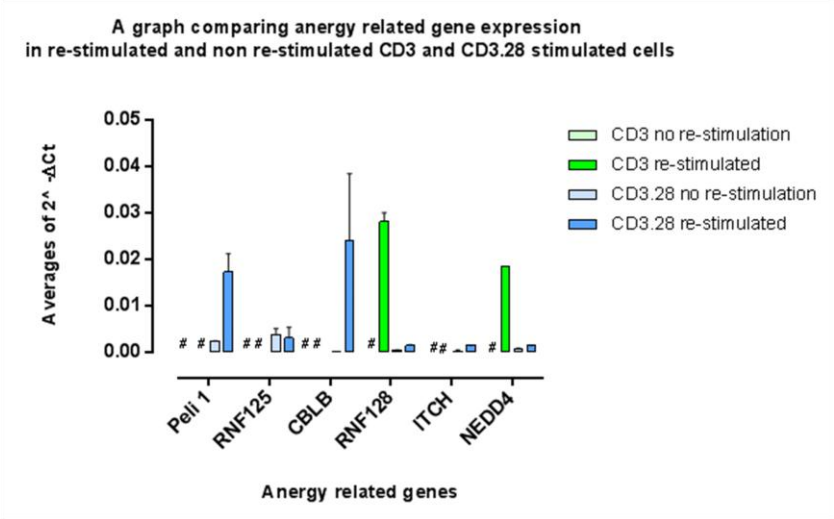

b.

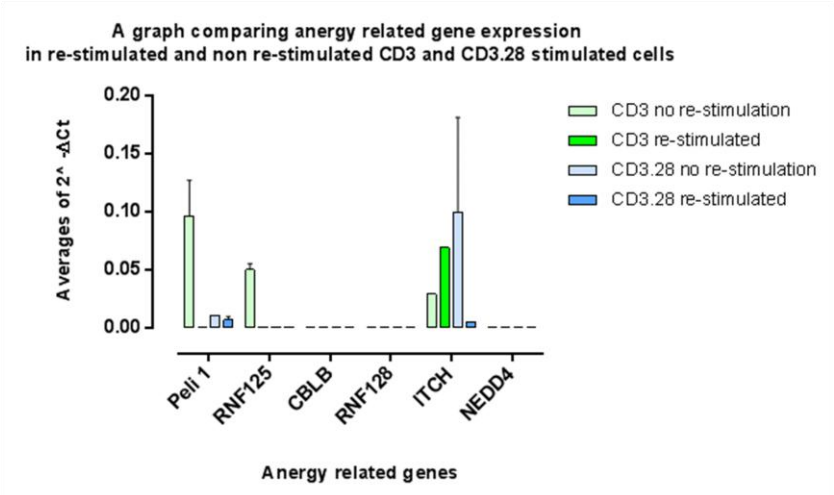

Figure 17- Graphs comparing E3 ubiquitin ligase expression between anti-CD3 stimulated and anti-CD3.28 stimulated conventional $CD4^+$T-Cells +/- CD3.28 Dynabead re-stimulation, measured by quantitative RT-PCR (n=2/3 except where there are no error bars in which case n=1). These T-cells were put through the anergy assays and frozen 3 hours after re-stimulation for PCR analysis. (a + b) represent the same experiment repeated using different donors. Each condition was repeated in triplicate and displayed as a mean. The error bars represent the SEM. The single lines on the graph represent where the gene was Not Detectable (N/D), where the reference gene GAPDH was detected however the target anergy gene was not. (#) indicates that there was insufficient material in these wells as the GAPDH reference gene was low and appearing late at ~34 cycles.

In Figure 17, when E3 ubiquitin ligase genes were detectable, the expression was very low. Higher expression of Cbl-b and Peli1 was found in CD3.28 re-stimulated populations in Figure 17a. Nedd4 and RNF128 were expressed at a higher level in the anti-CD3 re-stimulated population compared to the anti-CD3.28 re-stimulated population in Figure 17a.

In Figure 17b the majority of the genes were undetectable. Overall gene expression in this experiment was higher compared the donor used in Figure 17a based on the average 2^-Δct values. Peli1 and RNF125 were expressed in the anti-CD3 stimulated, non-re-stimulated population. ITCH was expressed in all four cell subsets in Figure 17b with the anti-CD3 re-stimulated and anti-CD3.28 non-re-stimulated populations showing the highest expressions.

Results show that anergy may be broken in some donors upon CD3.28 bead stimulation, and expression of E3 ubiquitin ligase genes in different T-cell subsets may donor dependant.

4. Discussion

The aim of this study was to investigate the E3 ubiquitin ligase expression in different $CD4^+$T-cell subsets. Previous studies indicate that some E3 ubiquitin ligases contribute to T-cell anergy(10, 20, 23). This study replicates previously described anergy induction methods and compares E3 ubiquitin ligase expression in different T-cell subsets using quantitative RT-PCR.

4.1. The effects of different initial stimulation methods on T-cell proliferation

Different methods of initial anti-CD3.28 stimulation were used to determine which method would be best to use in the 8 day anergy assay. It was essential that the initial stimulation activated the conventional $CD4^+$T-cells effectively whilst allowing them to return to rest prior to re-stimulation at day 4. This would prevent excessive 'boosting' of existing T-cell proliferation upon re-stimulation.

Figure 9 shows that anti-CD3.28 antibody is the best method to use to initially stimulate conventional $CD4^+$T-cells. This is because T-cell proliferation induced by antibody stimulation is still significantly higher compared to the resting population at day 4, demonstrating that the T-cells have been activated, but are able to come back down to rest. On the contrary, Treg bead and Dynabead stimulation hyperactivate the T-cells which causes significantly higher levels of T-cell proliferation, preventing the T-cells from returning to rest at day 4.

4.2. The effects of different re-stimulation methods on anergy induction

Previous results show that anergy is reversible with strong stimuli(10). It is possible that re-stimulation with anti-CD3.28 Dynabeads is too strong, and breaks anergy. In order to address whether Dynabeads were 'breaking' anergy, various methods were used to re-stimulate the T-cells (Figure 10).

Interestingly, the antibody re-stimulated population displayed similar levels of proliferation to the resting population, suggesting that mAbs may not be efficient at re-stimulating $CD4^+$T-cells. Previous literature shows that plate bound anti-CD3 is more effective than soluble anti-CD3 at cross-linking and inducing strong T-cell activation(32). It is possible that anti-CD3 mAb was not bound to the plate efficiently causing signal 2 to be absent upon re-stimulation. This would cause T-cell stimulation through anti-CD28 alone which has been linked to T-cell apoptosis(33, 34), therefore explaining the lower number of antibody re-stimulated populations compared to non-re-stimulated populations. It is also possible antibody re-stimulation re-stimulated the T-cells, but not strongly, allowing them to return to rest by Day 8,

4.3. Inducing anergy in conventional $CD4^+$T-cells

The higher level of proliferation in some of the the anti-CD3.28 stimulated re-stimulated populations compared to anti-CD3 stimulated re-stimulated populations shown in Figure 12a, may indicate that the anti-CD3 stimulated population is anergic upon re-stimulation. However, conflicting results from Figure 12a Experiment 4 and 12b show that the initially unstimulated population has a similar number of proliferating T-cells compared to the anti-CD3 stimulated population.

It is possible that the unstimulated T-cell population is unhealthy indicating that the anti-CD3 stimulated population may be truly anergic. Figure 13 demonstrates that the number of non-proliferating cells from Experiment 4 is lowest in the resting population indicating that unstimulated T-cells require additional factors other than media alone to survive. The reduced health of the resting unstimulated population is reinforced in Figure 11, where the resting, re-stimulated population shows the lowest T-cell proliferation and high T-cell death. This data suggests that the resting re-stimulated T-cell population is dying or non-functional, indicating that the anti-CD3 stimulated T-cells may be anergic upon anti-CD3.28 re-stimulation.

Figure 11 shows that T-cells which receive anti-CD3.28 stimulation survive better and proliferate more compared to those which receive anti-CD3 stimulation. This may be because dual stimulation through CD3 and CD28 fully activated the T-cells, causing them to continue proliferating at day 4. Re-stimulation at day 4, may have 'boosted' the existing proliferation, causing the high T-cell proliferation number at day 8. On the contrary, anti-CD3 stimulation may only provide few survival signals, therefore partially activating T-cells causing fewer T-cells to survive. To ensure all results were comparable, the samples were all run on the flow cytometer for the same length of time.

Figure 11a shows variability in results between experiments, which may be due to biological variability between donors. T-cells from some donors may have been more susceptible to anergy induction and less able to survive in conditions without survival signals.

4.4. Comparing E3 ubiquitin ligase expression between Tregs and Conventional $CD4^+$T-cells

Tregs represent a small population of the total $CD4^+$T-cell population making them difficult to isolate(8). Figure 14 demonstrates although the isolated population is enriched with Tregs, it is not as pure as it could be. It is possible that the contaminating $CD4^+CD25^-$ cells may have therefore affected the results when measuring the E3 ubiquitin ligase expression of Tregs.

Peli1 has a role in negatively regulating T-cell activation and is known to prevent autoimmunity(27). $Peli1^{-/-}$ T-cells *in vitro* demonstrate hyper-responsiveness to CD3.28 stimulation(27). However studies also show that Peli1 deficiency does not impair Treg cell development(27). This supports Figure 15 where there is no significant difference in Peli1 expression between Tregs and conventional T-cells. Peli1 has also been identified as having high expression in lymphocytes(27). Results from Figure 15 shows that Peli1 has the highest expression in conventional T-cells and Tregs compared to other E3 ligase gene tested.

GRAIL (RNF128), Cbl-b and ITCH have all been reported to play a role in peripheral tolerance(24, 35-37). One study made links between the expression of FOXP3, ITCH and Cbl-b mRNA with CTLA-4 expression on the surface of $CD4^+$CD25 high T-cells in MS(24). Furthermore, Cbl-b and ITCH activity in particular plays a role in Treg development by modulating parts of the TCR and interfering with TGFβ signalling(35)

Data from Figure 14 demonstrates expression of Cbl-b, RNF128 and ITCH in Tregs compared to conventional $CD4^+$T-cells where these genes were not detectable. This

shows that some E3 ubiquitin ligase expression may be upregulated in Treg cells therefore possibly contribute to their role in peripheral tolerance.

The overall expressions of all the E3 ubiquitin ligase genes tested were generally all low and in some cases not detectable. In order to gain robust data where accurate conclusions can be drawn, the assays and PCR must be repeated using purer samples with more material.

4.5. Comparing E3 ubiquitin ligase expression between anergic and non-anergic $CD4^+$T-cells

Many tested samples shown in Figure 17a had insufficient material (#) therefore accurate Ct values could not be collected. Consequently, an accurate conclusion could not be drawn from these results. Where E3 ubiquitin ligases were expressed in certain subsets, this expression was extremely low. In order to try and make accurate comparisons, the PCR was repeated using samples from a different donor (Figure 17b).

It was previously mentioned that anergy can be broken with strong stimuli(10). Peli1, ITCH and RNF125 expression were found in in anti-CD3 stimulated, non-re-stimulated cells, but were mostly undetectable upon re-stimulation. This suggests that anergy may have been broken due to strong re-stimulation therefore causing the T-cell to return to a normal activated phenotype. This would explain why these E3 ligase genes fell to an undetectable expression level.

Nedd4 is a positive regulator for T-cell activation(10, 20). In Figure 17b, Nedd4 expression is higher in anti-CD3 stimulated, re-stimulated populations than non-re-stimulated populations, which further indicates that the anergic state of the T-cells may be broken following re-stimulation.

The differences in gene expression between both PCR experiments could be explained by biological differences between donors. T-cells may react differently to anergy induction depending on the donor and therefore may demonstrate different expression of E3 ubiquitin ligase genes.

4.6. Future work

Anergic cells can be characterised by their reduced ability to proliferate, however previous studies also look for anergy induction by testing for reduced cytokine production such as IL-2, IL-3 and IFNɤ(10, 20). In future assays the cytokine production between anti-CD3 stimulated and anti-CD3.28 stimulated T-cells can be compared using cytokine secretion assays. This would confirm the anergic properties of the anti-CD3 stimulated T-cells. Anergy can also be reversed by adding exogenous IL-2(10, 17, 20). The expression of E3 ubiquitin ligase genes can be compared before and after IL-2 addition to define whether the gene expression changes with reversal of anergy.

The majority of previous studies used plate-bound anti-CD3 to induce anergy in jurkat cell lines and murine T-cells. However, the current study used the same method to induce anergy in $CD4^+$T-cells isolated from human peripheral blood. Previous studies demonstrated anergy induction *in vitro* using alternative methods such as mitogen concanavalin A, stimulation with the calcium ionophore ionomycin, MHC II-peptide complexes presented on a planar lipid bilayer, or peptides presented by APCs lacking B7 expression(10, 17, 18). It is possible that these alternative methods would be more efficient at inducing anergy in $CD4^+$T-cells isolated from human peripheral blood.

Past experiments also used thymidine incorporation to measure T-cell proliferation, whereas the current study used cell proliferation dye. Previous studies show that thymidine can disturb cell generation cycles(38). The difference

in methods when measuring T-cell proliferation may explain why it was difficult to replicate past results in this study.

A large proportion of T-cells died throughout the assay, making the cDNA recovery at the end of the assay minimal, therefore affecting the PCR and detection of E3 ligase expression. To avoid this problem, future assays would involve the isolation of larger cell numbers to ensure that there is enough material. Furthermore, the purity of the Treg population can be increased by using FACS following magnetic isolation. This would prevent $CD4^{+}CD25^{-}$ cells from contaminating the sample and affecting the PCR data.

Other E3 ubiquitin ligases such as TRAF6, MARCHVII and AIP2(28, 39) have also been reported to play a role in anergy and T-cell activation. It is possible that these genes are also differentially expressed in different T-cell subsets and so the expression of these genes in different T-cell subsets should be tested in future. Furthermore, differential expression of E3 ligases may occur between other subsets of $CD4^{+}$T-cells such as central memory and effector memory groups which may relate to their specific functions. This is another possible area of future research.

4.7. Conclusion

The results from the anergy assay demonstrate that anergy in T-cells may be induced via stimulation through plate-bound anti-CD3 antibodies, however further work would need to be performed to confirm the anergic state of these T-cells.

Unfortunately, accurate conclusions could not be drawn from the PCR data when comparing E3 ubiquitin ligase expression between T-cell subsets due to insufficient material and possible contamination of other T-cell subsets. In future, these challenges should be addressed so robust data may be collected and accurate conclusions drawn.

By understanding the role of specific E3 ligases in T-cell activation and different T-cell subsets, signalling pathways and consequent E3 ligase expression can possibly be manipulated therapeutically in the future. By manipulating E3 ligase expression to induce T-cell anergy, you may prevent the development of autoimmune diseases, allergic responses and immune responses after transplantations. It may also be possible reduce expression of E3 ligases which negatively regulate T-cell activation, to encourage non-responsive T-cells to become more activated. These active T-cells may then be able to target cancers and chronic infections, where T-cell activation may otherwise be impaired.

5. References

1. Sprent J, Kishimoto H. The thymus and central tolerance. Philosophical Transactions of the Royal Society of London Series B-Biological Sciences. 2001;356(1409):609-16.

2. Abbas AK, Lohr J, Knoechel B, Nagabhushanam V. T cell tolerance and autoimmunity. Autoimmun Rev. 3. Netherlands2004. p. 471-5.

3. Siegel RM, Katsumata M, Komori S, Wadsworth S, Gill-Morse L, Jerrold-Jones S, et al. Mechanisms of autoimmunity in the context of T-cell tolerance: insights from natural and transgenic animal model systems. Immunol Rev. 1990;118:165-92.

4. Xing Y, Hogquist KA. T-Cell Tolerance: Central and Peripheral. 2012.

5. Zhang W. Immunology Webnotes [Website]. University of Georgia2013 [updated 10/21/2007]. Available from: http://wenliang.myweb.uga.edu/mystudy/immunology/ScienceOfImmunology/index.html.

6. Ahmad E, Elgohary T, Ibrahim H. Naturally occurring regulatory T cells and interleukins 10 and 12 in the pathogenesis of idiopathic warm autoimmune hemolytic anemia. J Investig Allergol Clin Immunol. 2011;21(4):297-304.

7. Curotto de Lafaille MA, Lafaille JJ. Natural and adaptive foxp3+ regulatory T cells: more of the same or a division of labor? Immunity. 30. United States2009. p. 626-35.

8. Workman CJ, Szymczak-Workman AL, Collison LW, Pillai MR, Vignali DA. The development and function of regulatory T cells. Cell Mol Life Sci. 2009;66(16):2603-22.

9. Sakaguchi S, Ono M, Setoguchi R, Yagi H, Hori S, Fehervari Z, et al. Foxp3+ CD25+ CD4+ natural regulatory T cells in dominant self-tolerance and autoimmune disease. Immunol Rev. 212. Denmark2006. p. 8-27.

10. Fathman CG, Lineberry NB. Molecular mechanisms of CD4+ T-cell anergy. Nature Reviews Immunology. 2007;7(8):599-609.

11. Mueller D. Mechanisms maintaining peripheral tolerance. Nature Immunology. 2010;11(1):21-7.

12. Shevach EM. Regulatory T cells in autoimmmunity*. Annu Rev Immunol. 18. United States2000. p. 423-49.

13. Takahashi T, Kuniyasu Y, Toda M, Sakaguchi N, Itoh M, Iwata M, et al. Immunologic self-tolerance maintained by CD25(+)CD4(+) naturally anergic and suppressive T cells: induction of autoimmune disease by breaking their anergic/suppressive state. International Immunology. 1998;10(12):1969-80.

14. Alderson KL, Zhou Q, Berner V, Wilkins DE, Weiss JM, Blazar BR, et al. Regulatory and conventional CD4+ T cells show differential effects correlating with PD-1 and B7-H1 expression after immunotherapy. J Immunol. 180. United States2008. p. 2981-8.

15. Zhu J, Paul W. CD4 T cells: fates, functions, and faults. Blood. 2008;112(5):1557-69.

16. Gillespie KM. Type 1 Diabetes - Pathogenesis, Genetics and Immunotherapy. 2011.

17. Zheng Y, Zha Y, Gajewski TF. Molecular regulation of T-cell anergy. EMBO Rep. 9. England2008. p. 50-5.

18. Anandasabapathy N, Ford GS, Bloom D, Holness C, Paragas V, Seroogy C, et al. GRAIL: an E3 ubiquitin ligase that inhibits cytokine gene transcription is expressed in anergic CD4+ T cells. Immunity. 18. United States2003. p. 535-47.

19. Macian F. Albert Einstein College of Medicine: Yeshiva University2013. Available from: http://www.einstein.yu.edu/macian/page.aspx?id=22023.

20. Mueller DL. E3 ubiquitin ligases as T cell anergy factors. Nat Immunol. 5. United States2004. p. 883-90.

21. Andris F, Denanglaire S, Mattia Fd, Urbain J, Leo O. Naive T Cells Are Resistant to Anergy Induction by Anti-CD3 Antibodies. 2004.

22. Paolino M, Thien CB, Gruber T, Hinterleitner R, Baier G, Langdon WY, et al. Essential role of E3 ubiquitin ligase activity in Cbl-b-regulated T cell functions. J Immunol. 186. United States2011. p. 2138-47.

23. Paolino M, Penninger JM. E3 ubiquitin ligases in T-cell tolerance. Eur J Immunol. 2009;39(9):2337-44.

24. Sellebjerg F, Krakauer M, Khademi M, Olsson T, Sorensen PS. FOXP3, CBLB and ITCH gene expression and cytotoxic T lymphocyte antigen 4 expression on CD4(+) CD25(high) T cells in multiple sclerosis. Clin Exp Immunol. 2012;170(2):149-55.

25. Zhao H, Li CC, Pardo J, Chu PC, Liao CX, Huang J, et al. A novel E3 ubiquitin ligase TRAC-1 positively regulates T cell activation. J Immunol. 174. United States2005. p. 5288-97.

26. Yang B, Gay DL, MacLeod MK, Cao X, Hala T, Sweezer EM, et al. Nedd4 augments the adaptive immune response by promoting ubiquitin-mediated degradation of Cbl-b in activated T cells. Nat Immunol. 9. United States2008. p. 1356-63.

27. Chang M, Jin W, Chang JH, Xiao Y, Brittain GC, Yu J, et al. The ubiquitin ligase Peli1 negatively regulates T cell activation and prevents autoimmunity. Nat Immunol. 12. United States2011. p. 1002-9.

28. King CG, Buckler JL, Kobayashi T, Hannah JR, Bassett G, Kim T, et al. Cutting edge: requirement for TRAF6 in the induction of T cell anergy. J Immunol. 180. United States2008. p. 34-8.

29. Dure M, Macian F. IL-2 signaling prevents T cell anergy by inhibiting the expression of anergy-inducing genes. Molecular Immunology. 2009;46(5):999-1006.

30. Steenbakkers P, Boots A, Rijnders A. T-cell anergy induced by clonotype-specific antibodies: modulation of an autoreactive human T-cell clone in vitro. Immunology. 1999;96(4):586-94.

31. Zheng Y, Delgoffe G, Meyer C, Chan W, Powell J. Anergic T Cells Are Metabolically Anergic. Journal of Immunology. 2009;183(10):6095-101.

32. VANLIER R, BROUWER M, REBEL V, VANNOESEL C, AARDEN L. IMMOBILIZED ANTI-CD3 MONOCLONAL-ANTIBODIES INDUCE ACCESSORY CELL-INDEPENDENT LYMPHOKINE PRODUCTION, PROLIFERATION AND HELPER ACTIVITY IN HUMAN LYMPHOCYTES-T. Immunology. 1989;68(1):45-50.

33. Carpenter P, Pavlovic S, Tso J, Press O, Gooley T, Yu X, et al. Non-Fc receptor-binding humanized anti-CD3 antibodies induce apoptosis of activated human T cells. Journal of Immunology. 2000;165(11):6205-13.

34. VanParijs L, Ibraghimov A, Abbas A. The roles of costimulation and Fas in T cell apoptosis and peripheral tolerance. Immunity. 1996;4(3):321-8.

35. Venuprasad K. Cbl-b and Itch: Key Regulators of Peripheral T-cell Tolerance. Cancer Research. 2010;70(8):3009-12.

36. Venuprasad K, Huang H, Harada Y, Elly C, Subramaniam M, Spelsberg T, et al. The E3 ubiquitin ligase Itch regulates expression of transcription factor Foxp3 and airway inflammation by enhancing the function of transcription factor TIEG1. Nature Immunology. 2008;9(3):245-53.

37. Nurieva R, Zheng S, Jin W, Chung Y, Zhang Y, Martinez G, et al. The E3 Ubiquitin Ligase GRAIL Regulates T Cell Tolerance and Regulatory T Cell Function by Mediating T Cell Receptor-CD3 Degradation. Immunity. 2010;32(5):670-80.

38. BLENKINS.WK. EFFECT OF TRITIATED THYMIDINE ON CELL PROLIFERATION. Journal of Cell Science. 1967;2(3):305-&.

39. Chen A, Gao B, Zhang J, McEwen T, Ye SQ, Zhang D, et al. The HECT-Type E3 Ubiquitin Ligase AIP2 Inhibits Activation-Induced T-Cell Death by Catalyzing EGR2 Ubiquitination. 2009.